Institut für Nutzpflanzenwissenschaften und Ressourcenschutz (INRES)
- Allgemeine Bodenkunde und Bodenökologie -

Soil organic carbon pools and their spatial patterns – rapid assessment using mid-infrared spectroscopy

Inaugural - Dissertation

zur

Erlangung des Grades

Doktor der Agrarwissenschaften

der

Hohen Landwirtschaftlichen Fakultät

der

Rheinischen Friedrich-Wilhelms-Universität

zu Bonn

vorgelegt am 07.05.2010

von Ludger Clemens Bornemann

aus

Münster

Fraktionen von Bodenkohlenstoff und deren räumliche Muster – schnelle Erfassung durch Mittlere Infrarot-Spektroskopie

Organischer Bodenkohlenstoff (SOC) spielt eine wesentliche Rolle in globalen C-Kreisläufen, doch die räumlichen Muster unterschiedlicher SOC-Fraktionen sind bislang kaum erforscht – zu aufwändig sind die klassischen Analysemethoden. Wenig bekannt ist daher auch der Einfluss effektiver Steuergrößen auf die Verfügbarkeit der einzelnen SOC-Fraktionen auf der Feldskala.

Ziel meiner Arbeit war es, das Potenzial Mittlerer Infrarot-Spektroskopie (MIRS) zur schnellen und kostengünstigen Quantifizierung wesentlicher Kenngrößen des SOC-Haushaltes zu evaluieren. Des Weiteren sollten effektive Steuergrößen der räumlichen Heterogenität des C-Umsatzes auf der Feldskala identifiziert werden.

Neben der quantitativen Bestimmung von SOC habe ich hierzu black carbon (BC), drei Fraktionen partikulärer organischer Substanz (POM) sowie mineralisch gebundenen Kohlenstoff als Differenz in Probensätzen unterschiedlicher Herkunft bestimmt und mit Hilfe qualitativer spektraler Informationen Vorhersagemodelle zur Parameterschätzung erstellt. Effektive Steuergrößen räumlicher Variabilität der einzelnen SOC-Fraktionen habe ich mit Hilfe statistischer Strukturanalyse und Geostatistik identifiziert.

Zur erstmaligen quantitativen und qualitativen Bestimmung von SOC und BC mittels MIRS verwendete ich Grünland- und Ackerböden aus diversen Lössregionen der Welt (n = 309). Die BC-Referenzwerte wurden mit Hilfe einer Biomarker-Methode (Benzolpolycarbonsäuren, BPCA) bestimmt, die spektroskopiegestützte BC-Charakterisierung habe ich anhand unterschiedlich carbonisierter organischer Substanz, welche individuelle Stadien der Verkohlung repräsentierte, validiert. Ebenso habe ich basierend auf den Ergebnissen der SOC- und BC-Bestimmungen regionalisierte Probensätze für die MIRS-gestützte Bestimmung von POM dreier Größenklassen (POM1: 2000–250 µm; POM2: 250–53 µm; POM3: 53–20 µm) für 129 Rasterpunkte eines 1,3 ha großen Testfeldes verwendet. Die Validierung dieser Vorhersagemodelle erfolgte unter anderem durch Ligninanalysen der untersuchten Proben. Als potenzielle Steuergrößen des C-Umsatzes habe ich den Steingehalt, die Textur der Feinerde, den Gehalt von pedogenen Eisenoxiden, Hangneigung und Höhe über normal Null, die ^{137}Cs-Aktivität zur Abschätzung von erosiver Verlagerung sowie die Bodenfeuchte an allen 129 Rasterpunkten bestimmt. Die statistischen Methoden zur Identifikation effektiver Steuergrößen des C-Umsatzes umfassten Multidimensionale Skalierung einer Fuzzy-Kappa-Ähnlichkeitsmatrix, Hauptkomponentenanalyse, Korrelationsanalysen, multiple Regressionsmodelle sowie Semivarianzanalysen.

Durch die Anwendung von MIRS konnten alle SOC-Fraktionen verlässlich abgeschätzt werden. Lokale Kalibrationen erklärten ca. 99 % der absoluten Variabilität des SOC. Die Qualität der BC-Vorhersage war etwas geringer (R² > 0,8), was teilweise auf unterschiedliche BC-Qualitäten zurückzuführen war. Diese sind durch den Anteil an Mellitsäure im BPCA-Spektrum charakterisiert, welcher ebenfalls mit den spektralen Signalen korrelierte (R² ≥ 0,6). Die erreichten Bestimmtheitsmaße zur Vorhersage von POM lagen zwischen 0,77 und 0,96. Das Vorhersagemodell für POM1 basierte dabei hauptsächlich auf Absorptionsbanden von Cellulose und Lignin, die Gehalte von POM2 wurden durch spezifische Spektralbanden von Abbauprodukten organischer Materialien wie CH-Gruppen und aromatischen Strukturen charakterisiert. Absorptionen von Carboxylgruppen trugen wesentlich zur Vorhersage von POM3-Gehalten bei. Enge räumliche Beziehungen konnten zwischen POM1, POM2 und Lignin festgestellt werden, welche auch zu großen Teilen die Variabilität von SOC im Gelände erklärten. Im Gegensatz dazu zeigten die Gehalte an POM3 eine weniger deterministische räumliche Struktur und trugen nur wenig zur Heterogenität des SOC bei.

Mit Ausnahme von POM3 (R² = 0,20) konnte die Variabilität aller SOC-Fraktionen unter Verwendung des Steingehaltes, der Gehalte an pedogenen Oxiden und der Hangneigung in multiplen linearen Regressionsmodellen erklärt werden (R² = 0,68–0,79). Der stark variierende Steingehalt (4–60 %) erwies sich hierbei als dominierender Faktor der C-Dynamik auf der untersuchten Testfläche. Die räumliche Verteilung von BC war zusätzlich durch Bodenerosion bestimmt.

Zusammenfassend gilt, dass sich mittels MIRS schnell und kostengünstig räumliche Muster von SOC, BC und POM im Gelände ermitteln lassen. Die identifizierten räumlichen Muster zeigen hohe Anteile deterministischer Variabilität und lassen sich überwiegend mit Sättigungsprozessen erklären, welche aus relativ erhöhten Einträgen von Pflanzenstreu in durch zunehmende Steingehalte reduzierte Feinerdeanteile resultieren. Daher ist es gerade in Böden mit stark variierenden Steingehalten essentiell, dass Bodenskelett zu berücksichtigen, um effektive Kenngrößen des SOC-Haushaltes auf der Feldskala ermitteln zu können – ein Faktor also, welcher in konventionellen Bodenanalysen (auf 2 mm gesiebte Feinerde) bislang wenig Beachtung findet.

Soil organic carbon pools and their spatial patterns – rapid assessment using mid-infrared spectroscopy

Soil organic carbon (SOC) plays an important role in global C cycling. Until today, the spatial patterns of individual SOC fractions are, however, largely undiscovered as traditional methods for their determination are too time consuming. In consequence, also the interaction of regulating parameters governing SOC turnover on the field scale remains unresolved.

The aim of my work was to elucidate the potential of mid-infrared spectroscopy (MIRS) for time- and cost-effective quantification of constitutive parameters regulating SOC turnover, and to identify effective control parameters regulating the spatial heterogeneity of SOC dynamics on the field scale.

In addition to SOC quantification, I determined amounts of black carbon (BC), and particulate organic matter (POM) of three size classes in sample sets of different regional provenance. Quantitative prediction models for parameter estimation of the measured values were derived from MIR spectra. Mineral-bound SOC was calculated by difference. Further on, I identified effective control parameters regulating the spatial heterogeneity of SOC dynamics by statistical structure analyses and geo-statistical instrumentation.

Employing samples of various arable and grassland soils from loess regions all across the world (n = 309), I was able to conduct quantitative and qualitative determination of SOC and BC from MIR spectra for the first time. Black carbon contents were determined by a molecular marker method (benzene polycarboxylic acids, BPCA). The MIRS-based BC characterization was validated employing individual samples of charred organic matter which represented different stages of combustion. With regard to the results of the SOC and BC predictions, I employed regionalized sample sets for the MIRS-based determination of POM of three size classes (POM1: 2000–250 µm; POM2: 250–53 µm; POM3: 53–20 µm) for 129 subsites of a 1.3 ha test site ($R^2 = 0.77– 0.96$). At this, primarily analyses of the lignin contents were used for validation of the individual prediction models.

The stone content, texture of the fine earth, pedogenic oxides, hill slope, elevation above sea level, ^{137}Cs-activity as proxy for erosive translocation, as well as the soil moisture were considered as effective parameters regulating SOC turnover, and determined for all 129 subsites of the investigated test site. The statistical instrumentation for the identification of effective parameters for SOC turnover comprised multidimensional scaling of a fuzzy-kappa similarity matrix, principal component analysis, correlation analysis, multiple regression models, as well as analyses of semivariance.

All investigated SOC fractions were successfully determined by MIRS predictions. About 99 % of total SOC variability was explained by local calibrations. The precision of BC prediction was lower ($R^2 > 0.8$), partly reflecting different BC quality. A measure of the latter is the mellitic acid-C percentage, which also correlated with MIRS patterns ($R^2 \geq 0.6$).

Coefficients of determination for the predictions of POM of three size classes ranged between 0.77 and 0.96. The prediction model for POM1 chiefly relied on specific signals of lignin and cellulose; contents of POM2 were estimated by spectral bands assigned to degradation products as aliphatic C–H groups and aromatic moieties. Carboxylic groups essentially contributed to the prediction of POM3. There was a close spatial relation between the coarse POM1 and POM2 fractions and lignin, which largely also explained variations in bulk SOC. In contrast, POM3 exhibited a less deterministic pattern in the field, thus contributing little to spatial variation of the SOC content.

With exception of POM3 ($R^2 = 0.20$), multiple regression models employing the stone content, contents of pedogenic oxides, as well as the hillslope, successfully predicted the spatial distribution of all investigated SOC fractions ($R^2 = 0.68–0.79$). The highly variable stone content (4–60 %) proved to be the dominating factor regulating SOC dynamics on the investigated test site. The spatial distribution of BC was additionally affected by erosive translocation.

In summary, MIRS predictions facilitate a time- and cost-effective determination of spatial distributions of SOC, BC, and POM within landscapes. On the investigated test site, the observed variability is chiefly deterministic and can be attributed to saturation processes, caused by disproportionately high input of plant debris as amounts of fine earth are reduced by increasing stone contents.

Especially in soils that comprise highly variable stone contents, the coarse texture thus necessarily needs to be considered in case effective parameters of SOC turnover are to be identified – even though only rarely considered in conventional soil analysis (soil sieved to grain sizes of 2 mm).

List of figures

List of tables

List of abbreviations

ASL	elevation Above Sea Level
BC	Black Carbon
CPMAS	Cross Polarization Magnetic Angle Spinning
DOC	Dissolved Organic Carbon
DPM	Decomposable Plant Material
EF	modelling Efficiency
FE	Fine Earth
FIR	Far Infrared
FT	Fourier Transform
GC	Gas Chromatography
HUM	Humified Organic Matter
IR	Infrared
IRMS	Isotope Ratio Mass Spectrometry
LF	Light Fraction
MDS	Multidimensional Scaling
MIR	Mid-Infrared
MIRS	Mid-Infrared Spectroscopy
MS	Mass Spectrometry
NIR	Near Infrared
NMR	Nuclear Magnetic Resonance Spectrometry
PCA	Principal Component Analysis
PLFA	Phospholipid Fatty Acids
PLSR	Partial Least Squares Regression
POM	Particulate Organic Matter
PSRE	Proton Spin Relaxation
RMSECV	Root Mean Square Error of Cross Validation
RMSEP	Root Mean Square Error of Prediction
RPD	Ratio of Performance to Deviation
RPM	Resistant Plant Material
SOC	Soil Organic Carbon
SOM	Soil Organic Matter
SVA	Soil-Segetation-Atmosphere (continuum)
TOC	Total organic carbon
VSC	Sum of Vanilyl, Syringyl, and Cinamyl monomers
WEOC	Water Extractable Organic Carbon

I

General introduction

1 RATIONALE

Global warming and climate change are driven by man-made CO_2 emissions and simultaneously represent major challenges that have to be coped by mankind. At this, global C inventories in soil exceed those of plants or atmosphere more than twofold (Batjes, 1996). Accordingly, the Kyoto Protocol again manifested the increased environmental relevance of soil organic carbon (SOC) in 1997 and its "source and sink function" for greenhouse active CO_2 has received considerable interest ever since (Bellamy et al., 2005; Fierer et al., 2005; Davidson and Janssens, 2006). While agricultural and forestry activities are major contributors to increased CO_2 emissions since the 1950s (Lal et al., 2008), sequestration of atmospheric CO_2 in agricultural ecosystems may also mitigate parts of the greenhouse gas flux problem.

The stocks of soil organic matter (SOM) are balanced by inputs and outputs of organic C, but prediction of global CO_2 net fluxes from soils comprises high uncertainty (Prechtel et al., 2009). There is consensus that microbial decomposition of SOM is a main source of soil born CO_2 emissions, but turnover of SOM can be highly heterogeneous, even on the field scale. This variability is caused by the heterogeneity of its effective control parameters. Amount and quality of litter input, inorganic soil properties like contents of clay and pedogenic oxides, pH etc., as well as environmental conditions like soil moisture and temperature directly and indirectly affect the population of the decomposer community and its actual activity. The interaction of all these parameters determines the biotic transformation of animal and plant litter into the various decomposition products comprised by SOM. Quantity and quality of SOM could thus serve as an indicator for potential spatial patterns of soil born CO_2 emissions.

Studies aiming to derive measureable indices for the description of SOM decomposition commonly categorize bulk SOM into discrete pools with individual turnover times (Jenkinson, 1990). Practically, biomarker methods are applied to gain hints on the origin and composition of SOM species (Kögel, 1986; Brodowski et al., 2005) while physical (Christensen, 1992), or physicochemical soil fractionations (Cambardella and Elliott, 1992) represent the instrumentation for quantitative determination of SOM pools. Skjemstad et al. (2004) demonstrated for the first time,

that a conceptual carbon turnover model (RothC. Ver. 26.3) can be successfully initialized by measured soil carbon pools, comprising total organic carbon (TOC), particulate organic matter (POM), and black carbon (BC).

While such multi–pool models are clearly superior to models treating SOC as a single homogeneous pool (Jones et al., 2005), the classical determination of these pools is laborious and costly. Their applicability for large scale surveys is thus limited, especially under consideration of the apparent field scale heterogeneity. Techniques like nuclear magnetic resonance spectrometry (NMR) and biomarker analyses gave new insights regarding the composition of bulk soil and the chemistry of particular soil fractions (Amelung et al., 1999; Brodowski et al., 2007; Kögel-Knabner et al., 2008), but they share the drawback of being time-consuming and costly. However, recent evidence indicates that a rapid characterization of SOC may also be feasible by minimum-invasive techniques like mid-infrared spectroscopy (MIRS).

In combination with multivariate data analysis, MIRS has shown its potential for the rapid determination of various basic soil properties (Janik et al., 1998; Reeves et al., 2001; Viscarra-Rossel et al., 2006) like SOC or clay contents. The possibility to determine the field scale heterogeneity of individual SOM pools, however, still awaits clarification. Concerning their relevance for modelling of perennial SOM turnover, particular interest should be given to the determination of passive and slow cycling pools like BC and POM (Skjemstad et al., 2004). Given that such SOM pools are indeed predictable, MIRS-based screenings could allow for the fast assessment of comprehensive soil data, even in dense grids. Such datasets would facilitate the elucidation of effective control parameters regulating SOM turnover on the field scale by systematic integration of the observed spatial patterns of organic and inorganic soil parameters.

2 STATE OF THE ART

2.1 Spatial patterns

2.1.1 Why spatial patterns of soil organic carbon pools?

Major parts of global C cycling take place at the soil-vegetation-atmosphere (SVA) interface, where biogenic processes of C transformation are regulated by water and energy fluxes. The cycling and exchange between the involved compartments is thereby characterized by complex interactions among each other and the regulating parameters. Also the interference of human activity evokes mutual feedbacks on inherent exchange processes in the SVA system. These feedbacks may severely impact human living in many ways and represent a constitutive aspect of "global change".

Interactions between the SVA compartments are extremely complex due to their inherent spatial and temporal heterogeneity. At this, major parts of the observed heterogeneity are not random, but spatial patterns are formed by multidimensional non-linear coupling and feedback between the involved system compartments (Grayson and Blöschl, 2001). Predicting the reactions upon external changes thus represent a task of extreme complexity. An increasing number of numerical models aiming at different parts within the SVA system have become available and express a high demand for reliable input data. The use of point measurements and rather crude interpolations to deliver these input variables is limited as they inadequately smooth out much of the heterogeneity found in nature. This heterogeneity is, however, not random but highly organized, and a linear statistical representation of the variability will be hardly sufficient (Molz et al., 2004).

Except of single aircraft-based measurements of CO_2 and trace gases, measurement techniques to capture atmospheric properties on regional scales (> 100 km) concentrate on water and energy fluxes but the limited number of measurement stations restricts the parameterisation of meteorological modelling to rather coarse assumptions. Despite considerable spatial heterogeneity of relevant soil properties and hydraulic parameters, simple mean values or estimations of those are commonly applied and add further uncertainty to the gained results (Knorr and Heimann, 2001).

On the field scale, rapid turbulent mixing of the atmospheric boundary layer in SVA

systems limits the possibility to capture spatial patterns of atmospheric CO_2 concentrations. Thus, CO_2 fluxes in the field are usually assessed by eddy-covariance measurements above the vegetation canopy which capture the integrative signal of the turbulent layer. A large number of studies assessed the actual CO_2 exchange in various ecosystems, including grassland and forest soils (Chen et al., 2006), as well as cropped agricultural soils (Werth and Kuzyakov, 2009; Li et al., 2010). At this, soil moisture has been identified as one key parameter regulating the actual C dynamics under vegetation (Aiken et al., 1991; Reichstein et al., 2003).

Intensive research has improved our understanding of soil hydrology and a number of conceptual models are available for the simulation of subsurface water flow in the vadose zone (Van Genuchten and Simunek, 2004). But also here, multidimensional modelling demands data on spatial heterogeneity. Information on spatial patterns may be achieved by integrating data from remote sensing, geophysical surveys, and topographic information. A common limitation is, however, that the conversion of these datasets to the desired information for modelling is not straight forward and adequate ground truth data for validation is hardly available due to the considerable workload demanded for its acquisition (Braudeau and Mohtar, 2009).

While soil respiration plays only a minor role in daily or seasonal changes of net CO_2 fluxes, the soil born respiration is an indicator for SOC decomposition which co-determines the storage of carbon in soil in the long term (Ryan and Law, 2005). Practically, measures derived by the eddy covariance method are founded on limited numbers of soil data. The general assumption of uniformly distributed soil properties within the footprint area of eddy covariance measurements likely holds just as little as point measurements represent the actual spatial heterogeneity of parameters like soil moisture (Falge et al., 2001; Wilson and Meyers, 2001). The need for a better understanding of the spatial variability of SOC dynamics for the interpretation of eddy covariance measurements was also envisaged by Sanderman et al. (2003). There is consensus that beyond the consideration of rate parameters like soil moisture, the recognition of spatial patterns of soil organic carbon pools and inorganic soil parameters represents a key element for the elucidation of effective parameters of SOC turnover (Smith et al., 2003; Ahuja et al., 2006). Integrated attempts are needed that

combine CO_2 efflux measurements as well as soil properties to allow for a better understanding of SOC dynamics. At this, the recognition of spatial patterns has to be considered for the modelling of long term C sequestration in SVA systems on all scales (Anderson et al., 2003; Manzoni and Porporato, 2009). Effective parameters and their representative mean values that are applied on regional or even global scales should thus be based on knowledge gained by recognition of spatial patterns on the field scale (Izaurralde et al., 1998; Vogel and Roth, 2003).

In the past, field scale heterogeneity of basic soil properties like SOC or clay contents have been assessed by applying laborious lab-based measurements (Kern, 1994; Kuzyakova and Richter, 2003; Ye et al., 2008; Wang et al., 2009). Although a variety of different fractionation procedures have been proposed for the identification of individual carbon pools for the parameterisation of SOC turnover models (Paustian et al., 1997; Six et al., 2004; Skjemstad et al., 2004), the considerable expenditures for their determination renders the assessment of their spatial heterogeneity within larger areas almost impossible until today (von Lützow et al., 2007). Innovative methods that enable for the fast screening of organic and inorganic soil properties are thus a prerequisite for the recognition of spatial patterns and their implementation for SOC turnover modelling.

2.1.2 Statistical assessment of spatial patterns in soil

Early concepts aiming towards the prediction of specific soil properties based on factors of soil formation like climate, vegetation, or soil forming substrate, coupled with soil-landscape relationships (Jenny, 1941; Simonett, 1960). Applying climofunctions, Jones (1973) was able to derive relations between soil carbon, nitrogen, clay, annual rainfall, and altitude. These classical attempts, however, related to surveys on larger scales and are not capable of capturing spatial heterogeneity at the field scale. The spatial distribution of mineral soil constituents frequently co-determines patterns of different soil organic carbon pools, which may also be autocorrelated to each other. The high degree of co-linearity in such datasets severely limits the applicability of simple linear and multiple linear regression analysis for the determination of effective control parameters that explain the spatial distribution of individual SOC pools. At this, multivariate explorative techniques and higher non-

linear models are most suited for the identification of deterministic dependencies. Due to the limited number of spatial data achievable from classical soil survey, data intensive procedures like neural networks or partial least squares regression are usually restricted to applications in remote sensing or geophysical surveys (Cockx et al., 2009). Principal component analysis is, however, also applicable to derive structures in smaller data sets (Hasie et al., 2001). The application of fuzzy-sets with subsequent multivariate exploration of the similarity matrices by multidimensional scaling represents a possibility to account for uncertainty associated with lab based determination of soil properties and the fuzziness of their spatial patterns in the field (Kruskal, 1964; Zadeh, 1965; McBratney et al., 2003). Multivariate statistical exploration of the dataset, however, represents only the initial step in the geostatistical data analysis. As a second step, quantitative description of spatial heterogeneity is routinely achieved by semivariogram analysis, which represents the single most important geostatistical tool in soil science (McBratney and Webster, 1986; Atkinson and Lloyd, 2007). Quantitative measures for the dependencies between dependent and independent soil parameters can finally be derived by nonparametric statistical methods like correlation or regression analysis (Kuzyakova and Richter, 2003; Yavitt et al., 2009).

2.2 Soil organic carbon

2.2.1 Soil organic carbon in the arable soil environment

Summing up to about 1.4 billion ha, arable soils account for approximately 10 % of worldwide land area (WRB, 2007) and contain about the same percentage of its SOC stocks (Jenkinson et al., 1991). The organic carbon that is stored within a soil represents floral and faunal litter in various stages of decomposition, microbial biomass and its detritus, as well as products of incomplete biomass burning and fossil fuel combustion. In addition to the in-situ inputs of plant and animal litter, considerable amounts of ex-situ litter may be introduced to agricultural soils by organic manuring.

As arable soils have specifically been selected for cultivation, they are usually characterized by reasonably good aeration and drainage, allowing for vital plant growth with correspondingly high amounts of plant debris. Simultaneously these soil properties are favourable for decomposition and C stocks are thus rather low compared to the high biomass input (Davidson and Janssens, 2006). Upon cultivation, topsoil layers of native soils are homogenized and mixed with mineral soil horizons by varying kinds of tillage. The outcome of these practices is a soil profile with clear cut boundaries between two unequal sectors. Of these sectors, the tilled topsoil usually comprises the highest proportions of SOC as also indicated by data of Batjes (1996) who estimated 700 of the 2400 Gt of SOC in 0–200 cm to persist in the first 30 cm. Representing the active interface between pedosphere, atmosphere and vegetation, topsoils thus play a major role for carbon dynamics in SVA systems. Among arable soils, exceptions are represented e.g. by sandy soils that are prone to considerable leaching of SOC into deeper layers (Podzols), or by soils that naturally comprise SOC-rich subsoils like Fluvisols or Histosols.

2.2.2 Qualitative characterization of soil organic matter and its turnover

Owing to its manifold constituents, SOC exhibits a complex chemistry which has challenged researchers all times. Early procedures attempting to characterize the chemical composition of SOC derived relatively unspecific measures for its contents of e.g. carbohydrates (Lowe, 1978), lipids and polypeptides (Stevenson, 1966), or "humic substances" (Coulson et al., 1959). While these classical extraction procedures

yielded a rather coarse chemical classification, the actual understanding on the origin of the manifold SOC species stems from a variety of biomarker methods with a higher degree of specification.

Residues from incomplete combustion of biomass burning or fossil fuels are suspected to be most recalcitrant against biochemical degradation (Brodowski et al., 2007) and a variety of different methods have been proposed for the assessment of BC in soils (Hammes et al., 2007). These include the use of benzene polycarboxylic acids (BPCA) as biomarkers for highly condensed carbonatious material (Brodowski et al., 2005). In addition to the quantitative estimation of charred material, the gained biomarker spectrum delivers additional information about the degree of BC condensation, giving hints on its composition within the large spectrum from amorphous charcoal to highly condensed soot (Brodowski et al., 2007). The enhanced abundance of aromatic compounds in BC rich soils was also confirmed by studies applying pyrolysis GC/MS (De la Rosa et al., 2008; Kaal and Rumpel, 2009).

Several biomarkers are also available for the identification of chemically stabilized moieties in SOM. Lignins are formed by terrestrial plants and received particular attention, e.g. with regard to rates of litter decomposition (Parton et al., 1987; Amelung et al., 1999; Otto and Simpson, 2006a). Quantitave and qualitative information on lignin in soils can be assessed by gas chromatographic analysis of lignin derived phenols which are soluble upon alkaline CuO oxidation (Hedges and Ertel, 1982; Kögel, 1986; Otto et al., 2005). Other bio-molecules that are released upon CuO oxidation comprise proteinaceous aromatic compounds and plant derived phenols such as tannins (Otto and Simpson, 2006b). Also for the identification of lignin in soils, measurement techniques combining pyrolysis and mass spectrometry have been applied (Schulten and Leinweber, 1993). While the identification of specific sources for n-alkanes is difficult (Lichtfouse et al., 1998), long chained n-alkane precursors like carboxylic acids can serve as useful indicators of plant derived SOC (Ninel et al., 1990). The ester-bound biopolymers cutin and suberin are biomarkers that allow for root-shoot-differentiation of SOC from non-woody plants (Bernards, 2002; Nierop and Verstraten, 2004). Other lipids that are utilized as specific biomarkers comprise cutan and suberan (Buurman et al., 2007) or triterpenoids (Otto

and Simoneit, 2001; Otto et al., 2005).

Fresh plant and animal litter usually comprises high amounts of easily degradable compounds and represents SOM of short turnover times. Plant derived carbohydrates constitute the main source of energy for microbial litter degradation, and are rapidly converted after they have entered the soil. Also microbial biomass and their metabolites contain significant amounts of carbohydrates. Non-cellulosic polysaccharides can, however, be removed prior to carbohydrate analyses, thus allowing to discriminate between plant derived carbohydrates and microbial metabolites (Amelung et al., 1996). On agricultural soils, easily degradable material may also enter the soil in form of animal feces by organic manuring. At this, cholesterol, 5β-stanole, and bile acids represent specific biomarkers for metabolic processes of higher mammals (Voet and Voet, 1995; Evershed et al., 1997). Finally, dead biomass of microbes and fungi contribute to SOM, while living biomass is assigned to the edaphon. Total amino-sugar concentrations in soils are used as a quantitative measure for the contribution of microbial necromass (Amelung and Zhang, 2001). Ratios of the individual amino-sugars have been used as indicators for the relative abundance of fungal and microbial communities (Liang et al., 2007a; Liang et al., 2007b). Due to the significant accumulation of amino-sugars in soils (Glaser et al., 2004), total amino-suger concentrations reflect a combination of historical and actual microbial communities. Also phospholipid fatty acids (PLFA) are primarily derived from microbial cell membranes, but in contrast to amino-sugars they are quickly decomposed after cell death, thus representing a measure for living microbial biomass (Zelles, 1999). Information on living fungal biomass can be derived by the use of Ergosterol (Ruzicka et al., 2000). The combination of methods determining total microbial necromass and living bacteria or fungi may thus provide valuable information on the turnover times of amino-sugars in soil and the significance for microbial communities in nutrient cycling (Liang et al., 2008).

While the use of biomarkers provides valuable qualitative information on specific compounds and their origin within SOM, they hardly reveal quantitative estimations on the composition of bulk SOM (Amelung et al., 2008). Such information is, however, mandatory for the elucidation of compositional SOC patterns that are relevant for spatial distributions of SOC turnover.

The application of nuclear magnetic resonance spectroscopy (NMR) in soil science (Wilson, 1987) opened up new possibilities for the chemical characterization of intact soil samples. As the intensity of an NMR signal is proportional to the concentration of the nuclei that generate the signal, the integration of assignable NMR peaks allows estimating bulk SOC composition (Kögel-Knabner, 2000). Statistically analysing published NMR data, Mahieu et al. (1999) found humus rich top-soils to be dominated by O-alkyl C (45 %), alkyl C (25 %), and a combined carboxyl and amide C fraction (10 %). Although specific pulse techniques like cross polarization magnetic angle spinning (CPMAS), bloch decay, or proton spin relaxation (PSRE) widened the applicability of NMR, e.g. to the detection of ^{13}C labelled molecules (Webster et al., 1997) or to differentiate between structures from SOC pools like decomposed plant litter and charcoal (Golchin et al., 1997; De la Rosa et al., 2008), NMR still predominantly yields data on abundances of functional groups while little information is given on the molecular composition. This drawback has been overcome by recent investigations which successfully integrated NMR spectroscopy and biomarker analysis (Simpson et al., 2008). However, also the combination of biomarker analysis and NMR spectroscopy does not facilitate a quantitative estimation of particular carbon stocks. Its use for the rapid screening of large numbers of samples is further restricted by its requirement of time- and cost-intensive sample preparation, and the need for sophisticated instrumentation and expertise.

During the last two decades, several methods using isotope ratio mass spectrometry (IRMS) have successfully been applied for the discrimination of the naturally occurring carbon isotopes in SOM (Amelung et al., 2008). Due to individual ratios of ^{12}C and ^{13}C isotopes in C3 and C4 plants (Smith and Epstein, 1971), man induced land use changes by cropping plants with either of these photosynthesis pathways allows to discriminate between recent and ancient plant residues in SOC turnover studies

(Schwartz et al., 1996; Kramer and Gleixner, 2006; Krull et al., 2007). Also information on the role of fresh plant litter for soil aggregation can be obtained by natural δ^{13}C labelling, as demonstrated by Bol et al. (2004). In a recent study, Bol et al. (2009) determined the molecular turnover time of naturally labelled SOC in physical soil fractions. Even the analysis of compound specific carbon isotope ratios can be facilitated (Amelung et al., 2008), e.g. by coupling of methods like gas chromatography (Quenea et al., 2006; Mendez-Millan et al., 2010), or thermal analysis systems as isolation step prior to isotopic determination (Lopez-Capel et al., 2005). The applicability of natural carbon isotope ratios for SOC turnover studies is, however, restricted to sites with a rigorous change between cropping of C3 and C4 plants and thus, as biomarker analysis and NMR spectroscopy, not suited for the elucidation of naturally evolved SOC patterns in agricultural ecosystems.

Microbially mediated processes and chemical aspects of SOM dynamics have been in the focus of most soil scientists until Christensen (1992) highlighted the potential of physical soil fractionations for the elucidation of SOM turnover. Scanning physical soil fractions, Baldock et al. (1992) revealed a consistent change in the chemistry of SOC with particle size. While the sand fraction was characterized by signals of carbohydrates, the chemical shift of the NMR spectra indicated a dominance of aromatic moieties for the silt fraction and alkyl-dominated structures for the clay fraction. Contents of O-alkyl C in fresh organic litter are usually high but decline during a first stage of decomposition. On the contrary, contributions of alkyl-C increase (Baldock et al., 1997; Kögel-Knabner, 2000; Kögel-Knabner, 2002), supposedly caused by selective preservation and in-situ synthesis (Baldock et al., 1992). Baldock and Skjemstad (2000) proposed that as O-alkyl C depletes, a second stage of SOC decomposition is initiated. Within this stage lignin is suspected to degrade, as indicated by a decline of aromatic structures in aging plant debris. Based on the concept that SOM associated to mineral particles of certain particle size fractions differs in structure and function, Christensen (1992) pointed out the potential of physical soil fractionations to deliver measurable SOM pools as desired for the initialization and validation of the emerging SOM turnover models.

2.2.3 Soil aggregation and turnover of soil organic matter

There is growing evidence that physical stabilization mechanisms of structural debris in varying stages of decomposition are essential factors governing carbon dynamics in soil (Gulde et al., 2008; Stewart et al., 2008). Owing to its specific occurrence as stabilized SOM in soil aggregates of varying size or density, this SOC pool is commonly referred to as particulate organic matter (POM) or light fraction (LF). As major parts of it are biochemically readily available for decomposition, its stability is crucially affected by soil aggregation and several attempts were made to describe its formation and turnover in soils. While early models of soil aggregation proposed a direct relationship between specific surface area of clay minerals and SOC storage in soil aggregates (Emerson, 1959) most contemporary concepts are based on the model suggested by Oades (1984). According to his concept, microbially colonized plant debris initially forms macroaggregates ($> 250\,\mu m$) as the coarse organic material is glued together with the mineral matrix by microbial carbohydrates and mucilage. In a second step, these macroaggregates burst into large microaggregates ($20–250\,\mu m$) which continuously liberate small microaggregates ($< 20\,\mu m$). Other concepts adopted the basic structure of the model by Oades (1984) but modifications were suggested with regard to site and point in time of microaggregate formation (Six et al., 2000). The importance of interactions between SOM and the mineral phase as suggested by Christensen (1996) is firmly established in the actual understanding of soil aggregation. In opposition to the concept of Oades (1984), Christensen (1996) assumed the primary structure of soils to be defined by its texture. The concept proposes the formation of "primary organo mineral complexes" by sorption of SOM on mineral particles. "Secondary organo-mineral complexes" are supposed to form upon aggregation of several primary organo-mineral particles. Applying transmission electron microscopy, Chenu and Plante (2006) found that many of $< 2\mu m$ "particles" actually consisted of microaggregates and challenged the concept of primary particles. In line with these results, also von Lützow et al. (2007) concluded that several binding mechanisms are involved in the stabilization of clay sized SOM gained by particle size fractionation and highlighted the potential of emerging fractionation techniques like high gradient magnetic separation for characterization of clay sized SOM. In arable soils, the dynamics of SOM turnover are, however, dominated by sand and silt sized

SOM (Gulde et al., 2008) as protection of SOM by organo-mineral interactions is limited and saturation may occur (Hassink et al., 1997; Six et al., 2002; Wiseman and Puttmann, 2005).

Changes between cultivated and uncultivated soils were observed to occur primarily in aggregated particulate organic matter, while fine-clay sized SOC was hardly affected (Golchin et al., 1995). Here, high concentrations of O-alkyl C in combination with relatively young δ^{13}C ages suggested that fine-clay associated SOC was dominated by microbial biomass, its metabolites and detritus. Also Christensen (1992; 1996) found that different land-use strategies may have only moderate consequences for the chemical composition of SOM attached to < 20 µm aggregates. While none of the available models can explain the aggregate hierarchies in all soils, consensus prevails that in soils where SOC represents the main binding agent for aggregation, SOC turnover decreases with decreasing aggregate size. Generally, macroaggregation promotes the greater storage potential and microaggregation promotes long term sequestration due to enhanced physical stability. Positive relationships between soil aggregation and bulk SOC contents are indicated by long term studies of Watts and Dexter (1997). Also Six et al. (2000) observed a concurrent loss of bulk SOC and degradation of soil structure. Recently, Gulde et al. (2008) showed that elevated manure application resulted in a hierarchical sequestration of additional C in coarse fractions with relatively short turnover time.

In soils where a limited number of key mechanisms control SOM stabilization, particle size fractionation thus provides a rough differentiation between active, intermediate, and passive SOM (von Lützow et al., 2007) and could also provide a basis for the recognition of spatial patterns in SOM dynamics.

2.2.4 The pool concept of soil organic matter turnover

Growing evidence that SOM comprises different moieties of specific structure and reactivity has led to the development of fractionation techniques aiming at isolation of biochemically meaningful pools (Cambardella and Elliott, 1992; Amelung and Zech, 1999) as demanded for initiation and validation of SOM turnover models. Despite varying implementations used by the different concepts, all modelling approaches conceptualize SOM into pools of varying turnover times. The most popular models are

the Roth-C (Jenkinson and Rayner, 1977; Jenkinson, 1990), and Century (Parton et al., 1987), but also models like APSIM (McCown et al., 1996), and others (e.g. Jenkinson and Rayner, 1977; Paul and Beauchamp, 1995; Paul et al., 1997; Falloon and Smith, 2000) proved to successfully predict SOM dynamics under specific conditions. Commonly, the models comprise one or two labile pools, two or three physically or chemically protected pools and one pool considered to be slow or even "inert" (Falloon and Smith, 2000). The analytical identification of these pools, however, has challenged researchers ever since because of intrinsic difficulties.

The Roth-C model can be used to calculate the C dynamics for specific crop rotations of agricultural soils as well as for the prediction of long term changes in carbon due to changing climate. Skjemstad et al. (2004) demonstrated for the first time, that this conceptual carbon turnover model (RothC. Ver. 26.3) can successfully be initialized by measured soil carbon pools. The group of Skjemstad measured total organic carbon (TOC), particulate organic carbon (POC), and a black carbon pool (BC). A forth, so called "humic" pool (HUM) was obtained as the residuum: HUM = TOC – POM – BC. The measured carbon pools were then used to initialize the Roth-C model for two long term rotation trials in Australia. At this, the measured fractions served as representatives for the original model pools of "resistant plant material" (POM), the "humic model pools" (HUM), and "inert organic matter" (BC) were in good agreement to modelled data for 18 years of cultivation. With regard to actual critical literature on the inertness of BC in terms of SOC turnover (Czimczik and Masiello, 2007) I will refer to BC as "passive soil organic matter" in the following.

2.2.5 Passive soil organic matter (black carbon)

One of the chemically most recalcitrant forms of organic carbon is black carbon (BC), a major aromatic residue from the incomplete combustion of biomass and fossil fuels (Goldberg, 1985; Schmidt and Noack, 2000; Flessa et al., 2008). Repeatedly, BC was taken to be equivalent to the "inert" C pool for initialization of RothC soil carbon turnover models (Skjemstad et al., 2004; Rethemeyer et al., 2007). Beside its potential to act as an important sink for atmospheric CO_2, BC may positively impact soil functions. It is suspected to be involved in the stabilization of humus (Schmidt et al., 1999), soil aggregation (Picollo et al., 1997; Brodowski et al., 2006) and may promote

soil fertility (Schutter and Fuhrmann, 1999; Linker et al., 2006; Czimczik and Masiello, 2007). Due to its hydrophobic nature, BC substantially contributes to the sorption of organic pollutants in soils and sediments (Lohmann et al., 2005; Bornemann et al., 2007) and heavy metals (Hiller and Brümmer, 1997). In general, BC is assumed to comprise 1–6 % of SOC (Gonzalez-Perez et al., 2004) but accumulation via aeolian and fluvial transport (Patterson et al., 1987) as well as wildfires and anthropogenic BC input can enrich the content significantly (Laskov et al., 2002; Brodowski et al., 2007; Czimczik and Masiello, 2007). Proportions of BC in SOC of German soils range between 15–45 % (Schmidt et al., 2002), but up to 60 % have been reported to prevail in Canadian Chernozems (Ponomarenko and Anderson, 2001). While there is consensus that selective chemical preservation of BC inputs can be an important factor regulating quantity and turnover of SOC (Flessa et al., 2008), the paradigm of being biochemically inert is increasingly challenged. Incubation experiments (Baldock and Smernik, 2002; Hockaday et al., 2005), field measurements of loss rates (Flessa et al., 2008), and its presence in the dissolved organic carbon (DOC) pool (Wengel et al., 2006), however, indicate the dynamic nature of BC as SOC constituent. Recently, Czimczik and Masiello (2007) proposed a multi factor model for the prediction of BC storage in soils. Besides amount and quality of BC inputs, their concept also considers physicochemical soil properties, microbial activity, as well as anthropogenic impact as relevant control parameters for BC stocks in soil.

The heterogeneity of BC makes its estimation in soils a challenging task. The various analytical methods available all capture only parts out of the continuum of BC materials (Hammes et al., 2007). While optical examination allows for qualitative characterization by means of morphology and particle size, quantitative information is limited: Applying light microscopy for BC analysis, particles on the submicron scale might not be detected. Further, areal observations as performed by electron microscopy will most likely not be representative for heterogeneous sample matrices (Karapanagioti et al., 2004). For thermal detection methods, the analysis is based on changes in transmission spectra of carbon during heating (Yang and Yu, 2002). As these techniques were originally implemented for the detection of soot and other atmospheric forms of BC, the applicability to samples from soils and sediments is

limited. Probably most widely applied are techniques employing either chemical (Skjemstad et al., 1993; Song et al., 2002) or chemo-thermal (Gustafsson et al., 2001) oxidation procedures in order to remove non-BC carbon, followed by elemental analysis or semi quantitative NMR. All these procedures are prone to intrinsic experimental uncertainty due to losses, artificial BC formation, or alteration of the molecular structure (Nguyen et al., 2004). Black carbon contents may thus be significantly over- or underestimated as also demonstrated by Hammes et al. (2007) who declared the need for a fast and universally applicable quantification method for BC in soils and sediments by employing a comprehensive inter-laboratory comparison. Estimation of BC content with the use of benzene polycarboxylic acids (BPCAs) at least satisfies one of the claimed needs: it is universally applicable as it is directly derived from the oxidation products of condensed aromatic structures (Glaser et al., 1998). Additionally, the degree of condensation and thus the nature of the charred material, can be derived from different BPCA patterns. However, also this method is laborious and time consuming.

2.2.6 Resistant plant material (particulate organic matter)

Resistant plant material (RPM) has been shown to be closely linked to soil aggregation (Wander, 2004) and has been used for the initialization of slow cycling SOC pools in conceptual SOC turnover models (Skjemstad et al., 2004; Zimmermann et al., 2007b). Further on, different sub-fractions of RPM represent differently stabilized SOC (Kölbl et al., 2005), and the determination of biochemically meaningful RPM pools is needed for understanding and monitoring of SOC turnover processes (Olk and Gregorich, 2006). The physical determination of RPM implies that the association of SOC with the mineral phase and their three-dimensional structure is representative for SOC dynamics. The physical properties applied for the characterisation of these structures are basically particle size and / or density. Ideally, the different methods are tailored to meet the specific objectives of the study and the properties of the analysed soils (Wander, 2004). Density fractionations aiming to gain the so called "light fraction" (LF) typically involve the use of sodium or potassium iodide, sodium polytungstate, or silica gel with common densities varying between 1.85 and 1.40 g cm^3. Usually, the density fractionation is performed after a preliminary soil dispersion employing

prolonged shaking with glass beads. Density fractionations are most suited for analyzing the effects of different agronomic treatments as they have been shown to be most sensitive to changes in management practice (Carter et al., 1998; 2003). To separate the most active fractions as well as mineral protected SOC, density fractionations have also been combined with a precursor size fractionation to gain particulate organic matter (POM) (e.g. Cambardella and Elliott, 1992; Baldock et al., 1997). The use of chemical density solutions, however, likely causes unintended artefacts which may constrain the validity of the gained results. Iodide solutions and silica gel alter the chemical characteristics of SOC and sodium polytungstate can hardly be completely removed from RPM. In direct comparison, the LF exhibits a darker colour than the POM as gained from single size fractionation. The observed phenomenon has been attributed to contaminations of the LF with humified moieties and microbial residues (Baldock et al., 1990; Kerek et al., 2002). Further limitations may be caused by high-surface-area materials like BC which have also been identified to represent unintended constituents of the LF (Kleineidam et al., 1999). The recognition of spatial patterns in SOC turnover models requires large numbers of samples for appropriate initialization and validation. Due to the excess workload and expenditure demanded by density fractionations their use is, however, inappropriate to gain such data sets. At this, also the generally more robust POM fractionations have been proven to effectively document changes in land use, tillage practices, crop rotations, and climatic effects (Amelung et al., 1997; 1999; Bowman et al., 1999). Generally, the POM comprehends major parts of the LF (Cambardella and Elliott, 1992), but the recovered amounts of C and N are higher, while the C:N ratio is lower (Gregorich et al., 1996). Particulate organic carbon typically comprises 10–20 % of bulk SOC (Angers et al., 1997). For size fractionation, the suspended soil is most commonly dispersed by ultrasonication but also chemical reagents like sodium hexametaphosphate are used. For sonication, optimum values for energy and sonication time depend on the type of sample and the desired size fraction (Amelung and Zech, 1999). Stepwise procedures with initial low energy dispersion for the macroaggregate-containing coarse fraction, and high energy dispersion for the microaggregate fraction have been shown to deliver biochemically more meaningful fractions (Kölbl et al., 2005). The mesh-size limits commonly used for POM

fractionations are owing to their origin in procedures which were designed for the investigation of mineralogical controls over SOC dynamics and correspond to classically employed grain sizes for texture analyses. Typically, the lower boarder of POM is defined at 53 μm with an additional subdivision at 250 μm and upper boarders reaching from 2000–8000 μm, dependent on the envisaged questions (Hassink et al., 1993). Content and composition of lignin are classical parameters for the identification and characterization of POM (Monreal et al., 1997). According to Skjemstad et al. (2004) the 53–2000 μm POM fraction can be used as a surrogate for the RothC pool of RPM. Amelung et al. (1999), however, found that the lignin signatures of the 20–50 μm fraction and the 50–250 μm fraction were statistically identical, thereby challenging the commonly used lower border of 53 μm for POM fractionation. However, all disputed size boundaries for POM fractionation (250 μm, 53 μm, and 20 μm) should be determined in order to elucidate effective control variables on POM turnover.

2.2.7 Humified organic fractions

Within the Roth-C model, the turnover time of the humified organic matter (HUM) is subjected to the clay content of the soil by an exponential equation (Jenkinson, 1990). The adjustment aims to meet the specific concerns of this SOC pool with very slow turnover, which is considered to be effectively protected by microaggregation. While the residence time of partly processed SOC like POM falls below one year, organic C that is protected by clay minerals may prevail undegraded for longer than a hundred years. The basic mechanisms of SOC sequestration by microaggregation involve adsorption of organic molecules by clay particles, polymerization of humic substances on clay surfaces, and incrustation of polymerized organic compounds by clay crystals (Laird et al., 2001). The chemical bindings which facilitate these close interactions are mainly anion-cation-anion bridgings which are promoted by polyvalent cations between the predominantly negatively charged organic matter and clay surfaces. But also H-bonding, van der Waals forces and Coulombic attractions are involved in microaggregation. The type and amount of SOC that is accumulated by microaggregation has been shown to be dependent on the particle size and the mineralogy of the inorganic phase (Wattel-Koekkoek et al., 2001). Special emphasis

has also been addressed to the role of pedogenic Al and Fe oxides (Kögel-Knabner et al., 2008). Monreal and Kodama (1997) even found that total SOC was negatively correlated to bulk clay contents while increasing amounts of extractable pedogenic Fe and Al oxides positively affected SOC storage. Recent results of Gulde et al. (2008) and Stewart et al. (2008) suggest that in agricultural environments, hierarchical saturation processes have considerable impact on the storage of SOC in small sized mineral associated fractions. The relevance of saturation processes for the determination of spatial distributions of SOC varying SOC pools, however, demands further clarification.

2.2.8 Readily decomposable organic carbon

Although water soluble soil carbon represents only a small proportion of total SOC, its influence on biological and ecological soil functions is well recognized (Chantigny, 2003). This fraction with very fast turnover time is commonly defined as dissolved organic carbon (DOC) or water extractable organic carbon (WEOC). As the soil solution tends to equilibrate with the solid phase, both fractions largely represent the chemical composition of bulk SOC (Zsolnay, 2003) but spatiotemporal patterns of DOC and WEOC are controlled by numerous biotic and abiotic factors (Kalbitz et al., 2000). While they may be included in model pools of fast turnover times like the "decomposable plant material" (DPM) of the Roth-C model (Jenkinson, 1990; Zimmermann et al., 2007 b), results of Skjemstad et al. (2004) and Zimmermann et al. (2007 b) confirm its role for modelling of SOC turnover to be inferior. The negligible contribution of the WEOC to total SOC storage in soil (Chantigny, 2003), its short time fluctuations, and the manifold interactions with the solid matrix further constrain its implementation as individually estimated model pool (Kalbitz et al., 2000). I thus precluded DOC and WEOC from further considerations in the context of this work.

2.2.9 Conclusion

The results of Skjemstad et al. (2004) indicate that the essential mechanisms of perennial SOC dynamics are represented by SOC fractions that are accessible by determining BC, POM, and bulk SOC. The methods that are currently applied to determine BC and POM are either not quantitative or too laborious to be applied for routine analysis. The feasibility for fast screenings by economic measurement techniques like MIRS would provide the basis for recognition of their spatial patterns. The opportunity for simultaneous assessment of mineral soil constituents using MIRS further provides the basis for the determination of effective control parameters regulating SOC dynamics on the field scale.

2.3 Mid-infrared spectroscopy

2.3.1 Physical principles

At the beginning of the 18th century the German Astronomer Sir William Herschel discovered that invisible radiation beyond the red area of a light spectrum exhibited a higher heating potential than the visible light and named this spectral range "infrared" (IR). Further exploration of the IR range was hampered by the limited abilities for its detection and thus, the first fully automated instrument was not constructed before 1937. From there, the spectroscopic instruments were continuously improved and the accessible spectral ranges successively broadened. Especially the advent of the Fourier transform (FT) technique in the 1960s opened up new dimensions of spectral bandwidth (Jones, 1985).

As any other electromagnetic radiation, infrared light is characterized by its wavelength λ. The principle of infrared spectroscopy constitutes the interaction of infrared light and matter, that is molecules. As wavelength is, however, not a unit comprised by molecules, in spectroscopy the wavelength is classically translated into frequency values. Given that the IR radiation can spread with the velocity of light c, the frequency v is directly proportional to λ,

$$i)\ v = c * \lambda.$$

According to Planck's law, the energy E of electromagnetic radiation is proportional to its frequency v,

$$ii)\ E = h * v$$

where h is the Plack-constant (h = $6.26*10^{-34}$Js). In spectroscopy, v is typically further translated into "wavenumbers" to avoid inconveniently large numbers. The wavenumber is a measure for the amount of waves in a wavetrain of 1 cm length and its unit correspondingly is cm^{-1}. Ranging from $7.8*10^{-5}$ to $2.5*10^{-4}$ cm, the near infrared region (NIR) represents the shortest wavelength of the IR range. The mid-infrared region (MIR) follows up to $5*10^{-3}$ cm and at $1*10^{-1}$ cm, the far infrared region (FIR) reaches the maximum wavelength within the IR range. Electromagnetic waves with shorter wavelength comprise visible and ultraviolet radiation, longer wavelengths represent microwaves. Figure I.1 summarizes frequency v, wavelength λ,

wavenumber w, and corresponding energy E of electromagnetic radiation.

Whenever electromagnetic radiation impacts matter, it is either reflected, transmitted, absorbed, or transformed to fluorescence. Among these effects, the functionality of IR spectroscopy is based on the fact that the vibrational or rotational energy of a molecule gets enhanced upon absorbtion of IR radiation. At this, only molecules that express a change of dipole moment, that is where the center of charge is shifted during vibration, are IR active. The intensity of an absorbtion band is thereby proportional to the power of two of the change in dipole moment. Symmetric diatomic molecules like H_2 and O_2 are IR inactive but they are detectable by Raman spectroscopy. The frequency of vibration is dependent on the properties of the binding: it increases the smaller the mass of the involved molecules and the higher the strength of the bonding is. The term absorption is defined as the uptake of photon energy under increase of vibrational energy. According to the laws of quantum physics, a continuous energy uptake is invalid and a molecule is thus only able to oscillate on certain energy levels. Consequently, only radiation with a defined frequency, that is certain energy (see ii), can be absorbed by a molecule, thereby achieving a higher mode of vibration. Thus, I find characteristic energy levels for different bondings of which the first level is referred to as the basic tone and the following levels are referred to as the overtones of vibration. On the basis of the presented principles, each molecule expresses characteristic combinations of vibrational frequencies. Commonly, the basic vibrations are found in the MIR range, while the overtones are ranging among the NIR range. For detailed information on the principles of IR spectroscopy the reader might be referred to specialized textbooks (e.g. Colthup et al., 1990; Guenzler and Gremlich, 2002).

Raman spectroscopy is often linked to IR spectroscopy and I would like to briefly describe its basic principles for clarity. In contrast to IR spectroscopy, where the frequencies of molecule and photon are matching and the molecule is steadily shifted to a higher level of vibration, the Raman-effect represents an inelastic stroke of a photon with significantly higher frequency.
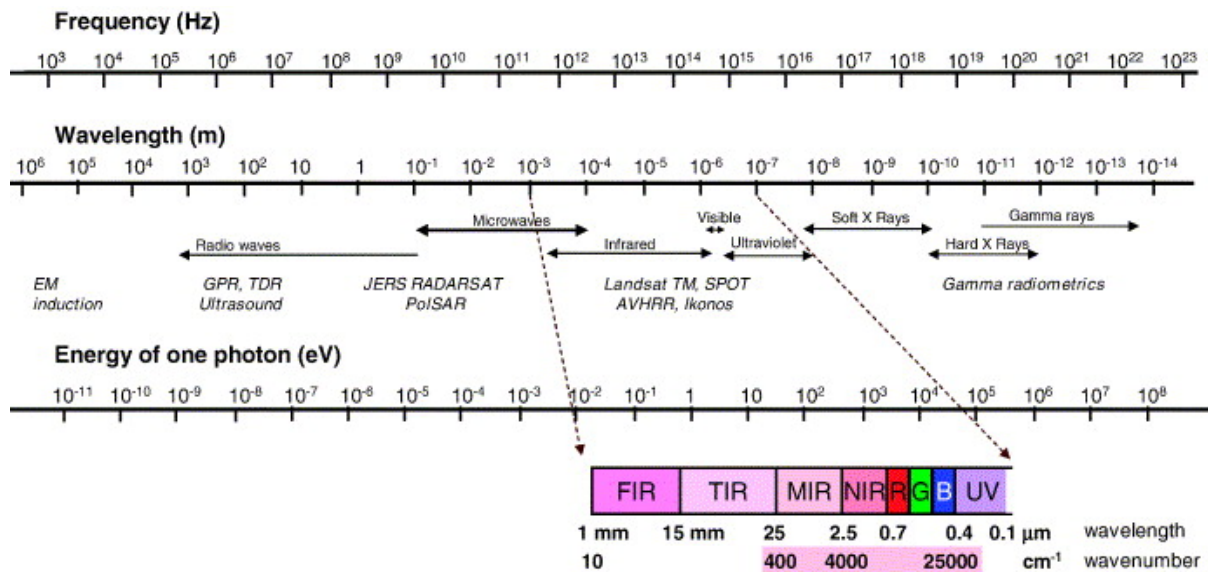
Fig. I.1 Frequency v, wavelength λ, wavenumber w, and corresponding energy E of electromagnetic radiation (modified after McBratney et al., 2003).

The photon looses only a part of its energy upon the impact and the molecule is temporarily shifted to a higher energy level. When the molecule falls back to the initial vibrational level, the previously immited energy is emitted by a secondary photon which comprises lower energy and is detectable as Raman radiation. Infrared spectroscopy and Raman spectroscopy are thus not competitive but rather complementary to each other as either technique is able to detect bondings which are undetectable by the other technique.

2.3.2 Infrared spectroscopy in soil science

Traditional lab analysis of solid soil properties and especially different C pools is very time consuming and destructive. These approaches are thus not suitable to understand spatio-temporal patterns of solid soil properties. Spectroscopic techniques like remote sensing and short-range reconnaissance are used instead to detect soil heterogeneity at the field scale. Satellite data, however, suffer from inadequate spatial and temporal resolution (McBratney et al., 2003). New satellites like RAPID EYE and Terra SAR-X will provide a better insight into small-scale variability of soil moisture and humus content (McNairn and Brisco, 2004). Still, remote sensing will not be sensitive enough for a detailed soil characterisation. Geoelectric and other ground based techniques employ radiowaves in the range of 1 to $1*10^6$ m. They are field tested and further progress can be expected from a refined data evaluation (Mertens et al., 2008; Pätzold

et al., 2008). Still, these methods are largely restricted to identify only textural differences among or within soils as they are based on a single signal which is influenced by multiple soil factors (Hedley et al., 2004).

NIR and MIR spectroscopy (NIRS, MIRS) are efficient in characterizing a large number of soil variables without elaborate sample preparation in a short time. For NIRS, online measurements in the field are available, at least up to 1800 nm; for MIRS, this opportunity is about to come during the next decade. Although the potential of NIRS for classification of soil organic matter has early been recognized (Ludwig and Khanna, 1998) and recently gained further support (Terhoeven-Urselmans et al., 2006), there is increasing evidence that MIRS is superior to NIRS in soil analysis regarding accuracy and the range of accessible parameters (Viscarra-Rossel et al., 2006). In soil science, the use of MIRS has been limited until multivariate statistical procedures (chemometrics) were established in the late 1980s (Martens and Naes, 1989). While the first attempts concentrated on the characterization of isolated humic substances (Geyer et al., 1997), Janik and Skjemstad (1995) were able to show that organic and inorganic soil properties can be predicted. Infrared-spectroscopic techniques provide chemical information without any alteration or chemical pre treatment of the sample. Errors due to mishandling or diverse sample characteristics during the sample preparation are thus avoided (Janik et al., 1998). Lab based MIRS has already been applied to characterize the composition of bulk soil organic matter (e.g., Reeves et al., 2001; Leifeld, 2006). For highly weathered Australian soils, Janik et al. (1998) proved that cation exchange capacity, texture and moisture content can be derived from MIR spectra. Later work reinforced these results and denoted the suitability for further soil components (e.g. Groeningen et al., 2003). McCarty et al. (2002) were able to gain substantial information on the content of organic and inorganic C in a set of soil samples representing most of the variability in North American soils and stated that "Development of instrumentation specific for soil analysis holds promise for rapid and automated means of C measurement." However, since only the total organic carbon was determined, the feasibility for an estimation of different carbon pools remained unclear. Also in a study by Mimmo et al. (2002), total organic C and N, as well as biological activity (reflected by three enzymes) were

successfully detected by MIRS. For dairy manures, MIRS allowed for the rapid estimation of the N mineralization potential (Reeves and Van Kessel, 2002; Boonmung and Riley, 2003). Recently, Zimmermann et al. (2007a) successfully determined SOC fractions with varying recalcitrance for a highly heterogeneous sample set of soils from Switzerland. Also Ludwig et al. (2008) and Reeves et al. (2006) were able to calibrate specific SOC pools by using highly heterogeneous sample sets. The identification of underlying spectral signatures for the apparently successful calibrations, however, remains unresolved. Furthermore, calibrations from such copious calibration models render their use for the exploration of spatiotemporal patterns on the field scale to a minimum as they are rather fitted for the discrimination of distinctive samples than for the quantification of sensible variations of soil properties.

The highly condensed aromatic structures of BC are characteristic and give rise to the feasibility of spectroscopic identification and quantification of BC in soils. Size fractions of physically isolated POM represent moieties of SOC whose chemistry and functional groups are determined by distinct stages of litter decomposition. I am thus confident that the determination of field scale heterogeneity of BC and POM is feasible by taking advantage of local calibrations and adapted sample sets (Linker et al., 2006). Further progress can be expected by improved spectrometer hardware, selective use of spectral ranges, tailored spectral pre-processing, and more effective mathematical routines (Viscarra-Rossel, 2007).

2.4 Sampling sites

To account for spatial heterogeneity in SOC turnover modelling we have to assess the spatial patterns of SOC fractions that are indicative for sustainable changes in SOC composition by fractionations that are suitable for initiation and validation of available turnover models. The test site that was chosen for this investigation features a smooth transition from a silt-rich to a sand-rich texture with moderate heterogeneity of soil clay contents. Correspondingly, significant differences across the test site can also be expected concerning size and stability of soil aggregates. Besides the physical properties of the mineral soil constituents, amount and quality of plant litter is the dominating factor regulating SOC dynamics in agricultural soils. The amount of plant litter that is incorporated into a certain volume of fine earth is, however, not only dependent on the productivity per area, but also on the fine earth content of the soil. On the investigated test site, the changes in mineralogy are accompanied by a drastic increase of the stone content in the sand rich areas (see also section V). As the test site has been under intensive agricultural management during the last decades, the relative litter input to amount of fine soil at identical litter quality can thus be expected to be significantly higher where amounts of fine earth are reduced. Hence, the investigated site is highly promising for detecting spatial patterns of different SOC pools and to derive further information on the role of hierarchical pool saturation for SOC dynamics in agricultural soils (Gulde et al., 2008; Stewart et al., 2008).

3 OBJECTIVES

The specific environmental conditions adjacent to potentially mineralizable organic matter control the organic carbon dynamics in soil. This study aims at determining effective parameters controlling soil organic carbon turnover at the field scale and their acquisition by mid-infrared spectroscopy (MIRS). Special emphasis is given to the ability of MIRS for the detection of i) the passive or "inert" SOC pool, represented by black carbon, and ii) the "resistant plant material" or slow pool as represented by particulate organic matter. Spatial patterns of the individual SOC pools will then be determined on the field scale and related to pedological, hydrological, and geographical control parameters.

I placed the main emphasis on the following questions

i. **Does MIRS-PLSR provide opportunity for rapid assessment and characterization of BC in the soil environment?**

I tested the ability of MIRS-PLSR for the prediction of the amounts and the composition of BC, as determined by a molecular marker method, on a sample set comprising soil samples from all over the world. Further on, I validated the MIRS based BC characterization by use of individual samples of charred organic matter representing different stages of combustion.

ii. **Is MIRS-PLSR suitable for the determination of POM and its spatial patterns on the field scale?**

I envisaged the determination of POM in three size classes by using regionalized sample sets for MIRS-PLSR predictions. Individual patterns of field-scale variation were identified by correlation analysis and fuzzy-kappa pattern recognition.

iii. **Is hierarchical saturation a relevant factor for field scale patterns of SOC storage in differently stabilized SOC pools?**

I employed a comprehensive data set containing stone content, texture, pedogenic Fe-oxides, elevation, erosive translocation, and soil moisture to determine the relevance of hierarchical saturation for the spatial distribution of SOC, BC, POM in three size classes, and nonPOM on a highly heterogeneous test site.

This PhD-thesis is part of the Transregional Collaborative Research Centre 32 "Patterns in Soil-Vegetation-Atmosphere Systems: Monitoring, modelling and data assimilation", which focuses on processes related to heat, energy, water and CO_2 fluxes in soil-vegetation-atmosphere systems on different spatial and temporal scales.

II

Material and methods

1 SITES

1.1 Main study site

The study site is a key-test site of the "Collaborative Research Center 32" of the German Research Foundation (DFG). This research association aims at understanding the spatio-temporal patterns of water and CO_2 fluxes between soil and atmosphere on different scales. The test site is located in Selhausen (50°52′09.34′′N; 6°27′00.58′′E) and is part of the Lower Rhine Embayment in Germany. The underlying sediments are fluvial deposits from the Rhine/Meuse River and the Rur River system, which were covered by aeolian sediments during the Pleistocene. The test site is weakly inclined (<4°) over ~180 m in east-west direction. Whereas in the lower part the texture represents a silt loam (WRB, 2007) and the stoniness is less than 3 %, in the upper part sand contents increase by ~20 % at the expense of silt and the texture represents a loam. Simultaneously the stoniness increases to at most 57 % of weight. The soil types cover a broad range from Dystric Leptosol in the upper part, Orthic Luvisol in the middle part, up to a Stagnic Luvisol in the lower part of the test site (WRB, 2007). Mean annual temperature and precipitation are 9.8 °C and 694 mm, respectively (means between 1961 and 2003). Quintuple drilling cores were taken in a ten times ten meter raster (one transect in a five times ten meter raster due to the dimensions of the field plot) from 0–30 cm depth. Two samples within the plot were obviously anthropogenically disturbed and thus removed from the set. In the north-eastern corner sampling was precluded by a mobile building. The resulting 129 surface soil samples were stored in sealed plastic bags, and immediately deep-frozen at -18 °C. Subsequently, samples were dried at 60 °C and sieved to grain sizes < 2 mm.

1.2 Mollisol samples

The majority (231) of the 309 soil samples discussed in section III stem from horizons of whole soil profiles taken for a study investigating soil sequences in the "typical Mollisol areas of the world" (Tab. II.1, sample set 1). According to soil taxonomy, these are basically the central plains of Russia, the Great Plains of the U.S.A., the Pampas regions of Argentina, the Manchurian plains of China, and the loess region of Germany near Halle. The samples were collected between October 1991 and June 2000.

An additional set of mollisols consists of 26 topsoils (0–25 cm) and 40 samples from the horizons of whole soil profiles, collected at three experimental field trial stations in Germany between 1958 and 2002 (Tab. II.1). While the site in Rotthalmünster is assumed not to be significantly influenced by anthropogenic BC input, especially the sites at Halle and eventually also the sites at Bad Lauchstädt have been subjected to considerable anthropogenic BC input, caused by heavy industry, steam engines, and above ground mining activity. Details of locations, sampling techniques, and soil parameters are given in Brodowski et al. (2007). Additionally, Iemployed eight topsoil samples (0–30 cm) and two times two subsoil samples (30–60 cm and 60–90 cm) of the main study site in Selhausen (Tab. II.1, Set 3). All samples were air-dried, passed through a 2 mm sieve and milled thoroughly with mortar and pestle.

1.3 Supplementary loess soils

Thirty topsoil samples (0–30 cm) of a field site in Sintsteden (51°2´55,47´´N; 6°38´37,13´´E), with similar geological and pedological situation as in Selhausen were supplemented in order to broaden the range of the investigated soil characteristics for MIRS calibrations as discussed in section IV. Detailed information on the sample set is given by (Pätzold et al., 2008).

Tab. II.1 Sites and soils employed for the BC predictions in section III.

	Country	MAT [°C]	MAP [mm]	arable [n]	steppe [n]	forest [n]	soil types (FAO)
	Argentina	13.8–15.6	582–844	48	12		Chernozem, Kastanozem, Phaeozem
	China	4.2–4.9	378–423	61			Chernozem, Kastanozem, Phaeozem
Set 1	Germany	8.8	479	27			Chernozem
	Russia	4.1–7	300–715	18	20	14	Chernozem, Greyzem, Kastanozem, Phaeozem
	USA	6.5–23.4	274–839		31		Calcisol, Cambisol, Chernozem, Kastanozem, Phaeozem
Set 2	Germany	8.2–8.8	479–890	66			Chernozem, Luvisol, Phaeozem
Set 3	Germany	9.8	694	12			Luvisol

2 SPECIFIC SOIL ANALYSIS

2.1 Texture

Texture of the fine earth (< 2 mm) was determined by a combination of wet sieving (sand fractions) and sedimentation (silt and clay fraction) after Köhn (ISO 11277, 2002). At the main test site, about 15 l soil of each sampling point were additionally sampled and dry sieved to determine the proportion of the coarse texture (> 2 mm). The exact bulk density of the soil was determined for five samples of two transects (n = 10) which were also employed for ^{137}Cs measurements. For this, cores of 25 cm diameter were drilled into the undisturbed soil to obtain soil samples of known volume. After air drying, samples were sieved to 2 mm and exact bulk density was determined for the coarse texture (> 2 mm) as well as for the fine earth (≤ 2 mm). The fine texture of soils may also be determined from infrared spectra as reviewed by Viscarra-Rossel et al. (2006). Recently, Pätzold et al. (2008) were able to successfully calibrate a model for the prediction of clay and silt contents employing a sample set comprising the soils of the investigated test site.

2.2 Total organic carbon, total nitrogen

The C and N contents of the sieved and milled soils was determined by elemental analysis (ISO 10694, 1995; ISO 13878, 1998).

2.3 Particulate organic matter (POM)

Fractionation of POM was conducted by ultrasonic dispersion according to Amelung and Zech (1999). Briefly, samples were gently sonicated (60 J ml^{-1}) so that microaggregates were preserved from disruption (Kölbl et al., 2005). The coarse fraction (POM1: 2000–250 µm) was separated by wet sieving, and the filtered remnant was sonicated a second time at 240 J ml^{-1}. Intermediate (POM2: 250–53 µm) and fine (POM3: 53–20 µm) material was also gained by wet sieving and all fractions were dried at 40 °C prior to elemental analysis. Sieving was supported by gentle agitating using small rubber paddles.

2.4 Black carbon (BC)

BC content was determined using the BPCA method (Brodowski et al., 2005b). In brief, about 500 mg of soil were digested using trifluoroacetic acid to remove metal cations and BC was oxidised to benzene carboxylic acids with sulfuric acid in a high pressure

digestion unit. After cleanup using a cation-exchange resin, BPCAs were derivatized to trimethylsilyl derivatives and analyzed using gas chromatography (GC) with a flame ionization detector (FID).

2.5 Lignin

For lignin analysis, about 100 mg sieved and milled soil was oxidized with alkaline cupric oxide at 170 °C for 2 h. The monomers of lignin-derived phenols gained by oxidation were isolated by centrifugation of the suspension and humic acids were precipitated. The lignin derived phenols in solution were then isolated on C18 columns, extracted with ethyl-acetate, and analyzed by capillary gas chromatography and flame ionization detection (Hedges and Ertel, 1982; Amelung et al., 1997). The sum of the vanilyl-, syringyl-, and cinamyl-biomarkers (so called VSC-lignin) are a measure for total lignin in soil. True lignin contents cannot be assessed in soil using wet chemical procedures, for intact lignin is insoluble (Hedges and Ertel, 1982).

2.6 Pedogenic oxides

Amounts of pedogenic Fe and Al oxides were determined by the dithionite-citrate-bi-carbonate (DCB) method as proposed by Mehra and Jackson (1960). On the investigated test site in Selhausen, DCB-soluble Al oxides continuously accounted for about 10 % of total pedogenic oxides, while Fe oxides dominated. Therefore, I considered only the DCB-soluble Fe oxides (Fe-Dith) in the context of this investigation.

2.7 Volumetric water content

The volumetric water content on the main test site was determined by time domain reflectrometry (Weihermüller et al., 2007). In order to obtain the water content of the fine earth, volumetric water content of the bulk soil was corrected by the stone content. The initial measurement was conducted at almost saturated conditions and compared with a repeated measurement after a dry period of 31 days (18th of May to 19th of June). The difference between both measurements ($\delta\theta$) was used to estimate patterns of varying soil moisture.

2.8 Soil erosion

To estimate the translocation of material by erosion or tillage I measured the activity of ^{137}Cs in topsoil samples. An aliquot of 50 g soil material with known bulk density (see II.2.1) was dried and the ^{137}Cs activity was subsequently determined by γ-spectrometry (Schuller et al., 2007). The activity of the aliquot was then transferred to the activity of the sampling volume by correcting for stone content and bulk density.

3. MID-INFRARED SPECTROSCOPY

3.1 Spectroscopic measurement

About 20 mg sample were transferred to microplates and compacted with a plunger to leave a plain and dense surface for spectroscopic measurement of the diffuse reflectance. Spectra were recorded using a Bruker Tensor 27 equipped with an automated high throughput device (Bruker HTS-XT). This extension for automated spectroscopic measurement is equipped with a liquid N_2-cooled mercury-cadmium-telluride (MCT) detector. Employing a broadband KBr beam splitter, spectra from 8000 to 600 cm^{-1} (1250–16700 nm), with a resolution of 4 cm^{-1}, were recorded in a single run. Five composite measurements, each comprising 120 scans, were conducted for each sample in order to minimize errors in spectroscopic measurement.

3.2 Data treatment and statistical analysis

The quality of the five repeat analyses, which were automatically corrected for water vapour and atmospheric CO_2, was verified by calculating root mean square (RMS) values. The RMS calculates the difference between a single spectrum and the average spectrum of all repeat analyses (Terhoeven-Urselmans et al., 2006). Spectroscopic measurement was repeated for samples exceeding RMS values of 0.00025.

PLSR quantification was performed using OPUS QUANT software (© BRUKER, 2006). Utilizing the PLS 1 algorithm (Martens and Naes, 1989), the software decomposes the data plotted in the spectral matrix X and the ground-truth matrix Y into latent variables (loadings), thereby maximising the covariance between spectral information and laboratory data. As forced by the algorithm, the first latent variable will exhibit the greatest predictive power. The following latent variables, always orthogonal to each other, will explain successively smaller parts until no further improvement is achieved. The rank of a prediction model nominates the number of latent variables needed to describe its spectral variability. Their corresponding multipliers (scores) represent the factors that would have to be applied in order to reconstruct a particular original spectrum from the loading weights of the PLSR model. Linking the spectral information for all samples in the data set to the sample property of interest, the first latent variable can also be interpreted as a first order approximation of the spectrum of the pure component

(Janik et al., 1998). Also, the plots showing the regression coefficients of the final calibration model at particular wave numbers may display chemical information. The regression coefficients highlight the most important spectral regions for the prediction of the analyte, even though riddled with disturbing effects such as interfering compounds and baseline deviations (Haaland and Thomas, 1988b). Further advantages of PLSR over classical univariate techniques are the significant compression of information, the ability to handle collinear data sets and some types of non linearity, as well as the discrimination between relevant spectral information and systematic error in measurement or spectral noise (Haaland and Thomas, 1988a). The latter becomes evident for consideration of changes in spectral information relating to varying analyte concentration. Accordingly, the algorithm employs identical scores for the respective latent variables in both spectral and laboratory data sets. As the scores are generated to fit the original laboratory data and the data estimated from the model in an optimum way, PLSR finds a compromise in describing the spectral variation and the correlation of the data sets. This is especially an advantage when laboratory methods are prone to appreciable measurement errors. In such cases, values calculated from PLSR calibrations may indeed be more accurate than the laboratory derived data used for the calibrations.

Information on the applied spectral ranges, data-treatment, validation techniques and statistical quality for the individual predicted parameters is given in sections III, IV, and V, respectively.

III

Rapid assessment of black carbon in soil organic matter using mid-infrared spectroscopy

Modified on the basis of

1 INTRODUCTION

To mitigate global warming, it is necessary that soils enduringly sequester soil organic carbon (SOC). One of the most chemical recalcitrant forms of SOC is black carbon (BC), a major aromatic residue from the incomplete combustion of biomass and fossil fuels (Goldberg, 1985; Schmidt and Noack, 2000; Flessa et al., 2008). The objective of this work was to test MIRS as a potential rapid method for SOC and BC quantification from soils from all over the world, using the BPCA method for calibration purposes. As the latter method affords mellitic acid C only for highly condensed BC material, my final objective was to investigate whether spectral properties might even provide information on BC quality.

2 MATERIAL AND METHODS

2.1 Soils

The quality of multivariate calibration procedures in spectroscopy is enhanced by investigating large numbers of samples. I utilized soils from three different studies where BPCA measurements had been conducted (see sections II.1.1; II.1.2). Even though partly comprehending samples from the same experimental field-trial stations, I did not merge the discrete sample sets for means of better identification of possible systematic measurement errors.

2.2 Ground truth measurement (see section II.2)

2.3 Spectroscopic measurement (see section II.3)

2.4 Data treatment and statistical analysis

Basic information on data treatments and statistical analysis of spectral data is given in sections II.3.2. The applied OPUS QUANT software supplies a routine that will automatically test combinations of varying spectral ranges and data treatment for the optimum prediction power of the model. The suggested model parameters for the applied sample sets were checked for plausibility and further optimized manually (Tab. III.1). For each sample set I conducted calibration procedures employing a leave-one-out full-cross validation (Efron, 2004). Samples that obviously did not fit the prediction model or exceeded the properly described range were treated as mavericks and removed from the

sample sets. After removal, the full-cross validation was repeated. The stability of the prediction models was verified by reciprocal test-set validation, with a desired ratio of calibration and validation samples of 50 %. For smaller sample sets, where bisection for test-set validation did not result in satisfactory results, the validation subsets were reduced to 30 % of the sample population.

Apart from the coefficient of determination (R^2) between measured and predicted values, the predictive power of the spectroscopic measurement was also described by other statistical parameters. The quality of the models was estimated by calculating the root mean square error of cross validation (RMSECV) and the root mean square error of prediction (RMSEP) for cross validation and test-set validation procedures, respectively (Geladi and Kowalski, 1986). Further on, I calculated the ratio of performance to deviation (RPD) and the modelling efficiency (EF) as dimensionless quality parameters. The RPD represents the quotient of standard deviation of the reference data and standard error of the calibration procedures, the EF is calculated as the relative deviation of the predicted data compared to the variation of the lab data (Loague and Green, 1991). The higher the RPD value, the better the predictive power of the calibration model; the EF should be as close to one as possible.

Tab. III.1 Data treatent and spectral ranges used in prediction models

Treatment	Data processing	Spectral range [cm^{-1}]
1	1st derivative and multiplicative scatter correction	5380 – 4944 4798 – 1238
2	1st derivative and multiplicative scatter correction	4719 – 1938 1246 – 550
3	1st derivative and multiplicative scatter correction	3658 – 2592 2299 – 1957 1620 – 1278
4	1st derivative and subtraction of a straight line	4719 – 3329 2634 – 1849 1751 – 550
5	2nd derivative	5415 – 3329 1940 – 550
6	vector standardisation	2634 – 550

3 RESULTS AND DISCUSSION

3.1 Prediction of soil organic carbon content

Compared with other studies predicting OC content of soils as reviewed by Viscarra-Rossel et al. (2005) the SOC predictions employing the whole sample set already indicated reliable predictions (Tab. III.2, model 1–3). The removal of six humus-rich samples from model 1, (Tab. III.2; Fig. II.1a) even resulted in further improvement of the RPD (4.75) while the EF stagnated (data not shown). For near infrared analysis of agricultural products, Williams and Sobering (1993) found RPD values between three and five to be satisfactory. Chang et al. (2001) even reported that RPD values > 2 might be sufficient for the prediction of various soil properties, provided that regression slopes were not significantly different from 1, and R² values exceeded 0.80. I assume, therefore, that model 1 predicted the SOC accurately in most cases.

Tab. III.2 Model parameters and statistical indices for prediction of SOC, BC in SOC, and contribution of mellitic acid-C within the marker spectrum

Fraction	Calibration-set	Model	Treatment[a]	Concentration range	Spectra (n)	Mavericks (n)	R²	RMSECV[b]	RPD[c]	EF[d]	Slope	LV[e]
SOC [g kg⁻¹ soil]	complete	1	1	0.8 – 80.1	1545	–	0.95	2.46	4.45	0.95	0.96	12
	steppe	2	2	1.6 – 45.4	298	17	0.97	2.01	5.8	0.97	0.97	11
	Germany arable (Tab. 1: set 2+3)	3	3	0.8 – 25.0	380	10	0.99	0.70	10.1	0.99	0.99	8
BC [g BPCA–C kg⁻¹ SOC]	complete	4	4	6.17 – 114.2	1270	30	0.63	13.80	1.64	0.63	0.68	10
	arable	5	5	6.17 – 114.2	900	4	0.70	12.20	1.83	0.70	0.73	11
	Argentina arable	6	4	6.17 – 64.43	170	10	0.81	6.08	2.31	0.81	0.85	6
Mellitic acid–C [% of total BPCA–C]	complete	7	6	10.6 – 54.6	1265	34	0.58	5.77	1.55	0.58	0.62	12
	arable	8	6	10.6 – 54.6	910	20	0.63	5.72	1.64	0.63	0.67	10
	Argentina arable	9	6	6.2 – 64.4	160	10	0.76	3.20	2.05	0.76	0.86	10

[a] Mode of data treatment used in the prediction models (see Tab. III.1); [b] root mean square error of cross validation; [c] ratio of performance to deviation; [d] modelling efficiency; [e] number of latent variables used for prediction.
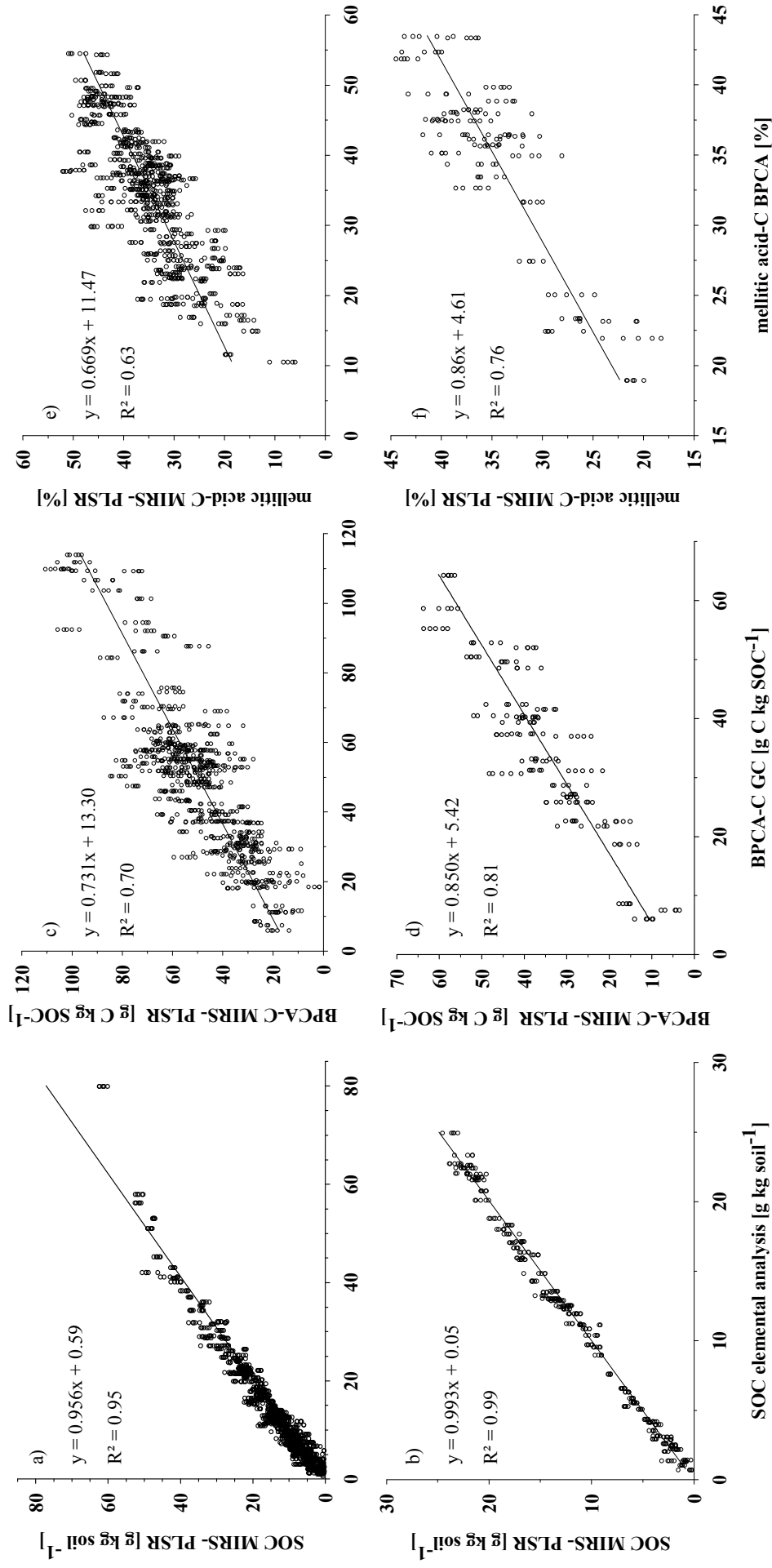
Fig. III.1 Prediction of soil organic carbon (SOC; a+b), BC content in SOC (c+d), and mellitic acid C (% of BPCA C) content (e+f) from mid-infrared spectroscopy and partial least squares regression (MIRS-PLSR) compared with the SOC content determined from elemental analysis, and BC content as well as mellitic acid-C determined using the benzene polycarboxylic acids (BPCA) method. Predictions from five individual spectroscopic measurements are plotted per sample. a) model 1; b) model 3; c) model 5; d) model 6; e) model 8; f) model 9. (Note that not all samples were analyzed for BC with the BPCA method due to low BC content).

Reducing the heterogeneity among the soil samples usually enhances the predictive power of PLSR models (Linker et al., 2006). I partitioned the samples into subsets according to varying land use, as it substantially affects SOC (Blanco-Canqui and Lal, 2004). Only for the steppe soils, the predictions improved clearly (Tab. III.2, model 2) after separation.

For further evaluation of possible structures within the applied data set, I conducted principal component analysis (PCA) of the spectral data. In contrast to PLSR, PCA decomposes the spectral matrix X into scores and loadings without consideration of the laboratory data. This way, the spectral information is condensed and can be utilized to visualize variability among the sample set. Distinct differences were revealed by plotting the first two PCA scores (Fig. III.2). Especially the soils from Argentina (turquoise) and from Germany (green) are clearly separated by the PCA scores. For the soils from China (magenta), the USA (blue), and Russia (red) the differentiation was not as unambiguous but certain clusters could be identified. Hence, I separated the sample sets with respect to their regional provenance for further calibrations. For all arable soils, the prediction of SOC content from MIRS improved considerably. After separation, each model reached RMSECV values of at least 1.33.
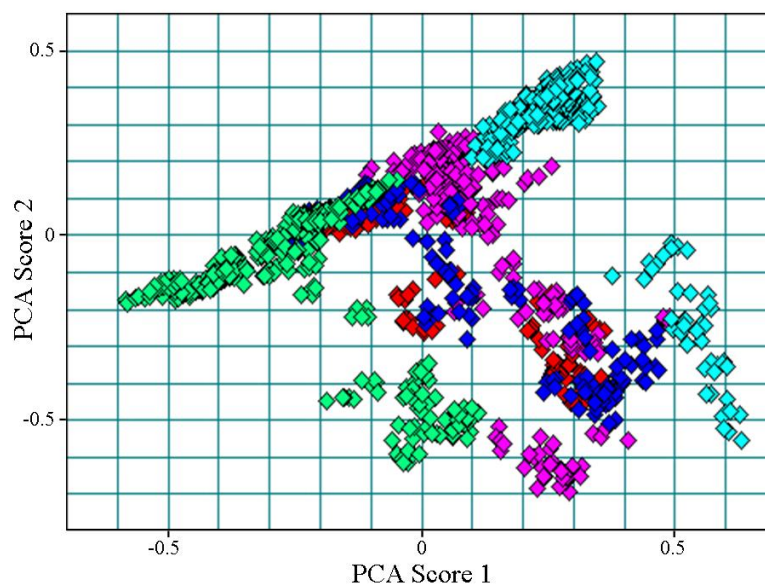
Fig. III.2   Scatter plot of the first two scores from PCA employing the spectral information for the whole data set (n = 1545). Colours indicate the regional provenance of the soils (Argentina: turquoise; China: magenta; USA: blue; Russia: red; Germany: green).

At the same time the number of latent variables required could be reduced to at most nine. Accordingly, local calibrations may even increase the strong predictive power of MIRS data. With R^2 and EF values reaching 0.99, as achieved for the arable soils from Germany (Tab. III.2, model 3; Fig. III.1b), further deviations from the calibration line may no longer be caused by lack of precision of MIRS but could as well reflect analytical errors in conventional SOC determinations. Variable agricultural cropping systems and input of debris from different plant species in the different countries may have affected the organic matter quality (Blanco-Canqui and Lal, 2004).

For the steppe soils, easily decomposable structures like aliphatic CH_2 and CH_3 (~2850 cm^{-1} and ~2925 cm^{-1}), carboxylic acids (~2140 cm^{-1}; ~1210 cm^{-1}), aliphatic OH (~1120 cm^{-1}), and cellulose structures (1020–1050 cm^{-1}) contributed to the prediction of SOC content as displayed by Fig. III.3a (Haberbauer et al., 1998; Rumpel et al., 2001; Tatzber et al., 2007). Further signals of organic constituents could be identified between 830 cm^{-1} and 730 cm^{-1} which might be addressed to secondary amines or aromatic CH bend vibrations (Smidt and Meissl, 2007; Zimmermann et al., 2007). Additionally, calcium carbonate (~2515 cm^{-1}), clay minerals (~3695 cm^{-1}; ~3650 cm^{-1}; ~690 cm^{-1}), and Fe/Al oxides (~920 cm^{-1}; ~890 cm^{-1}) added information that helped to improve SOC quantification in the steppe soils (Doner and Lynn, 1989; Haberbauer et al., 1998; Madejova et al., 2002). In contrast, for German arable soils, only aliphatic stretching vibrations (~2850 cm^{-1} and ~2925 cm^{-1}), small peaks of carbohydrates (2115 cm^{-1}–2180 cm^{-1}), and C=O stretching vibrations (1280 cm^{-1}) were observable besides the dominating aromatic signals (Fig. III.3b). The responses at 1560 cm^{-1} and 1500 cm^{-1} are likely indicating C=C stretches of lignin (Rumpel et al., 2001; Leifeld, 2006), the smaller peak at ~1400 cm^{-1} can be assigned to phenol-OH (Rumpel et al., 2001).
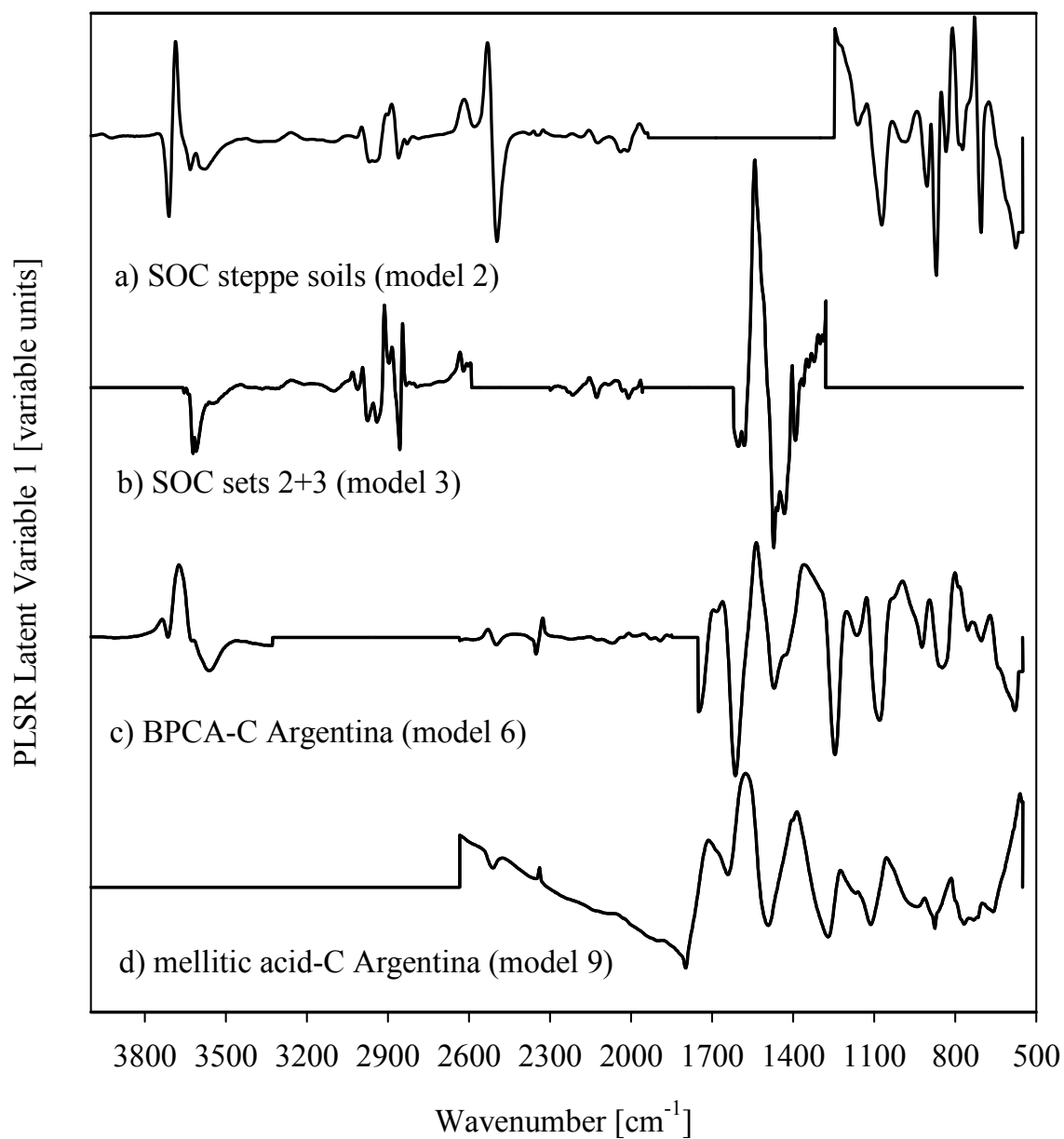
Fig. III.3   **Loading vectors for the first latent variable from partial least squares regression (PLSR) used in the various prediction models (Tab. III.2). (Note that due to the data pre-treatment (Tab. III.1) maxima and minima of the original peaks are located at zero values for Fig. III.3a–3c.)**

3.2 Prediction of black carbon content

Recently, Zimmermann et al. (2007) demonstrated that the chemically recalcitrant carbon after NaOCl oxidation may be predicted from MIRS-PLSR. Leifeld (2006) successfully predicted alkylic and carboxylic NMR regions of soil samples while the prediction of aromatic signals failed. Masking of the infrared absorptions as well as underestimation of aromatic signals of charred material by NMR (Baldock and Smernik, 2002) were discussed as possible reasons for the incompatibility. Using high resolution spectral recording, however, may help to decipher aromatic signals in SOM even if minerals are present. I thus tested the predictability of BC constituents by applying PLSR to BPCA-C.

BPCA-C predictions (g C kg soil^{-1}) of the complete data set resulted in an R² of 0.84 and the RPD of about 2.5 indicated secure predictions (data not shown). However, the first loading vector of this model (data not shown) was quite akin to the ones for SOC predictions of the arable soils (e.g., Fig. III.3b) and I suspect that an intrinsic coherency between SOC and total BC contents occurred. Such a correlation was also reported by Glaser and Amelung (2003) and indeed, there was also a high correlation between the total BC and SOC content within the applied sample set (R² = 0.76). In order to avoid such spurious correlations for BC predictions I normalized the BC content by the SOC content. In doing so, autocorrelations to SOC content in bulk soil could be ruled out (R² = 0.05; data not shown). I am not aware of any other study that has attempted such an approach before.

For the whole data set, the statistical parameters (Tab. III.2, model 4) did not match those reported by Zimmermann et al. (2007) for the recalcitrant organic matter fraction (RPD = 2; R² = 0.72). However, the latter might still be affected by autocorrelation effects to SOC. Again, as also done for bulk SOC, predictions could be improved by splitting the sample sets according to land use and country of origin, reflecting that both, SOM quality and BC dynamics are influenced by human management practices (Rodionov et al., 1999, 2006; Solomon et al., 2007). At intensive land management, light and readily decomposable SOM is degraded, leaving more stable forms of SOM behind (Schulten et al., 1992; Christensen, 1996). Splitting the complete set into arable and non arable soils resulted in enhanced predictions (Tab. III.2, model 5; Fig. III.1c),

although the RPD did not approach values of 2.0. The arable soils from Argentina (Tab. III.2, model 6; Fig. III.1d) allowed for predictions with RPD values as high as 2.31 and an EF of 0.81 in the cross validation. Even better predictions were achieved in the respective test-set calibration (data not shown).

The achievable quality of PLSR predictions is also dependent on the precision of the underlying conventional analysis. In our laboratory, the results of two repeated BPCA measurements differed on average by 6.9 %. However, the reproducibility between different laboratories applying the same method may be worse, as recently reported by Hammes et al. (2007) for BC analyses. Also the samples utilized in my study were analyzed in different laboratories and by different personnel, and I cannot rule out laboratory-specific deviations. The observed validation errors for the BC predictions were in the range of 20 % of the mean BC values measured among the sample sets (Tab. III.2). For the arable soils from Germany, the RMSECV even decreased, however, to values of ~ 10 % of the mean BC concentration (data not shown). My results indicate that reliable estimates of the BC content in SOC can be achieved, provided that a representative calibration set is available.

As for the determination of SOC, relevant spectral information can be discovered from the loading plots of the latent variables. The first loading vector of the BPCA prediction for the Argentinean arable soils (Fig. III.3c) is dominated by signals of aromatic C. Additional major signals can be addressed to acetylic groups of xylan (~1760 cm^{-1}), aromatic C=C and C-H bonds (~1510 cm^{-1}; ~830–730 cm^{-1}), as well as phenols (~1400 cm^{-1}; 1270 cm^{-1}; Rumpel et al., 2001; Leifeld, 2006; Nuopponen et al., 2006; Tatzber et al., 2007; Zimmermann et al., 2007). A signal of aliphatic OH occurs at ~1200 cm^{-1}. Signals of clay minerals are apparent at 3695 cm^{-1}, and 3630 cm^{-1}, Fe/Al oxides are indicated by bands at 2340 cm^{-1} (Clark et al., 1990) and 930–880 cm^{-1} (Madejova et al., 2002). The regression coefficients of the respective spectral regions (data not shown) display that clay minerals and Fe/Al oxides were negatively correlated to BC found in SOM. The negative correlations likely reflect the ability of clay minerals and pedogenic oxides to stabilize also other SOM constituents such as cellulose and polysaccharides (Kögel-Knabner et al., 2008), which then dilute BC relative to bulk SOC. In contrast, aromatic signals, especially at 1400–1600 cm^{-1} and

at 830–770 cm^{-1}, are positively related to BC. I am further assured in my hypothesis as in the models for the prediction of SOC (e.g. Tab. III.2, model 3; Fig. III.1a,) that the signals for clay minerals and pedogenic oxides were positively correlated to SOC content (data not shown).

3.3 Prediction of proportion of mellitic acid-C

Recently, Czimczik and Masiello (2007) emphasized the need for analytical approaches that would not only determine BC quantitatively, but also allow for qualitative interpretations. Applying the BPCA method provides a basis for such qualitative estimates by taking the percentage of mellitic acid-C of total BPCA-C as a measure for the degree of condensation (Brodowski et al., 2007). I was able to predict this proportion by means of MIRS (Tab. III.2, models 7–9). For all models, a vector normalization procedure yielded the best prediction of the % mellitic acid-C (Tab. III.1). Again, enhanced predictions were gained by grouping the samples according to their type of land use as a first step, but only for the Argentinean soils by grouping the countries of origin in a second step (Tab. III. 2, model 8, 9; Fig. III.1e, f), but statistical parameters of prediction were of poorer quality than for SOC and BC predictions (Tab. III.2). In view of the analytical challenge (i.e., low concentration range, quotient calculation with BPCA-C), this is not surprising. While for the complete set (model 7) the cross validation resulted in an RPD of only 1.55 and an EF of 0.58, the values rose to 2.05 and 0.76 for model 9, respectively. For models 8 and 9, standard errors of prediction comprised about 16 % of the mean value for mellitic acid-C. These values decreased to about 10 % for the steppe soils (data not shown). Considering the uncertainty in the conventional laboratory method, the accuracy of prediction is satisfactory. The dominating signals of the first latent variables in the prediction models for the percentage of mellitic acid-C in the Argentinean arable soils (Fig. III.3d) can be assigned to aromatic and phenolic responses, as already observed for the prediction of BPCA-C in SOC. On the contrary, mineral phases did not contribute notably to the predictions of mellitic acid-C proportions. Further evidence for the practicability of the method was gained in an additional experiment. Employing the calibration model of the non-tilled soils (data not shown) I predicted the percentage of mellitic acid-C in maize chars combusted at 400 °C and 500 °C. The predictions of

five repetitions resulted in mean mellitic acid-C proportions of 19.1 % (SD = 1.4) and 34.4 % (SD = 2.9) of total BC for the respective combustion temperatures. The BPCA analytical method yielded proportions of 26.7 % (400 °C) and 32.6 % (500 °C) of mellitic acid-C. The realistic MIRS-based prediction of mellitic acid-C proportion in charred plant material using prediction models developed from the spectra of soils implies that the spectral features were interpreted correctly. I take this as additional hint that MIRS is capable of distinguishing among BC fractions with varying degrees of condensation.

4 CONCLUSIONS

Utilizing a comprehensive sample set of soils from different continents and of varying land use, my investigations revealed that

i)   not only the total amount of SOC but also the proportion of BC in SOC can be predicted by means of MIRS coupled with multivariate data analysis (PLSR).

ii)   calibrations comprising the whole data set provided satisfactory results, albeit local calibrations accounting for varying type of land-use and country of origin allowed for an enhanced quality of the predictions.

iii)   the proportion of mellitic acid-C, serving as an indicator of the degree of BC condensation, can be modelled successfully.

iv)   analytical errors in elemental analysis and in the BPCA method may be alleviated by the opportunity to easily conduct large numbers of repeat analyses and by averaging the variable ground truth data assigned to spectroscopic akin samples.

IV

Particulate organic matter at the field scale – rapid acquisition using mid-infrared spectroscopy

1 INTRODUCTION

Comprising more than 60 % of the terrestrial carbon pool, soil organic carbon (SOC) is one of the principal factors regulating the global C cycle (Batjes, 1996). Recently, Gulde et al. (2008) showed that carbon sequestration in soils propagates by hierarchical saturation of different carbon pools. A homogeneous distribution of the respective pools and their potential for C storage within natural environments, however, is unlikely as the controlling soil parameters are subject to spatial and temporal heterogeneity (Cosby et al., 1984; Kögel-Knabner et al., 2008; Kölbl and Kögel-Knabner, 2004). Capturing of the spatio-temporal patterns of different SOC pools is thus required to improve C turnover modelling at the field scale. Yet, comprehensive datasets are hard to obtain, mostly due to the extreme workload associated with a geostatistically adequate C pool assessment (Blanco-Canqui and Lal, 2004). In this work I present the compilation of a raster data set including SOC, POM of three size classes, and lignin contents, for a discrete test site as derived by MIRS-PLSR. My aims were to evaluate if, i) a local calibration with satisfying prediction quality is attainable, in particular for deciphering the spatial patterns of POM at the field scale, ii) whether the predicted carbon pools can be characterized chemically by the loading weights of the PLSR prediction models, and iii) whether conclusions on the C dynamics can be drawn from the correlations between the respective C pools.

2 MATERIAL AND METHODS

2.1 Soils

The presented investigations apply to the main test site which is described in section II.1.1. For MIRS analysis, samples as described in sections II.1.3 were supplemented (n = 30) in order to broaden the range of the investigated soil characteristics. In the following, calibrations containing samples from these two sampling sites are referred to as local calibrations. Another 27 samples originating from varying cropped loess soils all over North-Rhine Westphalia (Germany) were supplemented to investigate the effect of a more diversified sample set. Calibrations comprehending all three sample sets are referred to as extended calibrations.

2.2 Ground truth measurements

Ground truth measurements were conducted as outlined in section II.2.

2.3 Spectroscopic measurements

Spectroscopic measurement was conducted as outlined in section II.3.

2.4 Data treatment and statistical analysis of MIR spectra

Basic information on data treatments and statistical analysis of spectral data is given in sections I.2.3, and II.3.

Particular precaution has to be taken to avoid over-fitting when PLSR is applied to spectra of soil samples (Viscarra-Rossel, 2007). At this, also the appropriate mode of calibration procedure is subject to an ongoing debate. While a separation of the sample set into calibration and validation samples is suspected to deliver more robust and realistic calibrations (Chang et al., 2001; McCarty et al., 2002; Islam et al., 2003), especially for small sample sets also full-cross validations are widely accepted (Reeves et al., 2001; Moron and Cozzolino, 2004; Bornemann et al., 2008). Highest robustness, however, can be expected when the statistical parameters of varying calibration and validation techniques deliver akin results for a common sample set (Janik et al., 2007). I thus conducted complementary test-set calibrations and leave-one-out full cross validations for each predicted soil parameter in order to assure the robustness of the models. For test-set calibrations, 10 % of the samples were randomly removed from the calibration set. The calibration was then independently validated by applying the derived models to the previously removed samples. An even more important factor challenging the applicability of MIRS-PLSR in soil science is the employed sample set. At this, the capability of PLSR to maximize the covariance between spectral information represented by PLSR loading weights and a property of interest is crucially affected by the spectral heterogeneity of the sample set and the variability of the previously determined property among the soil samples. Recently, Bornemann et al. (2008) showed for a highly diversified sample set that local calibrations can be advantageous for the determination of SOC and BC in soils from all over the world. Also results of Linker et al. (2006) indicate that a reduction of the spectral heterogeneity within a sample set facilitates more accurate predictions of delicate soil parameters as nitrate contents. As a result, also in this

investigation, the effect of enhanced variability among the calibration samples was explored by applying local and extended calibration sample sets. The number of necessary samples to achieve robust model calibrations for the local sample set varied depending on the investigated fraction. For POM3 contents in bulk soil a set of 36 samples was sufficient for reliable predictions, 24 additional samples were supplemented for the calibrations of POM2 and POM1. Ten samples that contained less than 0.05 g POM1–C kg^{-1} soil underwent the detection limit and were thus excluded from modelling. Predictions of the SOC contents within the fractions were conducted employing both samples of the repeated fractionation of the initial sample set, therefore comprising 72 samples for each fraction. Predictions of lignin contents were calibrated by 51 samples.

To avoid over-fitting during PLSR calibration, additional ranks were only accepted if the explanation of the spectral variability improved continuously. Additionally, the optimum number of calibration ranks was identified by applying an F-test determining a minimum error which does not differ significantly from the minimum error of validation (Geladi and Kowalski, 1986; Haaland and Thomas, 1988a). Apart from the coefficient of determination (R^2) between measured and predicted values, the predictive power of the spectroscopic measurement was also described by the root mean square error of cross validation (RMSECV) and root mean square error of prediction (RMSEP), which are measures for the standard error of the respective calibration procedures and can be compared to a standard error of a lab-method (Geladi and Kowalski, 1986). Finally I calculated the ratio of performance to deviation (RPD), which represents the quotient of standard deviation of the reference data and standard error of the calibration procedures. It is thus a dimensionless quality parameter and most meaningful for the rating of quantitative chemometric predictions. The higher the RPD value, the better is the predictive power of the calibration model. Chang and Laird (2002) classified chemometric prediction models for soil parameters with respect to their RPD values. According to their classification RPD values >2 provide accurate predictions.

2.5 Statistical analyses

In addition to classical correlation analyses, the maps representing different C pool distributions on the test site were analyzed by specialized software for the comparison of maps displaying different characteristics at identical locations (Visser and de Nijs, 2006). Originally developed for the comparison of nominal scaled maps, the actual release of this "Map Comparison Kit" also comprises an algorithm handling ratio scaled values. The so called "fuzzy-numerical" algorithm is based on a fuzzy-kappa comparison and features two essential advantages over classical cell by cell comparisons. Firstly, the expected percentage of agreement between two maps is corrected for the fraction of agreement which can be statistically expected by randomly relocating all cells in both maps by applying the kappa-statistic. Secondly, not the pure values of the original cells are compared. Based on fuzzy-set Theory (Zadeh, 1965), the neighbourhood of each cell is taken into account by creating a fuzzy-similarity map, comprising similarity values between 0 and 1. The resulting statistic, the κ-value, is the average similarity of the compared parameters over the whole map, where a value of 1 indicates absolute similarity, 0 indicates no similarity. In summary, the Kappa-statistic corrects the observed correlations by the statistically expected correlation of the randomly distributed values with regard to the observed frequency distribution. The quality of the correlations is thus corrected by the part of coherency that may occur by chance, and the gained results are thus more robust. For further information on the software and the methods applied the reader might refer to Visser and de Nijs (2006).

3 RESULTS AND DISCUSSION

3.1 MIRS predictions

By now, MIRS-PLSR is a well accepted technique for the reliable prediction of SOC contents (Viscarra-Rossel et al., 2006; Bornemann et al., 2008). Also for the soils of the investigated test site the prediction model for SOC proved to deliver excellent results (Tab. IV.1). To quantify particular SOC fractions independently from bulk SOC contents, the respective prediction models must rely on individual and characteristic chemical features. The POM fractions utilized in this study were gained by a physical fractionation procedure. Amelung et al. (1998; 1999) employed the same procedure and akin size boundaries for particle size fractionation of soils along a climosequence in the prairies. They showed that VSC-lignin contents decreased with decreasing particle size. At the same time oxidative side-chain alteration proceeded, thereby indicating a typical SOC decomposition gradient. Results of Ludwig et al. (2008) suggest that amounts of VSC-lignin in a sample set of soils and litter can be predicted by means of MIRS-PLSR. Presuming that a decomposition and oxidation gradient is given with decreasing particle size (see above), variations in the spectral absorptions of lignin and other substances can also be expected among the samples of the investigated test site. A prediction of different POM pools in soil could thus, however, be facilitated by means of MIRS-PLSR.

In agreement with Ludwig et al. (2008), the statistical parameters for the prediction of VSC-lignin in the investigated sample set suggest a good reliability as indicated by the RPD of 3.61 (Tab. IV.1). To safeguard that these calibration results rest upon the identification of VSC-lignin and to rule out autocorrelations to other soil C pools, I identified spectral bands that are related to VSC-lignin by setting up an artificial sample set: the same CuO-oxidation products of lignin as identified by GC-FID in the natural samples were added in ten concentration steps to four soils of the applied sample set. At this, the ratios of the added monomers remained unchanged. As these monomers are released from intact lignin upon CuO oxidation, MIRS-PLSR will be able to detect the monomers if it is able to detect intact lignins as presumed. Indeed, the spectral principal

Tab. IV.1 Statistical parameters of the employed MIRS-PLSR prediction models. Predictions were conducted for soil organic carbon (SOC), phenolic oxidation products of soil organic matter (VSC-lignin), carbon content in the particulate organic matter fractions (POM1–3–C), and content of particulate organic matter in bulk soil (POM1–3). Particulate organic matter fractions comprise particle sizes of POM1: 2000–250 µm, POM2: 250–53 µm, and POM3: 53–20 µm.

Soil constituent	Unit	n spectra	Mean	Median	Range	Rank	full cross validation				test set validation (10%)				
							R²	Slope	RMSCV[a]	RPD[b]	Rank	R²	Slope	RMSEP[c]	RPD[b]
SOC	g kg⁻¹	475	10.0	11.0	1.6 – 17.0	7[d]	0.97	0.97	0.67	6.04	7[d]	0.97	0.93	0.087	5.51
VSC lignin	mg kg⁻¹	255	161	191	10 – 328	6[d]	0.92	0.93	23.7	3.61	5[d]	0.96	0.99	26.4	2.78
POM1–C	g kg⁻¹	310	30.7	13.6	1 – 105	5	0.96	0.96	6.54	4.80	5	0.98	0.93	7.00	6.74
						14[d]	0.99	0.98	3.44	9.12	12[d]	0.99	0.97	4.14	12.8
POM2–C	g kg⁻¹	360	9.1	7.3	0.6 – 23.4	5	0.96	0.96	1.05	5.17	5	0.95	0.93	1.17	15.1
						13[d]	0.99	0.98	0.62	8.79	11[d]	0.99	0.99	0.63	9.35
POM3–C	g kg⁻¹	360	4.1	3.6	0.4 – 13.5	5	0.96	0.96	0.48	5.03	5	0.98	1.01	0.44	7.13
						13[d]	0.99	0.98	0.29	8.29	13[d]	0.99	0.99	0.26	15.1
POM1	gPOM1C kg soil⁻¹	300	0.52	0.43	0.05 – 1.43	5[d]	0.77	0.79	0.15	2.10	5[d]	0.86	0.72	0.14	3.14
POM2	gPOM2C kg soil⁻¹	300	0.66	0.69	0.09 – 1.17	7[d]	0.87	0.88	0.07	2.74	4[d]	0.84	0.78	0.09	2.74
POM3	gPOM3C kg soil⁻¹	180	1.78	1.44	0.15 – 6.26	5[d]	0.96	0.94	0.26	4.81	3[d]	0.97	0.94	0.28	6.20
POM1	gPOM1C kg soil⁻¹	435	1.06	0.75	0.05 – 1.58	4[d]	0.67	0.73	0.19	1.75					
POM2	gPOM2C kg soil⁻¹	435	0.68	0.62	0.09 – 1.17	6[d]	0.76	0.74	0.11	2.04					
POM3	gPOM3C kg soil⁻¹	315	1.65	1.40	0.15 – 6.26	6[d]	0.89	0.87	0.33	2.99					

local calibration

extended calibration

[a] Root Mean Squared error of Cross Validation
[b] Ratio of Performance to Deviation (of the PLSR prediction models)
[c] Root Mean Squared error of Prediction
[d] Optimum number of principal components as recommended by F-test of calibration software

component analysis revealed that beside the aryl and carbonyl groups ($\sim$1500 cm^{-1}; $\sim$1660–1700 cm^{-1}; Tab. IV.2) chiefly vibrations between $\sim$1340–1360 cm^{-1} were indicative of the added phenols. According to Zimmermann et al. (2007) and Tatzber et al. (2007), these wavelengths can be ascribed to stretching vibrations of C–OH, and CO–CH$_3$ groups which are prevalent side chains of lignin derived phenols (Hedges and Ertel, 1982). Especially the first, and to lesser extents also the second, and fourth latent variable of the prediction model for measured VSC-lignin expressed their major signals at these particular wavelengths (data not shown). While I am aware that these CuO derived oxidation products are not actually found in soil, they do resemble the chemical structures of natural lignin molecules. I am thus confident that varying amounts of VSC-lignin in natural soil samples can be identified and their quantities can be predicted correctly by means of MIRS-PLSR. Predictions of the oxidative side chain alteration and ratios of syringyl- to vanillyl-monomers, however, failed. I presume that such a characterization was not feasible, simply because the qualitative lignin parameters hardly changed among the calibration samples (acid to aldehyde ratio: mean = 0.35; coefficient of variation = 10.0 %; syringyl to vanillyl units: mean = 0.91, coefficient of variation = 6.5 %). But even if there was considerable variation within a calibration set, the chance for detection by means of MIRS-PLSR might remain low as the VSC monomers are produced by the action of CuO on the lignin. That is, only the precursor material is

Tab. IV.2 **Structural assignments of the main signals featured by the mean spectra (Fig. IV.1), and the loading weights (Fig. IV.2b), and cumulative loading weights (Fig. IV.2a) of the prediction models for the POM fractions.**

Wavenumber [cm^{-1}]	Structural assignment	Cited reference
3600–3700	OH of clay and iron oxides	Cornell and Schwertmann, 1996; Madejova et al., 2002
2850–2920	aliphatic C–H	Haberbauer et al. 1998; Leifeld, 2006; Tatzber et al., 2007
1700	C=O of carbonyl–C	Leifeld, 2006; Tatzber et al., 2007
1660	carbonyl–C	Rumpel et al., 2001
1630	carboxyl–C	Haberbauer et al., 1998; Leifeld, 2006
1600–1620	phenolic compounds	Nuopponen et al., 2006; Rumpel et al., 2001
1565	carboxyl–C	Rumpel et al., 2001; Haris et al., 1992
1500–1510	aromatic C–H and C=C	Haberbauer et al., 1998; Leifeld, 2006; Tatzber et al., 2007
1427	carboxyl–C	Rumpel et al., 2001
1410	aliphatic C–H	Solomon et al., 2005
1320	hydroxylic C–O–H	Zimmerman et al., 2007
1250	carboxylic COOH	Solomon et al., 2005
1160	polysaccharides	Rumpel et al., 2001
1000–1080	C–O stretch of cellulose	Solomon et al., 2005
870	aromatic C–H and C=C	Haberbauer et al., 1998; Leifeld, 2006; Tatzber et al., 2007

directly subjected to MIRS, and not the CuO treated soil which actually contains the monomers.

In order to evaluate if the fractionated POM pools comprise specific carbon species and to obtain evidence that discrimination between the pools via MIRS-PLSR is possible, I built prediction models for SOC contents within the sets of fractionated soils (in the following called POM-C). For this, spectra of the separated POM fractions were recorded and calibrated by their SOC contents which were previously determined by elemental analysis. The prediction models for the SOC contents of the discrete fractions delivered excellent results for all three POM-C fractions, and even outperformed the prediction model for SOC (Tab. IV.1). The latter applies to both, full-cross validations and test-set validations. Here, RPD values exceeded numbers of eight and R^2 values of 0.99 were achieved by the calibration models employing the number of loadings as recommended by the F-test.

Calibration models employing a small number of samples are vulnerable to over-fitting, especially when high numbers of loading weights are calculated. To ensure that my calibration results were not falsified by over-fitted calibration models I also build more parsimonious calibrations employing only five loading-weights (Tab. IV.1). The statistical parameters of all models indicated only a slight decrease in calibration quality and again, full-cross validation and test-set validation delivered approximately similar parameters. The very high correlation coefficients realized for the predictions of POM-C in the fractionated soil samples are in line with results of Reeves et al. (2006), who reported that R^2 values of up to 0.99 may be achievable for the prediction of POM in soil samples. I address the high quality of the predictions for POM-C to a homogenization of the sample set upon fractionation: only parts of total SOM are isolated in individual C pools, still comprising varying contents of chemically distinct SOC. In such samples, the specific SOC features are better displayed than in bulk SOM, i.e. such sample sets ideally comply with the requirements for successful application of MIRS-PLSR (Geladi and Kowalski 1986) and the extraction of qualitative information (Haaland and Thomas, 1988a). For soil fractions, highly significant results are thus likely achievable even a with reduced number of samples as compared to predictions employing bulk soil samples. Besides, these predictions rely on the identification of different C species in soil fractions

where former wet chemical analyses have given independent evidence that these species are truly abundant. On the other hand, the analyses remained robust against both, changes in degrees of freedom and sample size.

While statistical parameters give indications for the quality of prediction models, evidence can be provided by chemical interpretations of spectral features and loading-vectors of the prediction models. Characteristic differences between the investigated soil fractions are already evident from the mean spectra of the calibration samples. In Fig. IV.1, the attenuation of the peak at ~1000–1080 cm^{-1} indicates a decrease in the content of cellulose (Solomon et al., 2005) from POM1 to POM3. Simultaneously, the contribution of hydroxylic groups (1320 cm^{-1}) and carbonyl-C (1660 cm^{-1}) is increasing with decreasing particle size (Rumpel et al., 2001; Zimmermann et al., 2007).
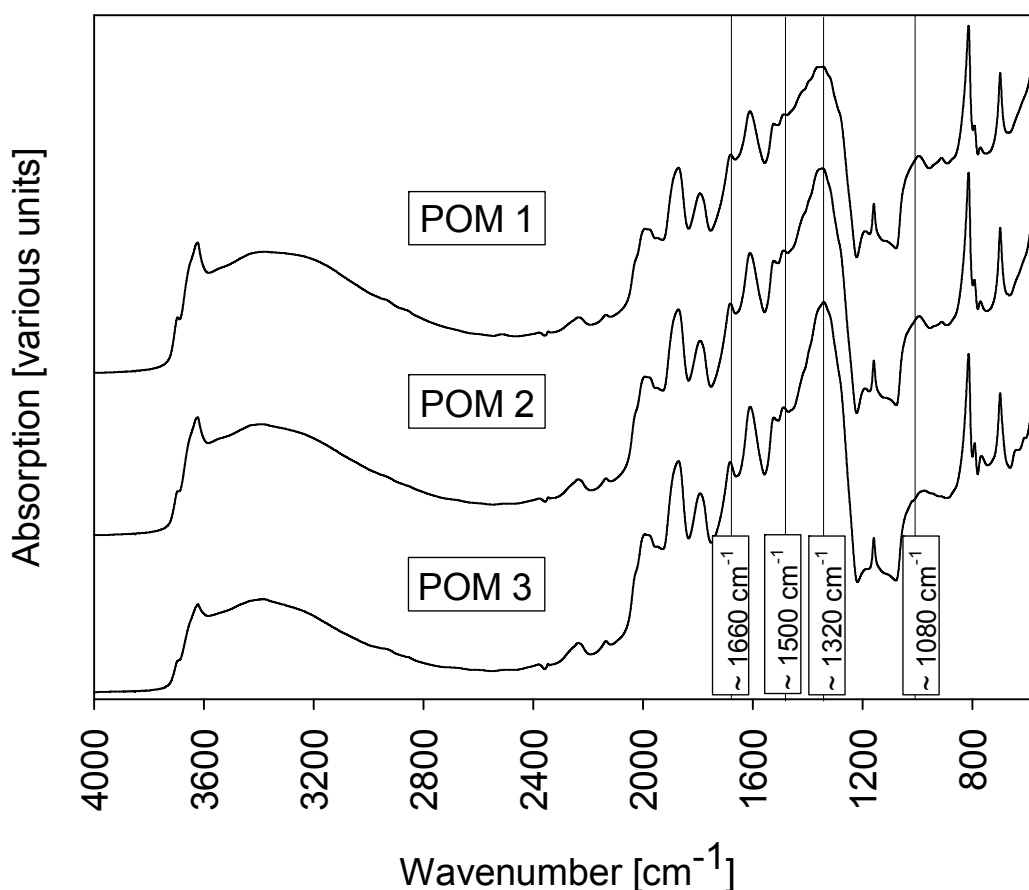
Fig. IV.1 Mean spectra of the separated particulate organic matter fractions (n = 72). Particulate organic matter fractions comprise particle sizes of POM1: 2000–250 µm, POM2: 250–53 µm, and POM3: 53–20 µm.

According to Haaland and Thomas (1988b), generally only the loading weights of the first single latent variable of a PLSR model should be interpreted chemically. Yet, in case of excellent predictions also the cumulative loading weights of all latent variables used in the particular prediction model may be used for structural interpretation (Haaland and Thomas, 1988b). Indeed, I also found distinct differences between the cumulative loading weights of the prediction models for the organic carbon contents of the soil fractions (Fig. IV.2a). Structural assignments for the main absorptions are given in Tab. IV.2. For POM1–C, C–O vibrations of polysaccharides, as well as aromatic C–H and C=C vibrations were dominating. Besides the vibrations at 1340–1360 cm^{-1} which were identified to be indicative for the VSC-lignin, also a strong phenol related signal at~1620 cm^{-1} was clearly observable.

As already indicated by the mean spectra (Fig. IV.1), there was a lesser contribution of polysaccharides in the finer fractions (POM2–C and POM3–C), and aliphatic C–H stretching vibrations, especially at 2920 cm^{-1} and 2850 cm^{-1}, were more pronounced (Fig. IV.2a). Also OH groups of mineral soil constituents like clays and Fe-oxides were positively related to carbon contents in soil fractions.

Distinct differences between POM2–C and POM3–C were observable between 1800 cm^{-1} and 1100 cm^{-1}. The signals for POM2–C primarily indicated C=O bondings of carbonyl–C and aromatic C=C. The major phenol derived peak at ~1620 cm^{-1}, which was observable for POM1, was weaker, and only a small shoulder was present at ~1340 cm^{-1}. Also in contrast to POM1–C, aliphatic C–H deformation and to a lesser extent hydroxyl groups were now more important. This trend was even fortified for POM3–C, where the cumulative loading weights were dominated by carboxylic absorptions while phenol- and lignin-related signals vanished. Hydrophilic moieties in POM3–C further comprised carbonyl groups, hydroxyl groups and C–O stretches of polysaccharides.

As a result, the fractionation borders of 20, 53, and 250 µm were indeed distinct enough for spectroscopic discrimination of the chemically different POM–C pools. The chemical properties of the POM fractions are also consistent with the current state of knowledge concerning degradation pathways of organic matter (Bachmann et al., 2008; Kögel-Knabner et al., 2008). The POM1–C fraction consists of relatively fresh and

undecomposed plant debris, which primarily contains cellulose and unaltered lignin (Marschner et al., 2008). The POM2–C fraction already contains aliphatic CH_2 and CH_3 groups as decomposition products. Kögel-Knabner et al. (2008) concluded from NMR analyses that mineral associated and thus protected organic matter of sandy soils is dominated by long-chained aliphatic molecules.

Organic matter in POM3–C appeared to be depleted in VSC-lignin, and the band at ~1030 cm^{-1} (C–O stretching vibration of cellulose) was missing. These changes in SOC composition suggest that structural carbohydrates have largely been metabolized. Also oxidation of plant lignin can be expected to be at a higher stage, due to a comparatively longer residence time of POM3 in soil (Christensen, 1992; Amelung et al., 1999). Yet, no significant differences in acid to aldehyde ratios were observable (see above), suggesting at least some of the aromatic and carboxylic moieties were selectively preserved during the decomposition of more labile substrates like cellulose in this POM pool. This hypothesis is also supported by the slight increase of vibrations from aromatic C=C bondings (Tab. IV.2) from POM1 to POM3 which are indicated by a small signal at 1500 cm^{-1} in Fig. IV.1, and an observable shoulder in Fig. IV.2b. In fact, the loading weights and mean primary spectra of POM3–C are rather dominated by carboxylic acids and aliphatic moieties, most likely indicating products of microbial metabolism (Fig. IV.1; IV.2b).

Having evidence that the POM–C fractions featured different chemical structures identifiable by MIRS-PLSR, I finally developed prediction models for the respective POM contents of the bulk samples (gPOM–C kg soil^{-1}; in the following called POM1, POM2, and POM3). According to the classification of Chang et al. (2002), the statistical parameters of the local calibrations indicated reliable predictions for all POM fractions, with an excellent quality of POM3 predictions (Tab. IV.1). The latter applies for both, full-cross validations and test-set validations, where consistent statistical quality parameters indicate robust prediction models. Although the extended calibration models involved more samples, and for POM1 also a wider range of POM contents, a slight decrease of prediction quality was observable compared to the local calibrations (Tab. IV.1).
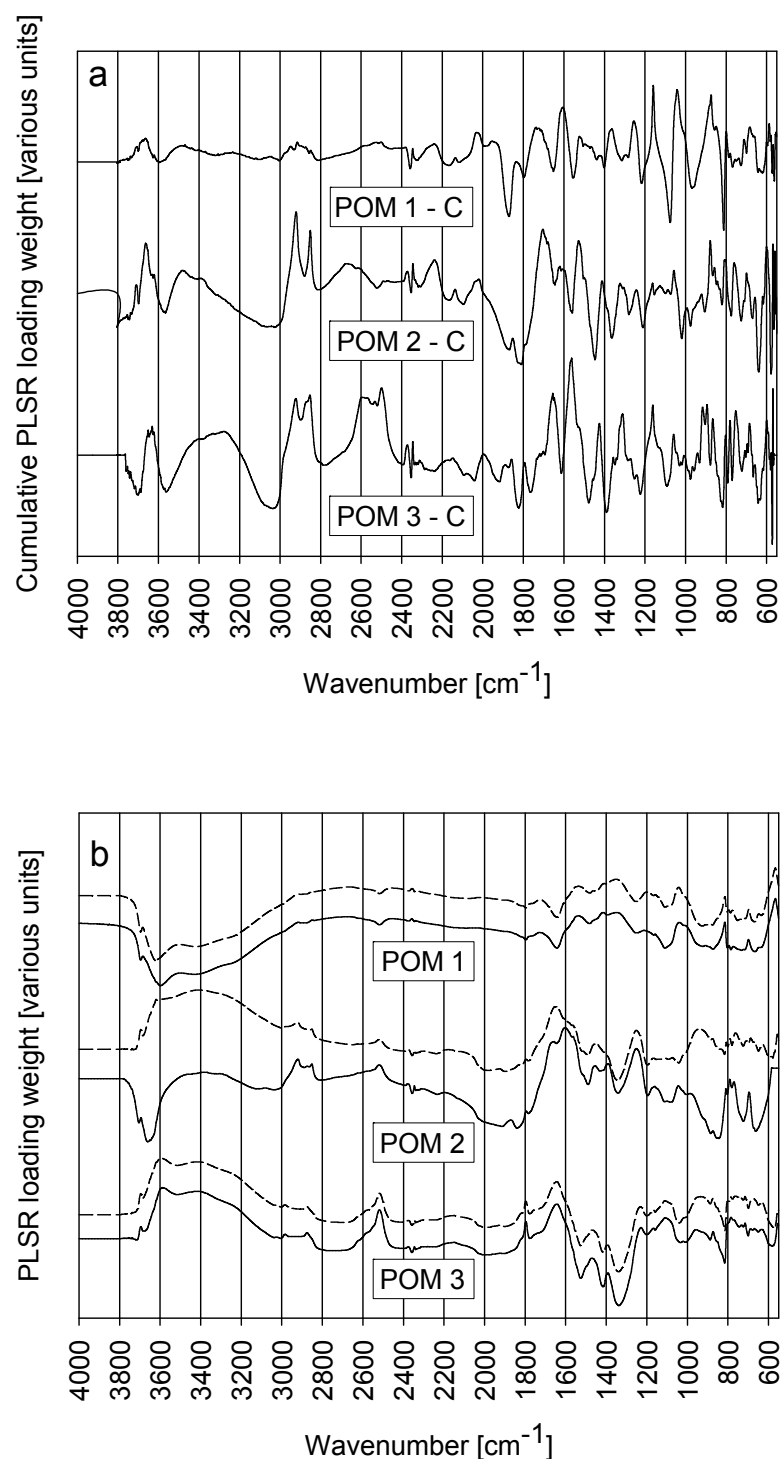
Fig. IV.2 Cumulative loading weights of the PLSR prediction models of soil organic carbon (SOC) in the separated particulate organic matter fractions (POM–C; Fig. IV.2a), and the loading weights of the first latent variable of the PLSR prediction models for the respective POM fractions in bulk soil (Fig. IV.2b) employing local calibration (continuous line) and extended calibration (dashed line). Particulate organic matter fractions comprise particle sizes of POM1: 2000–250 µm, POM2: 250–53 µm, and POM3: 53–20 µm.

Quantities of specific SOC fractions may be related to bulk SOC contents (Stewart et al., 2008). Particular precaution has thus to be taken when spectroscopic data is used to predict such fractions from MIR spectra of bulk soil. I reassured that the good calibration results which were achieved for the predictions of the POM fractions from spectra of bulk soil rested on fraction-specific signals by comparing the loading weights of the first latent variables (Fig. IV.2b) to the cumulative loading weights of the prediction models for POM–C (Fig. IV.2a). Representing only the first loading weight relating to the particular contribution of a given POM fraction to bulk SOC, I obtained a better resolution and less peaks than using the cumulative loading weights as employed for the POM–C predictions (Fig. IV.2a). In accordance to the predictions of POM1–C, the first loading weights for the local and extended predictions of POM1 in bulk soil featured C–O vibrations of polysaccharides and the indicative signal for VSC-lignin at 1340–1360 cm^{-1} were characteristic. These features vanished for POM2 and POM3 which exhibited stronger vibrations of aliphatic C species. For POM2, the phenol-C signal at 1600 cm^{-1} was dominating besides carboxylic vibrations. According to the spectral bands for POM3, carboxylic groups and polysaccharides were most characteristic. Other discernable signals in the loading weights for POM2 and POM3 comprised aromatic C and C–H deformation vibrations. Overall, the signals of the organic carbon species were essentially identical for local and the extended calibration sets of all three POM fractions (Fig. IV.2b). For POM2 predictions, however, differences were particular apparent for the mineral absorptions at 3800–3600 cm^{-1} and below 800 cm^{-1} (Cornell and Schwertmann, 1996; Madejova et al., 2002). I suppose that the integration of samples from 27 individual sites, as performed for the extended calibrations, lowered the prediction quality for POM by addition of interfering spectral variability (Tab. IV.1).

The spectral signals that were indicative for the C content in the fractionated samples (POM–C; Fig. IV.2a) were identical with those which I used for predicting total POM contents (Fig. IV.2b), irrespective of the applied sample set. Keeping in mind that the compared loading weights are based on three totally different sets of spectra (fractions for POM–C, two sets of bulk soil for POM in bulk soil) and originate from individual calibration models, the analogies between the PLSR models indirectly prove the reliability and applicability of the MIRS technique for POM prediction.

A small positive relation between mineral absorptions ($3000–3600$ cm^{-1}) and POM–C predictions was apparent for all size fractions of the fractionated soils (Fig. IV.2a), suggesting that varying amounts of minerals were associated with the organic fraction or present as thin coatings on the separated sand grains. In contrast, this effect was ambivalent considering the MIRS recordings of the bulk soil (Fig. IV.2b). In case of the local calibration, positive signals of mineral phases were detected only for POM3. The supplementation of variable samples in the extended calibration resulted in positive relations to POM2 and POM3. Kölbl and Kögel-Knabner (2004) found positive relations between occluded POM and clay contents, whereas the amounts of free POM were not affected by clay contents of the soil. The occlusion of SOC in soil is, however, dependent on the mineralogy, texture, and management (Blanco-Canqui and Lal, 2004) and observed relations between POM and mineral soil constituents likely depend on the applied sample set.

3.2 Interrelationships and spatial patterns

The consensus between the spectral signals of POM1, POM2, and VSC-lignin was confirmed by the high spatial correlations ($\rho = 0.91$) between these parameters at the investigated test site, as derived from a rigorous cell-by-cell comparison (Tab. IV.3). On the contrary, the correlations of POM3 to VSC-lignin were rather poor ($\rho = 0.29$), though still significant, reflecting the lower contribution of VSC-lignin to the finer POM3 pool. Also the spatial distribution of the varying C pools revealed individual patterns. The contents of SOC, POM1, POM2, and VSC-lignin show a clear increase in north-eastern direction (Fig. IV.3). In contrast, the POM3 contents are rather randomly distributed, only partly following the pattern observed for the other C pools. Here, the highest contents were detected in the south-eastern corner with a spotty distribution of extreme values throughout the remaining area.

Tab. IV.3   Correlations and fuzzy-kappa coefficients of the compared soil organic carbon (SOC), particulate organic carbon fractions (POM1–3), and VSC-lignin contents (n = 129).

	POM1		POM2		POM3		Lignin	
	ρ	κ	ρ	κ	ρ	κ	ρ	κ
SOC	0.88**	0.77	0.90**	0.74	0.54**	0.64	0.86**	0.77
POM1			0.88**	0.72	0.51**	0.57	0.91**	0.77
POM2					0.47**	0.54	0.91**	0.77
POM3							0.29**	0.56

ρ: correlation coefficient after Pearson
κ: fuzzy-kappa coefficient of map comparison algorithm

With respect to the spatial heterogeneity of the gained data, a rigorous cell-by-cell comparison as realized by correlation analysis would likely overemphasize local extreme values. I thus applied fuzzy-kappa statistics, which smoothes the effect of local extrema and allows for better spatial pattern recognition by integration of the neighboring values (Visser and de Nijs, 2006). Furthermore, artifacts due to spatial microscale heterogeneity, imperfect field sampling, and measurement error are alleviated.

The map comparisons by fuzzy-kappa statistics attenuated the estimated similarity of the maps, indicated by κ-values of 0.54 to 0.77 (Tab. IV.3). High degrees of conformity were again confirmed for SOC, POM1, POM2, and VSC-lignin. Contrasting to the correlation coefficients, the similarity of the patterns of SOC and POM1 was now considered higher as that between SOC and POM2, while both POM fractions and SOC resembled the same patterns of VSC-lignin in a similar way. The disparity of POM3 to the spatial patterns of the other C pools was displayed by low correlation coefficients (ρ) and was reapproved by the low κ-values.

The map comparison of the predicted C pools yielded unambiguous results concerning the similarities and differences in C pool patterns. Moreover, these results suggest that POM1 and POM2 are regulated by akin control mechanisms. The correlations to the lignin contents can be interpreted as additional evidence that high contents of VSC-lignin are indicative of weakly degraded POM. The close relations of bulk SOC to lignin likely are an artifact due to a spurious correlation, resulting from the correlation between the
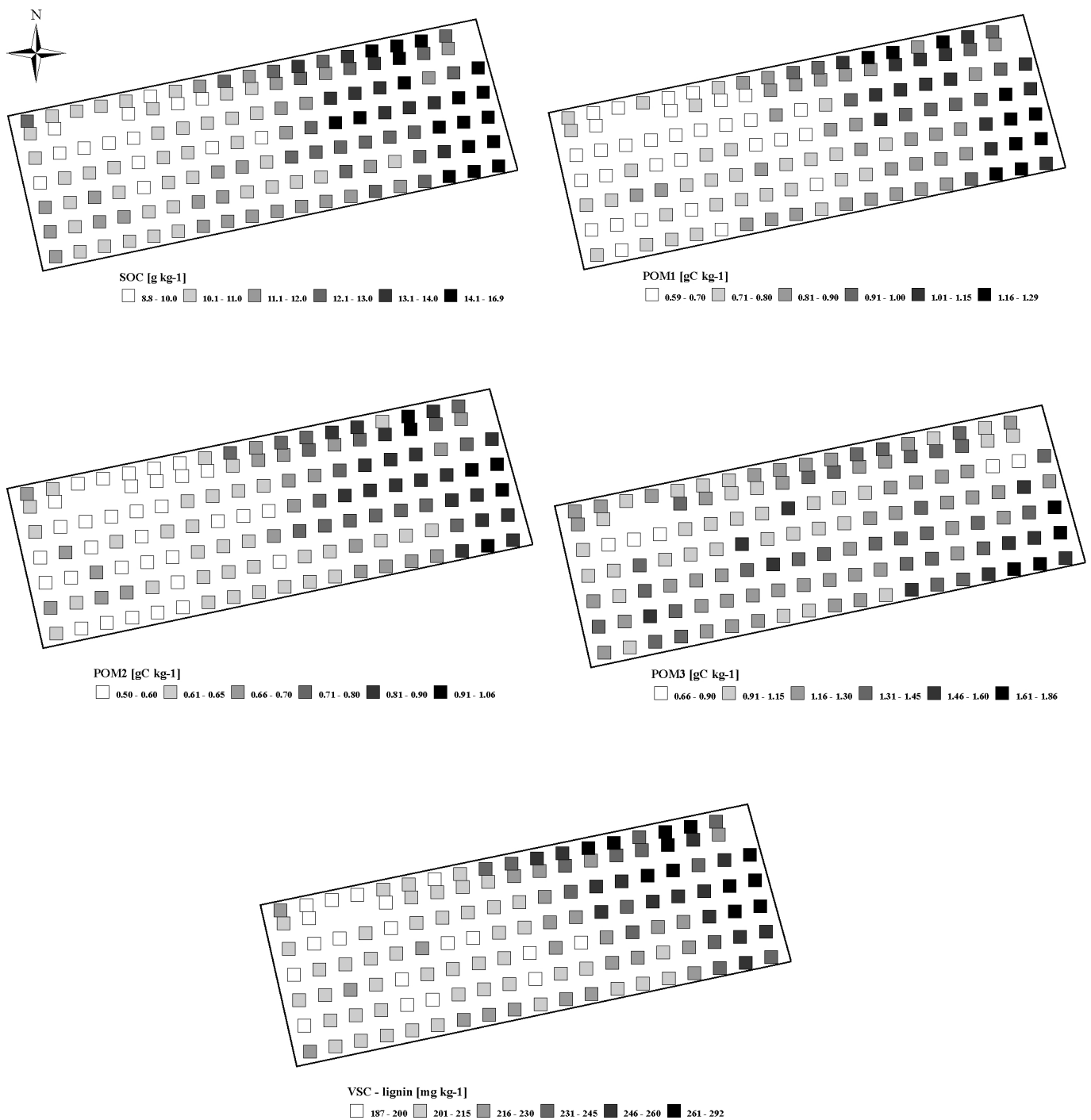
Fig. IV.3 Spatial distribution of soil organic carbon (SOC), particulate organic matter of three size classes (POM1: 2000–250 µm, POM2: 250–53 µm, POM3: 53–20 µm), and phenolic oxidation products of lignin (VSC-lignin) in topsoil samples at the investigated test site in Selhausen (50°52´09.34´´N; 6°27´00.58´´E). The sampling points represent a 10x10 m grid, with a 5x10 m grid for the northern borderline.

coarse POM fractions and lignin content. The smallest POM fraction seems, however, to be controlled by individual control mechanisms as it distributes independently from the other pools.

Caused by the individual spatial patterns, also the proportions of the individual POM fractions to bulk SOC are distinct. Those of POM1 and POM2 are less variable (POM1: 5.8–10.1 % of bulk SOC; POM2: 4.7–7.3 % of bulk SOC) as their fine earth contents distribute analogously to that of bulk SOC. On the contrary, the POM3 contents in fine earth exhibit an individual pattern, resulting in a more pronounced variability (5.8–15.0 % of bulk SOC).

Gulde et al. (2008) and Stewart et al. (2008) showed that hierarchical C pool saturation can explain the C dynamics under variable input of organic carbon to cropped soil systems. Thereafter, accumulation of SOC is proposed to proceed by a sequential saturation of differently stabilized C pools. Once the physically stabilized microaggregate fraction is saturated, storage of SOC is considered to proceed in coarser, rather labile fractions. In the SOC rich parts of the test site, the available solum is severely reduced by elevated stone contents. Under such conditions, there is an increased litter input to the remaining fine earth which could, at least principally, affect pool saturation at this point. To which extent, however, hierarchical saturation processes of differently sized C pools truly contribute to the observed C pool patterns warrants further clarification.

4 CONCLUSIONS

From my results I conclude, that

i.   the creation of suitable MIRS-PLSR prediction models for differently sized POM pools at the field scale is possible.

ii.   at this, the application of localized calibration samples is advantageous over more diversified sample sets.

iii. the predicted carbon pools can be characterized and chemically distinguished by the loading weights used in the PLSR prediction models, chiefly by specific absorptions of VSC-lignin, cellulose, and microbial metabolites.

iv.   on the investigated sampling site, the coarse POM fractions are regulated by akin control mechanisms, while the smallest sized POM distributes individually.

V

Stone contents control organic carbon pool sizes in agricultural topsoil

Modified on the basis of

Submitted manuscript

1 INTRODUCTION

The pedosphere constitutes an essential compartment of atmospheric C exchange with the land surface. Evaluating the role of soils as either sink or source of atmospheric C, chemical and biological analyses are classically performed on fine soil, sieved to grain sizes < 2 mm. However, many soils contain considerable amounts of stones. For instance, Stendahl et al. (2009) reported that the average content of stones and boulders could be as high as 43.4 % for forest soils all across Sweden. More than 60 % of the Mediterranean land surface comprises major amounts of stones (Poesen and Lavee, 1994). Miller and Guthrie (1984) reported that soils with high stone contents comprise considerable parts of the agricultural land in the US (~16%). Furthermore, they presume that this proportion will increase due to erosion and cultivation of marginal land. In fact, only a very limited number of soil-forming substrates are entirely free from stones. Ignoring highly variable stone contents by interpreting results from sieved soil samples may thus lead to erroneous conclusions on soil C dynamics.

High stone contents may limit plant growth due to a reduced solum and an accelerated leaching of dissolved nutrients (Poesen and Lavee, 1994). However, in arable ecosystems, nutrient deficiencies are usually alleviated by organic and inorganic fertilization. Hence, the biological productivity of agricultural soils, and thus also the amount of added plant debris, may be less dependent on stone contents than the turnover of SOM when soil solum, and thus the supply of moisture and mineral surfaces is reduced at high stone contents.

Turnover models for SOC like the RothC-model are more and more initialized on the basis of measurable SOC pools: black carbon (BC), particulate organic matter (POM), and humified organic matter (Skjemstad et al., 2004; Zimmermann et al., 2007). Varying chemical (Skjemstad et al., 1993; Brodowski et al., 2005), physical (Christensen, 1996; Feller and Beare, 1997), physico-chemical (Six et al., 2000), and isotope-based (Rethemeyer et al., 2007; Amelung et al. 2008) isolation procedures have been applied to calibrate and test SOM turnover models. Recently, advances in fast screening detection methods like mid-infrared spectroscopy coupled with partial least squares regression (MIRS-PLSR) also allowed quantifying these parameters in

large quantities and at high spatial resolution (e.g., Zimmermann et al., 2007; Bornemann et al., 2008, 2010).

Soil clay minerals and pedogenic oxides have been identified as important parameters regulating the storage of SOC by mineral associations (Chenu and Plante, 2006; von Lützow et al., 2006; Wiseman and Puttmann, 2006). Mineral associated SOC is thereby effectively sequestered and is characterized by slower turnover rates in soil carbon models compared to POM fractions (Balesdent et al., 1987; Skjemstad et al., 2004; von Lützow et al., 2007). Also the potential for SOC storage by micro-aggregation is significantly affected by clay and silt contents (Mayer et al., 2004), turning texture into key factor of C saturation concepts. Results of Kölbl and Kögel-Knabner (2004) showed that even at field scale, the amount of SOC stored as occluded POM may reveal a significant spatial variability, depending on the spatial variation of the clay content. Results of Bornemann et al. (2010) confirmed that the amount of coarse POM in FE can be highly heterogeneous throughout a single agricultural site which was homogeneously managed but also contained variable stone contents. However, to my knowledge the relation between SOC pool sizes and the presence of coarse texture has not been considered in detail, yet.

When artificially applying disproportionately high inputs of organic material, Gulde et al. (2008) and Stewart et al. (2007, 2008) found that the storage capacity of individual soils to sequester organic C was limited. In all three studies cited, the observed accumulation of organic matter was addressed to a systematic saturation hierarchy of increasingly stabilized SOC pools. In this respect, chemically and biochemically protected carbon pools have been observed to saturate after incorporation of high amounts of litter, and subsequent C accumulation then proceeded in the rather labile interaggregate-protected or even unprotected POM pools. However, one limitation of such studies is lacking comparability between results of the varying field trial stations as C dynamics are influenced by a range of factors as for instance climatic effects (Amelung et al., 1997; Lal, 2008), hydrology (Meersmans et al., 2008), parent material (Wagai et al., 2008), land use (Soussana et al., 2004), management practice (von Lützow et al., 2002; Metay et al., 2009) and fertilisation (Heitkamp et al., 2009, Sèquaris et al., 2010). This problem could be solved by investigating a single field site

with areas of highly different long-term C inputs to the fine earth.

In this study I investigate the effect of highly variable stone contents on the SOC dynamics in the topsoil of a homogeneously managed agricultural site. I hypothesize that the reduced solum at high stone contents induces saturation of mineral bound SOC like nonPOM and accumulation of weakly decomposed plant material like POM, while BC stocks are less affected.

2 MATERIAL AND METHODS

2.1 Test site

The presented investigations apply to the main test site which is described in section II.1.1. According to the digital elevation model as displayed in Fig. V.1a, the investigated test site can be segmented in three main areas of different geomorphology. The toe of the slope is characterized by a rather plain area reaching up to about 80 m longitude at latitude of zero and about 50 m of latitude at a longitude of 50 m. From here, the inclination reaches to about 180 m of latitude at longitude zero and about 150 m at longitude of 50 m. The remaining summit again represents a plain area. The distinct microrelief of the test site is perceptible by the disproportionately plotted z axis.

Caused by the described geomorphology, also the amount of available solum varies considerably. While at the lower plane, the Aeolian substrate completely covers the underlying sediments from the Rhine and Rur-River systems and only small gravel contents (in the following referred to as "stones") were mixed into the topsoil by soil-fluction, the fluvial deposits with their high stone contents more and more penetrate the Pleistocene loess layer towards the summit where a gravel-stripe crosses the test site in north-western direction. Hence, the varying stone content as displayed in Fig. V.1b roughly reproduces the geomorphologic properties. However, not only the stone content but also the texture of the fine earth (FE) is affected by this change of soil forming substrate. The spatial pattern of the silt content (Fig. V.1c) represents the diminishing loess coverage and is accordingly almost reciprocal to that observed for the stone contents (Fig. V.1b). The sand contents distribute almost complementary to the silt contents as indicated by a strong negative correlation ($R^2 = -0.93$).

2.2 Ground truth measurements

Ground truth measurements were conducted as outlined in section II.2.

2.3 Statistics

Using fuzzy-kappa statistics, automated map comparison of the spatial distributions of all investigated parameters was performed by using the Map Comparison Kit (Visser and de Nijs, 2006). Automated map comparison algorithms like fuzzy-kappa statistics allow for the quantification of similarities between spatial distributions of soil parameters (Bornemann et al., 2010). Multidimensional scaling (MDS) is a complementary statistical procedure for visualization and interpretation of structures within large similarity matrices. The observed similarities, as represented by the distances d_{ij} in a multi-dimensional room, are forced into a much smaller m-dimensional room (usually m=2 or 3) where the Euclidian distances resemble the d_{ij} as good as possible. The "stress" value relates the variance of the disparities of the observed similarities to the spatial distances within the multidimensional space of the MDS. The stress is thus a normalized measure of the variance and the routine quality index of MDS procedures. According to Kruskal (1964) a good representation of the observed similarities is indicated by stress values < 0.2. Multidimensional Scaling (MDS), correlation coefficients after Spearman (φ) and stepwise multiple linear regression models (MLR) were calculated using the software package STATISTICA for Windows. For MLR analyses, BETA values were calculated to quantify the contribution of the individual parameters to the MLR models. BETA values are calculated after datasets have been standardized to m=0 and stdv=1 and are thus independent from the individual units of the varying parameters. Semivariogram analysis was conducted by the software package Vesper (© University of Sydney: Australian Centre for Precision Agriculture).
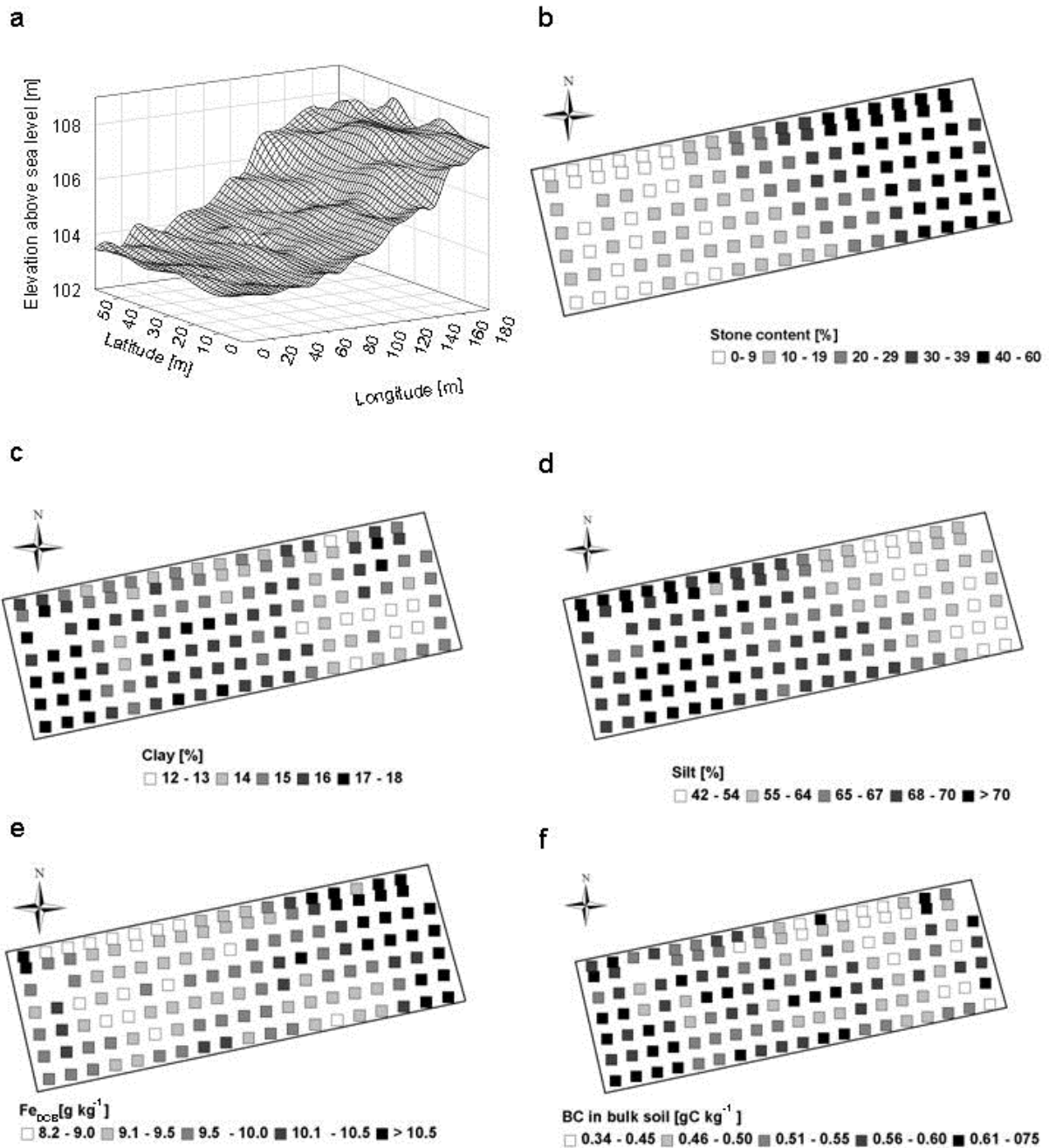
Fig. V.1 Digital elevation model (a), stone content and sampling scheme (b), contents in fine earth of silt (c), clay (d) dithionite soluble Fe oxides (e), and black carbon contents in bulk soil at the investigated test site in Selhausen.

3 RESULTS AND DISCUSSION

3.1 Spatial distribution of POM and nonPOM

Constituting ~71–81% of bulk SOC, nonPOM represented the quantitatively most relevant SOC fraction at this field site. The remaining 19–29 % of total SOC were comprised by the POM fractions, with decreasing proportions in the order POM3 ≥ POM1 ≥ POM 2 (calculated from Tab. V.1). Investigating the potential of mid-infrared

Tab. V.1 Descriptive statistics and statistical parameters of the empirical variograms for the contents in fine earth of soil organic carbon (SOC), particulate organic matter of three size classes (POM1: 2000–250 μm; POM2: 250–53 μm; POM3: 53–20 μm), non-particulate organic matter (nonPOM), black carbon (BC), texture, and dithionite soluble Fe oxides (FeDCB), for the contribution of the individual SOC fractions to SOC in FE, as well as for the stone content, difference of soil moisture between two dates of measurement (δθ), hillslope, and elevation above sea level (ASL).

		mean	min	max	Cv [a]	range[b] [m]	N/S ratio [c]
SOC	[g kg^{-1}]	11.75	8.76	16.85	0.15	30	0.09
POM1	[g kg^{-1}]	0.85	0.59	1.29	0.21	32	0.14
POM2	[g kg^{-1}]	0.68	0.51	1.06	0.17	30	0.67
POM3	[g kg^{-1}]	1.24	0.66	1.86	0.16	28	0.29
nonPOM	[g kg^{-1}]	9.01	6.51	13.09	0.15	32	0.27
BC	[g kg^{-1}]	0.75	0.51	1.23	0.23	48	0.56
Sand	[%]	20.0	12.0	45.7	0.36	55	0.24
Silt	[%]	65.1	41.9	72.6	0.10	47	0.22
Clay	[%]	14.9	11.7	18.3	0.09	32	0.23
Fe$_{DCB}$	[g kg^{-1}]	9.79	8.18	12.15	< 0.01	58	0.41
SOC	[g kg^{-1}]	8.55	5.76	11.06	0.15	52	0.29
POM1	[g kg^{-1}]	0.61	0.37	0.76	0.12	35	0.70
POM2	[g kg^{-1}]	0.49	0.27	0.63	0.14	36	0.39
POM3	[g kg^{-1}]	0.91	0.39	1.38	0.24	52	0.32
nonPOM	[g kg^{-1}]	6.54	4.30	8.62	0.15	50	0.39
BC	[g kg^{-1}]	0.54	0.34	0.75	0.13	60	0.63
Stones	[%]	25.0	3.9	59.4	0.68	58	0.09
δθ	[%]	5.7	2.4	9.8	0.28	34	0.24
Slope	[%]	1.5	0.1	3.8	0.58	n/a[d]	n/a
ASL	[m]	105.2	103.4	108.4	0.01	60	0.18

[a] Coefficient of variation
[b] Correlation length of the empirical semivariogram
[c] Nugget to sill ratio of the empirical semivariogram
[d] Data not applicable for semivariogram analysis

spectroscopy for the fast determination of SOC pools, Bornemann et al. (2010) revealed that bulk SOC, POM1, and POM2 exhibited a close spatial correlation on the investigated site, while POM3 showed a rather independent pattern. The spatial distribution of nonPOM and BC, as well as the effects of other soil properties on these patterns were, however, not investigated by Bornemann et al. (2010).

In the light of the numerous parameters to be compared I computed a similarity matrix employing fuzzy-kappa statistics and visualized the determined similarities applying multidimensional scaling (MDS). As indicated by good to very good stress values (stress 1= 0.065, stress 2= 0.034; Kruskal, 1964), the similarity matrix was reproduced satisfactorily by the Euclidian distances of the first three dimensions of the MDS (Fig. V.2). According to the first dimension, silt exhibited the highest positive values (~2.5), followed by clay (~1.5), and POM3 (0.7). All other parameters were collocated between values of 0 to ~0.6, where two distinct clusters were indicated by dimension two, and three. Besides nonPOM, the first cluster comprised POM1, POM2, and SOC, whose close relation was already indicated by Bornemann et al. (2010). The MDS analysis thus indirectly supported their hypothesis of an independent distribution of POM3, and suggested individual control mechanisms for the distribution of BC. The second cluster included sand, ASL, stone contents, and $\delta\theta$, whose close relation could be explained by the layering of the soil forming substrates and the inter-dependency of $\delta\theta$ and soil texture. However, statistical structure analysis by MDS did not facilitate the direct assignment of individual control variables to the patterns of the investigated SOC fractions.

Parameters that are deterministically dependent can be identified by an identical directional variability. The possibility to differentiate directional variability and stochastic heterogeneity is a prerequisite for the elucidation of any deterministic relation between C dynamics and regulating soil parameters. A classical method for the identification of spatial dependence is the semivariogram analysis (Cressie, 1993).

Due to distinct directional heterogeneity within the data set, I de-trended all determined parameters using second order polynomial functions to meet the requirements of this geostatistical procedure. As summarized in Tab. V.1, the FE contents of all SOC fractions except BC exhibit similar correlation lengths of ~30 m.

Against the background of strong correlations between SOC, POM1, POM2 and nonPOM with stone contents (Spearman´s rank correlation coefficient: φ= 0.75 – 0.85), the correlation length of ~60 m observed for the stone content appears contradictory at a first glance. Anticipating that the varying stone content resembles the main directional trend of the contents of the coarse POM fractions within the FE, the de-trending procedure would largely eliminate this trend before the variogram is calculated. As a result, the spatial distribution of the de-trended data of contents in FE and in bulk soil would be akin and matching correlation lengths could be anticipated. Indeed, the correlation lengths of the coarse POM fractions
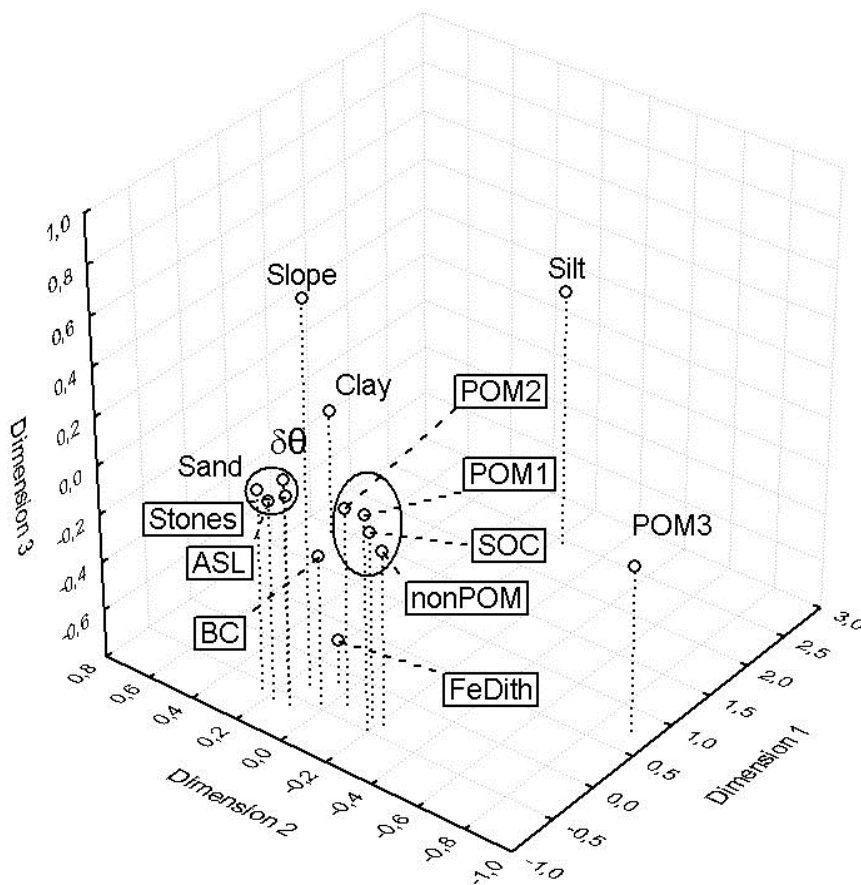
Fig. V.2   Three-dimensional alignment of the Euclidian distances of the investigated soil parameters as derived by a multidimensional scaling procedure of a fuzzy-kappa similarity matrix. Investigated parameters include contents in the fine earth of soil organic carbon (SOC), particulate organic matter of three size classes (POM1: 2000–250 μm; POM2: 250–53 μm; POM3: 53–20 μm), non-particulate organic matter (nonPOM), black carbon (BC), dithionite-soluble Fe oxides (Fe$_{DCB}$), sand, silt, and clay, fine earth contents of stones, difference of volumetric soil moisture between two dates of measurement (δθ), as well as hillsope (slope) and elevation above sea level (ASL).

(POM1 and POM2) remained constant whether the variogram of the FE contents or the contents in bulk soil were computed (Tab. V.1). As there are no mechanisms by which high stone contents could directly enhance the storage of coarse POM, indirect effects as for instance the reduction of the available solum has to be responsible for the observed phenomenon.

A close coherency between $\delta\theta$ and its driving forces, i.e. the delimited solum, high sand contents of the fine texture, and the top-slope location (ASL) was already indicated by the MDS analysis (Fig. V.2). A limited solum and reduced water holding capacity within the very gravelly topsoil likely also delimits microbial degradation, leading to the accumulation of weakly decomposed plant material. There are two indications that suggest $\delta\theta$ to co-determine the spatial distribution of the coarse POM beyond the dominating effect of the variable stone content. Firstly, the correlation lengths of the contents of coarse POM in bulk soil match the one of $\delta\theta$ (Tab. V.1). Secondly, a positive relation is indicated between the stone content and the C/N ratio of the bulk SOC ($R^2 = 0.53$), thereby documenting that SOC in the very gravelly areas of the test site is in deed enriched with weakly decomposed plant litter. Retarded decomposition and disproportionately high biomass input thus likely explain the enhanced contents of POM1 and POM2 in those areas of the test site that comprise high stone contents.

3.2 Carbon storage in dependence of potential storage capacity

In contrast to the coarse POM fractions, the correlation lengths of bulk SOC, POM3, and nonPOM shifted considerably after their contents in FE were transformed by the stone content. The correlation lengths of these fractions (~50m), thus suggest other secondary control factors (apart from the stone content) as indicated for POM1 and POM2. From literature, we know that the storage capacity of a particular SOC fraction is regulated by multiple protective mechanisms (von Lützow et al., 2006). Results of Wiseman and Puttmann (2006) suggest that the interaction of pedogenic Fe (Fe_{DCB}) and Al oxides and clay minerals play an important role for aggregation and stabilization of SOC in soils of temperate climates. According to Mayer et al. (2004), preservation of organic matter by micro-aggregation particularly includes abiotic networks of Fe and Al oxides. For my test site, the highest concentrations of Fe_{DCB} in

FE were located at areas with high stone contents. Nevertheless, elevated contents of Fe_{DCB} also represented a random component in the spatial distribution (Fig. V.1e). Indeed, the correlation length of Fe_{DCB} actually matched that of nonPOM (Tab. V.1). A stepwise multiple regression analysis proved the significant positive influence of Fe_{DCB} on SOC beyond the effect of varying stone contents (Tab. V.2). The SOC storage of the nonPOM, thus in part also resulted from higher Fe_{DCB} contents.

As already pointed out above, POM3 shows the smallest variability among the investigated POM fractions. Hence, the high CV of its content in bulk soil (Tab. V.1) is not founded on the variability of its FE contents, but rather on the variability of the FE contents of the other SOC pools. Accordingly, no close relation to any of the control variables could be identified by statistical structure analysis (Fig. V.2), and even the correlation coefficient to the highly variable stone content did not exceed values of 0.34.

However, akin correlation lenths (~50 m) suggest that the control mechanisms observed for the nonPOM also drive the spatial distribution of POM3. In contrast to the nonPOM fraction, the individual fractionation data revealed that the C content of the isolated POM3 fraction did not change despite changing fraction yield (data not shown). Apparently, the POM3 fraction does thus not only consist of very fine, degraded POM,

Tab. V.2 Multiple linear regression models for the predictions of contents of black carbon (BC), non-particulate organic matter (nonPOM), and particulate organic matter (53–20 µm: POM3) in fine earth, from stone content, contents of dithionite soluble Fe oxides (Fe_{DCB}) in FE, and hillslope (Slope). The asterisks indicate significances at the probability level of p < 0.05.

dependend variable	independend variable	BETA [a]	muliple R^2 [b]
BC	stone cont.	0.73	
[g kg^{-1}]	Fe_{DCB}	0.30	
	Slope	-0.15	0.79*
nonPOM	stone cont.	0.71	
[g kg^{-1}]	Fe_{DCB}	0.15	0.68*
POM3	stone cont.	0.65	
[g kg^{-1}]	Fe_{DCB}	-0.43	0.20*

[a] partial regression coefficients of the data if standardized to mean=0 and stdv=1
[b] coefficient of determination of the multiple regression analysis

but also of SOM attached to the surfaces of coarse silt (20–53 µm) – an assumption that is further backed by matching correlation lengths of POM3 and silt (Tab. V.2).

3.3 Indications for hierarchical saturation of SOC fractions

The concept of hierarchical C pool saturation implies that pools of mineral associated C fractions (i.e. nonPOM) saturate first and additional input of organic material will increase the amount of SOC fractions of larger particle size as soon as the next smaller fraction converges to the point of saturation (Stewart et al., 2007, 2008; Gulde et al., 2008). In line with this concept, nonPOM should saturate first, then POM3, while other fractions may continue to accumulate to a certain degree. According to my findings, the nonPOM fraction is close to saturation and thus also the POM3 fraction may become increasingly saturated as the SOC inputs in the gravelly areas are subjected to a limited volume of FE. The MLR model for the prediction of POM3 from stone content and Fe_{DCB} revealed a negative correlation of Fe_{DCB} to the residual of the correlation between stone content and POM3 (BETA = –0.43; Tab. V.2). This finding points to lower POM3 contents at areas where the storage capacity of the nonPOM fraction is enhanced by elevated Fe_{DCB} contents. In terms of a hierarchical saturation concept this indicates a more efficient C uptake by the nonPOM fraction, taking away the pressure from the POM3 to storage of SOC.

The hypothesis of hierarchical structures concerning the relation between stone content and the individual POM fractions is further backed by a systematic variation of the dependency between stone content and SOC fraction (Fig. V.3). Here, the strong positive relation of the stone content to POM1 successively decreases for POM2, and POM3. In accordance with a proposed hierarchical saturation of individual SOC pools, this points to a steady-state concentration of POM3 while additional organic material is either stored in the coarser POM2 and POM1 or, also in dependence of Fe_{DCB}, within the nonPOM fraction.

Intriguingly, much of the relative distribution of SOC among different particle-size pools can be explained with the concept of hierarchical saturation. The stone content influences the SOC pools because saturation of the FE is reached more rapidly when the FE content is lower at high stone contents.

3.4 Spatial distribution of BC

Processes of C saturation are naturally limited to C species that are formed in situ and depend on the specific environmental conditions of each particular soil. However, soils also contain BC even if they are located offsite from anthropogenic point sources and when vegetation burning is of minor concern as BC deposition also takes place by aerial immission. These immissions are considered to be rather homogeneous throughout larger areas (Brodowski et al., 2007). Comprising about 6 % of the total SOC (calculated from Tab. V.1), BC constitutes an essential SOC fraction on the investigated site. Its individual
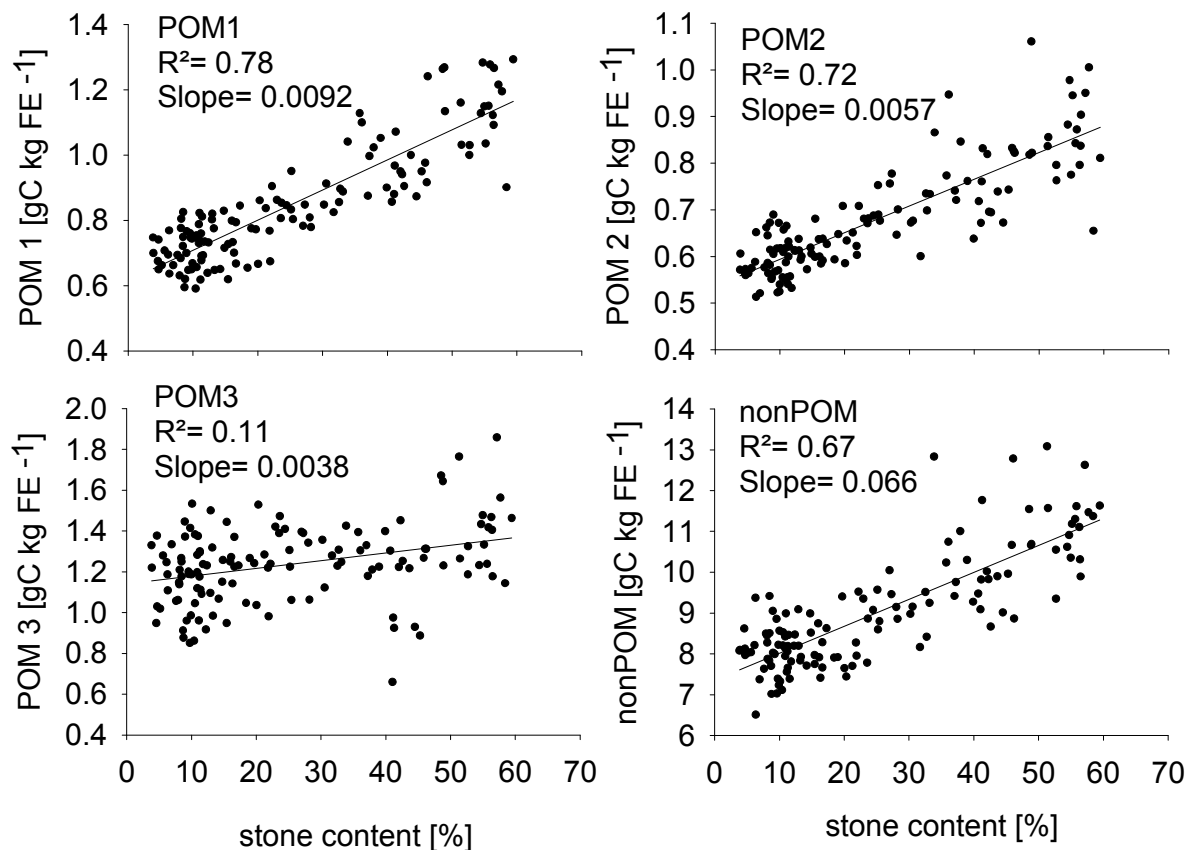
Fig. V.3 **Scatter plots displaying the relation between the stone content and contents of particulate organic matter of three size classes (POM1: 2000–250 µm; POM2: 250–53 µm; POM3: 53–20 µm), as well as non-particulate organic matter (nonPOM) in fine earth at the individual sampling locations of the test site Selhausen, respectively. All regressions are significant at p<0.001.**

spatial distribution is already indicated by the correlation length of its FE contents, which differs from that of all other investigated SOC pools and amounts to approximately 50 m (Tab. V.1).

With respect to the small size of the field plot and generally very slow turnover times of BC (Brodowski et al., 2007; Flessa et al., 2008), I expected the BC stocks to be distributed homogeneously across the whole test site. However, the highly variable stone contents determined the amount of FE to which supposedly homogeneous deposited BC was incorporated (plough layer). Indeed, the variability of the BC contents in FE showed the strongest variability of all SOC fractions (CV= 0.23; Tab. V.1). It was, however, also closely correlated to the stone content (φ= 0.80; data not shown). When related to bulk soil, the CV of BC contents in bulk soil was lower (CV= 0.13). While the latter probably results from a homogeneous deposition and extensive biochemical recalcitrance, the stone content was obviously not the sole deterministic parameter driving the spatial distribution of BC. Figure V.1f shows that despite the lower CV, also the BC contents in bulk soil were not homogeneously distributed. They were low at the upper end of the slope where the site had also high slope gradients. Large BC contents in bulk soil were, in turn, detected at the toe of the slope. With respect to the hillslope position (up to 4° slope gradient, Fig. V.1a), these results suggest that BC from the upslope may have been horizontally transported to downslope positions by erosion. This coherency to erosion processes was also corroborated by corresponding correlation lengths for ASL and BC in bulk soil (Tab. V.1).

In order to investigate a potential influence of erosive translocation on C-pool patterns, I applied γ-spectroscopy to identify ^{137}Cs as an isotopic tracer. Corresponding to the related topography, similar patterns of ^{137}Cs activity were observed for both investigated transects (B and F; Fig. V.4). Lowest ^{137}Cs activities were apparent at the uphill positions of the test site (B18, F17). The activity then increased significantly along the inclined intersections at intermediate positions (B16, F6) and decreased again towards the bottom of the slope (B2, F2). The ^{137}Cs activities even varied along the micro-relief at the sampling points at the upper part of the slope (Fig. V.4: B16, B18, F14, F17). Assuming a fairly homogeneous deposition of ^{137}Cs with the fallout

event of Tschernobyl, the observed ^{137}Cs patterns thus clearly support the assumption that erosion impacted the spatial patterns of BC. Also Rumpel et al. (2006) concluded that a preferential erosion of BC is "a crucial process determining its fate in terrestrial ecosystems". They attributed the potential translocation of BC by water erosion to its small density. Irrigation experiments by Rumpel et al. (2009) revealed that 7–55 % of burned harvest residues were subject to horizontal translocation by splash erosion, which is the first step towards water erosion. Translocation of BC was also observed as a result of downslope tillage by Zhang et al. (2008), who identified significant downslope transport of bulk soil by altered ^{137}Cs signatures of summit and toe slope following repeated hoeing of an orthic Regosol. In my study, multiple linear regression analysis also indicated a significant contribution of the hillslope to the observed spatial pattern of BC (Tab. V.2).

Besides, particularly the coarse POM fractions may also be affected by erosive downslope transport. Yet, the rather short turnover times of POM1 and POM2 likely constrain the detection of spatial patterns originating from eroded POM.
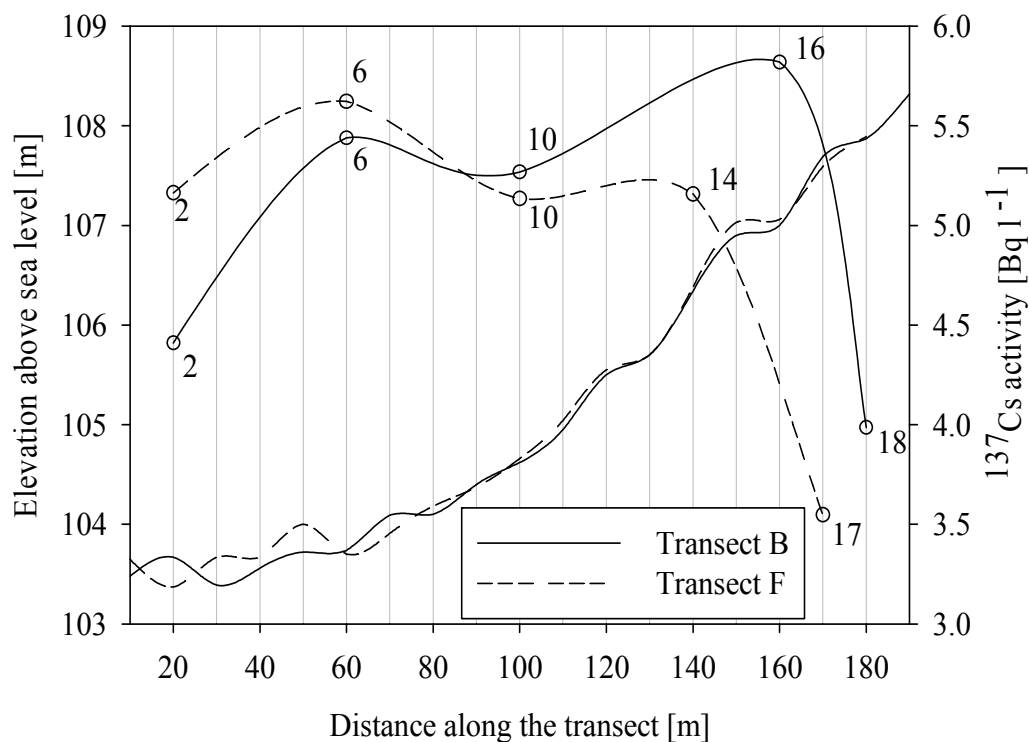
Fig. V.4   Elevation above sea level of the transects B and F (see also Fig. V.1a,b) and corresponding ^{137}Cs activities at five points along the individual transects.

4 CONCLUSIONS

My investigations revealed that variable stone contents on the investigated test site determine the patterns of all investigated SOC fractions. My results also suggest fundamental differences in the underlying mechanisms. High stone contents result in a disproportionately high biomass input to thus smaller volume of FE material. High stone contents also reduce amounts of water in the top soil and the resulting dryness probably prevents rapid SOM decay, thereby promoting the accumulation of POM1 and POM2 in the respective gravely subsites. Smaller FE contents at given biomass input are more prone to saturation processes when stone contents increase. The contents of POM3 and nonPOM within the fine earth are thus likely governed by such C saturation processes. Varying contents of pedogenic oxides additionally influence the C saturation capacity and therewith the spatial distribution of nonPOM. In contrast to the other C pools, patterns of BC are significantly driven by erosion.

VI

Synopsis

1 INTRODUCTION

World estimates for SOC reach from 2300 Gt for belowground organic carbon (1–3 m; Davidson and Janssens, 2006) to 1500 Gt within the first meter of the pedosphere (Eswaran et al., 1993), equalling nearly three times that of aboveground biomass and about twice the amount found in the atmosphere. Indeed, about one third of the worldwide SOC stocks can be found in non-cultivated soils of the tropics and another 25°% is stored in Histosols of which the largest moieties are inherent to swamps and soils of the arctic permafrost region (Jenkinson et al., 1991). The contribution of the spacious boreal forests is estimated at ~180 Gt. While these native ecosystems comprise a considerable proportion of worldwide SOC stocks, there is little opportunity for man induced increase in C sequestration. Actually, the SOC stocks of many ecosystems are subject to dramatic decrease. In the tropics, Brown and Lugo (1984) estimated the potential loss of stored SOC by deforestation and erosion of organic surface horizons at 20–50 %. Permafrost soils are endangered to loose significant shares of the stored C (~400 Gt) by global warming induced thawing, peatlands may diminish by changing water balances and man made drainage.

In view of the poor prospects for an active C sequestration in native ecosystems, efforts for sequestration of atmospheric CO_2 have to concentrate on agricultural environments. Here, the potential for (re-) storage of atmospheric CO_2 is high, as native soils have lost big amounts of SOC upon cultivation (Smith, 2008). In temperate regions, native soils lost 30–50 % of SOC in 50–100 years (Lal, 2008). It appears virtually paradox that our biggest knowledge gaps concerning storage and turnover of SOC apply to arable ecosystems (Prechtel et al., 2009).

While the invention of carbon trading programs and increasing bio-fuel production claim for better estimates of potential C storage in agricultural soils, a database for the site specific definition of baseline values, steady-state C levels, and potential C sequestration is lacking. Previous studies were largely conducted at a limited number of field trial stations and were designed to address specific issues, and individual or modified methods have been applied for soil survey. The resulting poor comparability, however, restricts the interconnection of the gained data sets for large scale surveys (Düwel and Utermann, 2008). The establishment of nation-wide or even world-wide

SOC monitoring programs involves the projection of local soil survey data to considerably larger areas. At this, the field scale heterogeneity of differently stabilized SOC pools and their regulating parameters have to be known in order to account for variable SOC dynamics, e.g. by adapted sampling strategies (McBratney et al., 2003; Mueller et al., 2004), or consideration of spatial variability in SOC turnover modelling (Aiken et al., 1991; Rochette et al., 1991). As efficient methodology for the acquisition of the required comprehensive datasets is currently lacking, the effective parameters that regulate SOC dynamics on the field scale remained precluded until today. Recent studies, however, suggested that besides the storage capacity of the mineral fraction, especially hierarchical saturation of differently stabilized SOC pools determines the storage of SOM in agricultural soils (Gulde et al., 2008; Stewart et al., 2008). My objectives were, *i)* to test the opportunity for rapid MIRS-PLSR based assessment and characterization of BC in the soil environment, *ii)* to evaluate the potential of MIRS-PLSR for the determination of POM and its spatial patterns on the field scale and *iii)* to elucidate the role of hierarchical saturation for the storage of SOC in differently stabilized SOC pools on the field scale.

2 SUMMARY OF THE RESULTS

i) Does MIRS-PLSR provide opportunity for rapid assessment and characterization of BC in the soil environment?

Comprehensive data sets for understanding the global distribution of black carbon (BC) in soil are currently lacking because of the considerable expenditure of time needed for BC analyses. Here I report that reliable screening of soil BC can be achieved using mid-infrared spectroscopy (MIRS) and multivariate data analysis. Calibration models were built employing 309 samples from different soil depths and land-use systems in America, Asia, and Europe, characterized for soil organic carbon (SOC) and benzene polycarboxylic acids (BPCA) as specific BC markers. About 99 % of total SOC variability was explained by local calibrations with an error of prediction < 0.1 g SOC kg^{-1} soil. Also BPCA-C was assessable. The precision was lower (R² > 0.8), partly reflecting different BC quality. A measure of the latter is the mellitic acid-C percentage. It also correlated with spectral absorbtions (R² ≥ 0.6), which thus even allowed a MIRS-based classification of BC according to its degree of condensation.

ii) Is MIRS-PLSR suitable for the determination of POM and its spatial patterns on the field scale?

Modelling global C cycles requires in-depth knowledge about small scale C stocks and turnover processes. Yet, different soil organic carbon (SOC) pools reveal considerable spatio-temporal heterogeneity at the field scale which is scarcely known due to the considerable workload associated with traditional fractionation procedures. Here I investigated the potential of mid-infrared spectroscopy combined with partial least squares regression (MIRS-PLSR) for rapid assessment of different particulate organic matter (POM) pools and their spatial heterogeneity at field scale. Locally calibrated prediction models estimated the contents of SOC, POM of three size classes (POM1: 2000–250 µm; POM2: 250–53 µm; POM3: 53–20 µm), and lignin contents for 129 subsites of a 1.3 ha test field. Relations between the parameters were described using correlation analysis and fuzzy-kappa statistics (κ).

All parameters were predicted successfully by applying local calibrations for MIRS-PLSR (R² = 0.77– 0.96). The prediction model for POM1 chiefly relied on specific signals of lignin and cellulose, contents of POM2 were estimated by spectral bands

assigned to degradation products as aliphatic C–H groups and aromatic moieties; carboxylic groups essentially contributed to the prediction of POM3. There was a close spatial relation between the coarse POM1 and POM2 fractions and lignin ($\kappa = 0.77$), which largely also explained variations in bulk SOC. In contrast, POM3 exhibited a less deterministic pattern in the field, thus contributing little to spatial variation in SOC content.

iii) Is hierarchical saturation a relevant factor for field scale patterns of SOC storage in differently stabilized SOC pools?

Stones are basic constituents of the pedosphere and may severely reduce the amount of fine earth per soil volume. However, little attention has been paid to the role of reduced solum on soil C dynamics. This study was designed to quantify the effect of variable stone contents on spatial patterns of bulk soil organic carbon (SOC), particulate organic matter (POM) of three size classes, non-particulate organic matter (nonPOM), and black carbon (BC). One-hundred and twenty-nine soil samples (0–30 cm) were taken in a regular grid on an arable field (1.3 ha) nearby Selhausen (Germany). The weakly inclined site featured a strong gradient in stone contents, soil types covered Dystric Leptosols, Orthic Luvisols, and Stagnic Luvisols. In addition to C-pools patterns and stone contents, we determined texture, Fe oxides, soil moisture, as well as hillslope and elevation above sea level. Additionally, ^{137}Cs measurements were conducted to indicate soil erosion.

Multiple regression analysis indicated BETA values of 0.65–0.73 between stone content and BC, nonPOM, and the finest POM. Also C contents of the coarse POM fractions were positively correlated with the stone content ($R^2 = 0.72$–0.78) and their spatial patterns were assumed to be caused by disproportionate input of plant litter to a reduced solum. Statistical structure analysis and variography pointed to hierarchical C saturation of nonPOM and POM3, which was additionally regulated by Fe-oxide contents. Erosive translocation affected only the spatial distribution of BC (BETA= – 0.15). Varying stone contents thus crucially affected all investigated SOC pools.

3 SYNTHESIS

The results of sections III and IV proved the applicability of MIRS-PLSR for simultaneous quantification and qualitative description of differently stabilized SOC pools. At this, local calibrations were continuously superior to calibrations including a wide variety of different samples. The use of specialized calibration sets allowed for improved prediction qualities and revealed qualitative aspects of the targeted SOC fractions. While the flexibility of the PLSR technique gives opportunity for the assessment of SOC fractions from different soils which may be determined by various methods, the superiority of local calibrations simultaneously focuses its use to studies where representative calibration samples are available.

Irrespective of the method applied for quantification and characterization of any relevant SOC pool, the key for an effective SOC monitoring is a periodic screening with sufficient accuracy to detect SOC changes in relevant time frames. The investigated test site in Selhausen was explicitly chosen with regard to its considerable field scale heterogeneity and proved to be an ideal choice to demonstrate the detectability of spatial patterns of organic and inorganic soil constituents employing MIRS-PLSR. As outlined in section V, the different SOC pools in the employed test site are subjected to explicitly variable properties of the mineral phase, and as a reason of this, express a higher variability as compared to a sample set of 27 loess soils taken all across North-Rhine-Westphalia (section IV).

In comparison to the variability on the investigated test site in Selhausen, the response of SOC pools on changes in management practice is usually considerably lower (Blanco-Canqui and Lal, 2004). The possibility for the detection of such effects in reasonable time frames by employing non-specific calibrations for MIRS-PLSR may thus be limited by lacking accuracies of prediction. In the past, alternative statistical methods to PLSR have been applied for the extraction of information from sets of infrared spectra of soil samples. These methods included neural networks (Fidencio et al., 2001; Daniel et al., 2003), wavelet analysis (Jahn et al., 2006), multivariate adaptive regression splines (Shepherd and Walsh, 2002), and others (Viscarra-Rossel et al., 2006). However, none of these procedures consistently outperformed PLSR, leaving it as the most popular technique for analysis of MIRS spectra until today. In

defiance of that, enhanced prediction accuracies of soil properties from MIR spectra can be anticipated by the application of specialized sample sets for calibration (sections III; IV; Linker et al., 2006). A set of ideal calibration samples comprises an unchanged matrix with varying quantities of the targeted property (Haaland and Thomas, 1988b). The high number of samples taken for large-scale monitoring programs would allow for the composition of specialized sample sets with regard to soil types and soil genesis, thereby allowing for higher accuracies of prediction. Finally, the periodic re-sampling of georeferenced sites as claimed for the implementation of national SOC inventories (Prechtel et al., 2009) would further improve the attainable accuracies of a MIRS based carbon pool assessment. The technical infrastructure to handle such large numbers of samples is already given: full automated spectrometer hardware facilitates 24h operation, while automated sample recognition and application of best suited calibration models is implemented in spectroscopic software-packages. In summary, MIRS-PLSR has proven its ability for identification and quantification of bulk SOC, physically separated particulate organic matter pools, and BC. Its capability to handle large numbers of samples at low running costs makes it a well suited analytical instrument for national and international SOC inventories.

While SOC is presumed to be a continuum of related material rather than a series of discrete pools (Paul et al., 2006) there is consensus that the identification and quantification of SOC stored in meaningful soil carbon fractions is a prerequisite for any SOC surveying or carbon trading programs (Olk and Gregorich, 2006; Prechtel et al., 2009). Possible modes for stabilization of SOC include physical, chemical, and biological aspects. At this, especially physical fractionation procedures have been shown to display effects of varying management practice at appropriate timescales in quantity and quality (Christensen, 2001; Six et al., 2004; Gregorich et al., 2006). Physically uncomplexed organic matter responds most quickly to changes in land management as it is mainly comprised by unaltered plant material (Gregorich et al., 1996). The similarity of their spatial distribution (see sections III, IV) and an improved MLR model (see section V) would legitimate the combination of POM1 and POM2 for purposes of SOC monitoring. The structural information gained by the PLSR

loading weights of the MIRS-PLSR predictions, however, revealed well defined structural differences between POM1 and POM2. As also the influence of the regulating soil parameters (Section V) was variable, a separate examination of POM1 and POM2 would still be mandatory for future studies aiming at elucidation of turnover processes.

Structural composition and spatial distribution of POM3 differed substantially from those of the coarse POM fractions. While the latter is in contradiction with results of Amelung et al. (1999) who identified similar characteristics of POM2 and POM3 for grassland soils, it confirms the findings of Skjemstad et al. (2004) and Zimmermann et al. (2007) who successfully applied the 2000–53 µm boundary for initialization of the RPM pool in the Roth-C turnover model. However, although these results suggest that the 53–20 µm fraction should not be referred to as POM, its separate isolation facilitated the identification of saturation processes of nonPOM. The possibility for calculation of a complementary nonPOM fraction opens up opportunities for estimations of long term sequestration potential by combining information of actual fraction-C contents and the mineralogy of the nonPOM fraction (Section V). Applying scanning electron microscopy, Brodowski et al. (2005) evidenced organo-mineral interactions between BC and heavy mineral fractions. Particles of varying morphology were identified across different physical particle size fractions, indicating that BC from different sources is not selectively enriched (Brodowski et al., 2005). Despite the possibility to characterize BC in soil by means of MIRS-PLSR (Section III), an estimation of its distribution across physical particle size fractions thus remains precluded. A homogeneous distribution of BC contents among all individual SOC fractions should thus be anticipated in C turnover modelling.

Until today, the considerable expenditures of time and money restricted the feasibility of studies on the field-scale heterogeneity of different SOC pools to small sample sets. The results presented in chapter V were only attainable by application of MIRS-PLSR for the rapid acquisition of a comprehensive data set. My results indicated that hierarchical saturation of differently stabilized SOC pools can indeed be a relevant factor governing the spatial distribution of nonPOM and POM3 on the field scale. Moreover, the elucidation of the effective parameters discovered that multiple factors

simultaneously determine the SOC storage within individual SOC pools. The complexity of the system thus enforces the acquisition of sufficient background information to draw conclusions on SOC dynamics or the C sequestration potential of a particular soil from SOC pool measurements. The latter was demonstrated by the inverse pattern of the SOC contents in FE and in bulk soil (section V).

The relevance of the heterogeneity of individual SOC pools can be demonstrated by projecting the data to larger areas. In appendix A, I demonstrate the effect of different soil pre-treatments (ultrasonic vs. chemical dispersion) and physical POM size classes on CO_2 emissions as predicted by the Roth-C turnover model. Just by combining individual particle size thresholds and fractionation techniques, the cumulative differences in modelled CO_2 emission may rise up to almost 10 % of the total C loss. The spatial heterogeneity of the POM pools on the test site in Selhausen, however, exceeds the differences as modelled in appendix A by several times (POM1: more than tenfold, POM2: approx. threefold, POM3 approx. sevenfold). The ignorance of spatial heterogeneity on the field scale may thus lead to considerably over- or underestimations of soil born CO_2 emissions in C turnover modelling.

Applying the presented methods I was able to detect spatial patterns of individual SOC pools, and to identify regulating parameters and processes that lead to the observed field scale heterogeneity. This heterogeneity may be linked to heterotrophic soil respiration by application of geostatistical procedures that allow the use of multiple covariates. A short introduction on field scale heterogeneity of heterotrophic soil respiration and methodical approaches for their prediction and mapping are given in appendix B. The application of external-drift kriging for the prediction of heterotrophic soil respiration on the investigated field from the determined SOC pools (POM, nonPOM, and BC), however, improved the predictions by only 3–12 % (Herbst et al, in prep.). As also the gain of prediction quality by stochastic simulation using simulated annealing was immaterial, the results of Herbst et al. (in prep.) challenge the sufficiency of the determined SOC fractions for enhanced predictions of soil born CO_2 respiration.

4 OUTLOOK

While my results demonstrated that the spatial distribution of different SOC pools can be regulated by multiple processes, the determination of SOC pools like POM, nonPOM, and BC may not be sufficient for the prediction of soil respiration. In fact, the discrimination between factors regulating soil respiration on different time scales is a prerequisite to identify the potential of POM pool measurements for predictions on soil born CO_2 emission. While POM pools exhibit variability in the time scale from seasons to years, the microbial biomass, as for instance determined upon chloroform fumigation, has been proposed to be a suitable parameter reflecting actual soil respiration (Ocio and Brookes, 1990; Smith et al., 2002). Previous work has shown that also microbial biomass and measures of biological activity are predictable by MIRS (Reeves et al., 2001). Beyond that, a combination with partial combustion of soil samples for identifying thermo-labile SOM appears to be promising for the identification of potentially degradable SOM (Dorodnikov et al., 2007). Representing readily accessible SOC, also water extractable soil organic matter (WESOM) can be an indicator for actual microbial activity (Chantigny, 2003). The possibility for MIRS-transmission measurements of inspissated aqueous soil extracts on silica plates thus offers further opportunity for a rapid quantification of additional control parameters for short-term variability of soil respiration.

The simultaneous assessment of indicators for soil respiration on different spatial and temporal scales in soil (e.g. microbial activity, WESOM, POM), together with temporal series of local CO_2 efflux measurements by using soil-chambers, combined with spatially averaged measurements employing the eddy-covariance method would provide the basis to identify the participation of POM in actual soil respiration. Without the possibility to distinguish between respiration from readily decomposable material like WESOC and slowly turning pools like POM, the elucidation of the chain of causes between actual CO_2 evolution and deterministic soil properties will remain precluded. At this, also the opportunities of stable isotope chemistry should be used: altered $\delta^{13}C$ signals of recently incorporated C4 plants can be identified if soils were formerly cropped with C3 plants (Balesdent et al., 1987); $\delta^{18}O$ measurements allow to distinguish between soil carbonates and soil organic matter as sources for soil-born

CO_2 emissions (Cerling, 1984). Finally, patterns that are observed in the field could be backed up with long-term incubation studies in the laboratory (analyses of soil respiration).

VII

Appendix A

Role of particulate organic matter isolation for estimating CO_2 release from soils

On the basis of :

Bornemann[a], L.; Sequaris[b], J.-M.; Welp[a], G.; Amelung[a], W.; Herbst[b] M. (2010)

[a] Institute of Crop Science and Resource Conservation – Soil Science and Soil Ecology, University of Bonn, Nussallee 13, 53115 Bonn, Germany

[b] Agrosphere, ICG–4, Forschungszentrum Jülich GmbH, 52428 Jülich, Germany

Manuscript in preparation

1 INTRODUCTION

Concepts for modelling carbon turnover usually partition soil organic matter into discrete pools with different turnover times (Smith et al., 1997). Several attempts were made to approximate the modeled pools by measurable soil fractions (Smith et al., 2002; Skjemstad et al., 2004). Particulate organic matter (POM), for instance, is a proxy for the so-called slow C pool in the RothC approach (Zimmermann et al., 2007). Yet, the procedures used for soil dispersion and subsequent POM isolation vary among scientists and little is known how the order of magnitude in modeled C turnover is affected by the fractionation procedures and boundaries for the assessment of the initial C pool sizes (Trumbore and Zheng, 1996; Sohi et al., 2001; Kölbl et al., 2005). My objective was, therefore, to document the effect of different soil pre-treatments (ultrasonic vs. chemical dispersion) and physical POM size classes on the initial pool sizes and modeled C turnover.

2 MATERIAL AND METHODS

Two sample sets were fractionated into three POM classes (fine: 20–53 μm, intermediate: 53–250 μm, and coarse: 250–2000 μm) using ultrasonic (Amelung and Zech, 1999) and polyphosphate dispersion (Cambardella and Elliott, 1992). Sample set 1 comprised twelve Luvisol samples of a heterogeneous arable site in Selhausen, Germany (50°52′09.34′′N; 6°27′00.58′′E; Bornemann et al., 2008). For means of diversification, a second set with soils of Germany included two Gleysols and two Stagnosols under forest, two Stagnosols under grassland, four samples of an artificially bare Arenosol (Bornim experimental plot; Herbst et al., 2008), as well as a Chernozem and a Cambisol under arable management. Bulk soil samples were air dried and material >2 mm was removed. For chemical dispersion, 10 g of soil was shaken on a flat-bed shaker overnight in 50 ml sodium-polyphosphate solution (5 g l^{-1} $[NaPO_3]_n$). For physical dispersion, samples were gently sonicated (60 J ml^{-1}) for coarse-sand (>250 μm) isolation (Amelung and Zech, 1999). The filtered remnant was sonicated a second time at 240 J ml^{-1}. For both procedures, the three POM fractions were isolated by wet sieving. Organic carbon contents (OCC) of bulk samples and fractions were determined by elemental analysis (ISO10694, 1995).

The fractionation data were used to initiate the SOILCO$_2$-RothC model, which is a coupled CO_2 flux and carbon turnover model (Herbst et al., 2008). The calculated respiration flux at the surface, as an integral signal, equals the carbon loss of the pools distributed over the whole soil profile. Based on a validated model run with SOILCO$_2$-RothC for the Bornim experimental plot, four scenarios were established for the four Arenosol samples. All boundary conditions and parameters were identical to the original model run (Herbst et al., 2008), except for the input of fresh plant material which was omitted for the scenarios in order to focus on the effect of the carbon pool initialization. Further, eight years of meteorological data were looped twice to provide an adequate period for modelling.

According to Skjemstad et al. (2004) the 53–2000 μm POM fraction can be used as a surrogate for the RothC pool of resistant plant material (RPM). However, Amelung et al. (1998) found that the POM fractions of 20–50 μm and 50–250 μm were chemically identical. With respect to these results, the lower threshold of 53 μm for the RPM pool remains questionable. I tested the impact of the two particle size boundaries (53–2000 μm and 20–2000 μm) as well as the two dispersion methods (polyphosphate and ultrasonic) on the cumulative CO_2 output. For each scenario, the stable carbon humus pool (HUM) was calculated from SOC after subtraction of the estimated inert organic pool (IOM) and microbial carbon pool (BIO) (Herbst et al., 2008) while it was assumed that the decomposable plant material pool (DPM) was zero.

3 RESULTS AND DISCUSSION

The mean differences (δm) of fractionation yields (soil mass distribution) indicate that for both sample sets, more material was gained by ultrasound in the fine (20–53 μm) POM fraction than was gained by chemical dispersion (Tab. VII.1).

The differences for the intermediate (53–250 μm) fraction were inconsistent and those for the coarse fraction (>250 μm) were not significant. In contrast, more organic carbon remained in the coarse fractions using ultrasound dispersion, while this carbon was lacking in the intermediate fraction. Different axis intercepts suggest that a translation of the results of one dispersion procedure into those of the other is difficult.

According to the different fractionation results I set up four different scenarios to be

used in the SOILCO2-RothC approach. The cumulative respiration of three of the four scenarios is displayed in Fig. VII.1. Due to the large overlap with the scenario "ultrasonic 53–2000 µm" I omitted the scenario "polyphosphate 20–2000 µm" in Fig. VII.1 for means of clarity. In all scenarios, respiration decreased during the 16 years because there was no plant input implemented into the model and the RPM pool was thus predetermined to run empty. Due to its relatively short half life of 2.3 y, the RPM pool depleted almost completely after six to seven years and respiration was now mainly fed by the more stable pools. For the 53–2000 µm fractionation scheme, the differences in the modeled cumulative CO_2 release over 16 years between the scenarios 'polyphosphate' (15.62 t ha^{-1}) and 'ultrasonic' (16.31 t ha^{-1}) are lower (4 %), compared to the 20–2000 µm particle size threshold ('ultrasonic': 17.33 t ha^{-1}; 'polyphosphate': 16.33 t ha^{-1}). Here, the data provided by the ultrasonic procedure indicates a carbon loss that is ~6 % higher as the data indicated by the polyphosphate alternative. However, combining thresholds and fractionation techniques, the cumulative differences may rise up to almost 10 % of the total C loss. The concern of these differences becomes especially evident by an exemplary projection of the gained data. According to the model results, the difference in estimated CO_2 loss by either "polyphosphate 53–2000 µm", or "ultrasonic 20–2000 µm" scenario would be 1.71 t ha^{-1} within 16 years.

If this data is extrapolated to the potential arable land of $4.14*10^9$ ha in the world (FAO, 2000), these differences would sum up to ~$1.9*10^9$ t of emitted C within 16 years. As reviewed by Davidson and Janssens (2006), Jones et al. (2005) estimated the potential worldwide C loss of SOC down to 1 m depth to be about $43*10^9$ t in 95 years, which equals $7.2*10^9$ t within 16 years. While Jones et al. (2005) admit that their study was limited by some generalized assumptions, my experiments indicate that the assessment of the initial RPM pool on the basis of two different fractionation schemes may already result in differences as high as 26 % of the total estimated SOC loss.

VII Appendix A: Role of POM isolation for estimating CO_2 release from soils

Tab. VII.1 Statistical comparison of ultrasonic and polyphosphate fractionation

Sample set[a]	Size fraction μm	Method	Mean g kg⁻¹ soil	Min g kg⁻¹ soil	Max g kg⁻¹ soil	CV[b] %	δm[c] g kg⁻¹ soil	b[d]	a[e] g kg⁻¹ soil	R²
			Soil mass distribution (SMD)							
1	20–53	Ultrasonic	337	179	412	2.3	32.2***	1.16	−17.04	0.86
		Polyphosphate	305	179	360	2.5				
	53–250	Ultrasonic	123	111	142	2.9	9.3**	0.50	65.61	0.48
		Polyphosphate	113	100	142	2.1				
	250–2000	Ultrasonic	110	52	311	6.2	5.3[n.s.]	1.15	−10.23	0.96
		Polyphosphate	105	53	257	3.5				
2	20–53	Ultrasonic	147	65	324	6.5	6.5*	1.02	4.10	0.99
		Polyphosphate	141	72	320	5.4				
	53–250	Ultrasonic	251	50	599	1.8	−30.7**	1.09	−55.21	0.99
		Polyphosphate	282	58	630	4.4				
	250–2000	Ultrasonic	127	22	221	9.6	−5.1[n.s.]	1.11	−20.2	0.92
		Polyphosphate	132	19	206	9.0				
			Organic carbon content (OCC) g kg⁻¹ fraction	g kg⁻¹ fraction	g kg⁻¹ fraction	%	g kg⁻¹ fraction		g kg⁻¹ fraction	
1	20–53	Ultrasonic	2.9	0.5	5.2	4.1	0.6**	1.04	0.44	0.89
		Polyphosphate	2.3	0.4	5.3	9.0				
	53–250	Ultrasonic	4.5	0.7	9.7	5.6	−3.7**	0.71	0.10	0.96
		Polyphosphate	6.2	0.7	12.1	2.6				
	250–2000	Ultrasonic	7.8	0.8	17.6	11.7	1.6**	1.29	−1.6	0.94
		Polyphosphate	6.2	0.7	13.3	12.0				
2	20–53	Ultrasonic	13.9	0.9	49.8	6.0	−2.1[n.s.]	0.75	1.92	0.98
		Polyphosphate	16.0	0.4	69.8	12.0				
	53–250	Ultrasonic	16.6	0.0	55.9	6.6	−10.1*	0.62	0.03	0.91
		Polyphosphate	26.7	0.0	87.2	3.5				
	250–2000	Ultrasonic	32.5	0.0	152	6.2	7.8[n.s.]	1.35	−8.7	0.98
		Polyphosphate	24.7	0.1	104	4.1				

[a] set 1: twelve samples of an arable luvisol; set 2: twelve samples of various soil types and land cover

[b] coefficient of variation (repetition: n = 2)

[c] absolute difference of the mean values and the level of significance (T-test for paired data sets)

[d] gradient of the regression slope (dependent variable in regression analysis: OCC and SMD obtained from ultrasound treatment)

[e] axis intercept of regression (dependent variable in regression analysis: OCC and SMD obtained from ultrasound treatment)

[f] linear regression of OCC and SMD contents between "polyphosphate" and "ultrasound" fractionation
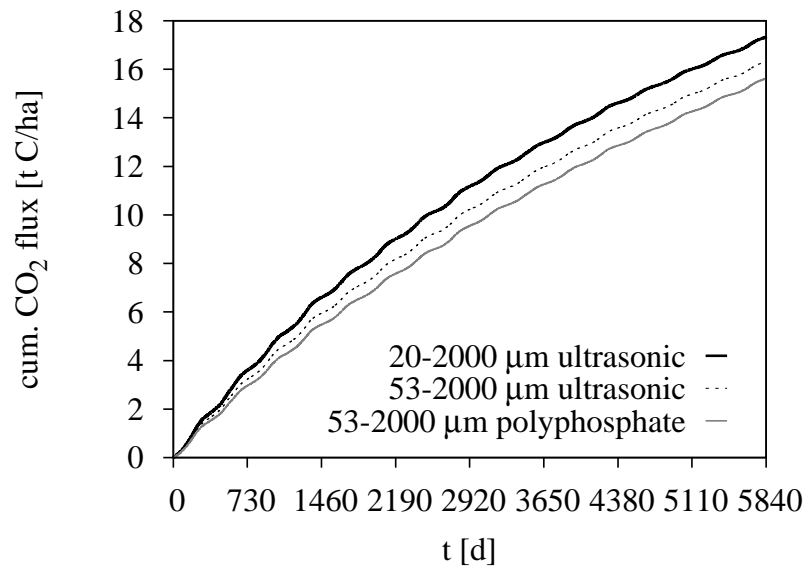
Fig. VII.1 Cumulative heterotrophic respiration flux of an Arenosol soil profile for 16 years according to three different scenarios of POM fractionation.

VIII

Appendix B

The use of covariates for the detection of field scale variability in heterotrophic soil respiration

1 INTRODUCTION

It is generally recognized that soils heterotrophic and autotrophic respiration components bare an essential spatial variability at field scale, even within land use or soil taxonomic units (Kravchenko and Hao, 2008; Herbst et al., 2009; Martin et al., 2009). This tremendous spatial variability was detected at an early stage (Aiken et al. 1991; Rochette et al., 1991; Dugas, 1993) and basically every scientist trying to measure chamber-based soil respiration has to tackle this problem. For specific land covers like a pine plantation (Fang et al., 1998), an oak-grass savanna or agricultural fields (Rochette et al., 1991; Han et al., 2007) parts of this spatial variability in soil respiration could be attributed to the spatial pattern introduced by natural topologies or planting certain geometries like crop rows. However, even only bare soil (heterotrophic) respiration shows a considerable spatial variability (Dugas, 1993; La Scala et al. 2000; Herbst et al., 2009; Graf et al., 2010).

Soil properties like organic carbon content (Kravchenko and Hao, 2008) or C:N ratio (Khomik et al., 2006) as well as state variables like soil temperature and soil water content (Aiken et al., 1991; Foti et al., 2008) were used to explain the spatial pattern in respiration. Experimentally determined soil organic matter fractions are increasingly used as a proxy for pool sizes in turnover models (Smith et al., 2002; Skjemstad et al. 2004, Leifeld et al. 2007). Linked to the spatial variability this would indicate high respiration rates at those locations, which show larger amounts of labile organic matter, since the high turnover of the labile carbon would cause higher CO_2 emissions. However, experimental evidence of this spatial coherence could not be found in literature yet. In one study the spatial pattern of a rather labile carbon fraction, potentially mineralizable carbon, was investigated at large field scale (Yanai et al., 2005), but without linking this to local CO_2 flux measurements.

The effect of spatial autocorrelation of environmental variables like soil respiration is twofold: On the one hand, spatial autocorrelation needs to be taken into account in case uncorrelated samples, e.g. in order to derive a representative spatial average value, are intended (Herbst et al., 2009). On the other hand, it allows the application of geostatistical mapping techniques. However, all studies using this approach for respiration measurements are limited to kriging techniques without using covariates

(Kosugi et al. 2007, Konda et al., 2008; Panosso et al., 2009), which generally have some essential disadvantages in terms of reproducing the variogram and the probability density function of the original point data (Gooveaerts, 2000).

Naturally, chamber-based measurements of soil CO_2 efflux bare a certain inaccuracy (Pumpanen et al., 2004). Among all the sources of measurement errors, the small surface area covered by the chamber in relation to the underlying spatial variability seems to be one of the major drawbacks. This probably also explains the rather large nugget effect detected in almost all of the studies applying variography to chamber-based respiration measurements (Konda et al., 2008; Panosso et al., 2009).

2 STATISTICAL INSTRUMENTATION

2.1 Variography and kriging

Spherical variogram functions can be fitted to the experimentally determined semivariances,

$$\gamma(h) = \begin{cases} c_0 + c_1 \left[1.5 \dfrac{h}{a} - 0.5 \left(\dfrac{h}{a} \right)^3 \right] & for \quad h \le a \\ c_0 + c_1 & for \quad h > a \end{cases} \tag{1}$$

where h is the separation distance, c_0 is the nugget, c_1 is the structural semivariance and a is the spatial auto-correlation range. In the following the nugget effect is referred to as the ratio between the nugget and the total sill ($c_0 + c_1$; Cambardella et al., 1994). Prior to the computation of the variograms and the kriging the data of the co-variates has to be spatially detrended for variables that exhibit a strong spatial trend in slope direction. The latter can be done with linear regressions between the variable values and the x coordinate. After applying the geostatistical procedures, the linear trend has to be added back to the estimates.

Kriging estimates are a kind of weighted mean of the neighbouring sampling location values. The weights λ_i are usually chosen according to the semivariance γ as a function of distance h (Eq. 5) between prediction location x and the neighbouring sampling location values x_j,

$$\begin{cases} \displaystyle\sum_{i=1}^{n} \lambda_i \gamma(x_j - x_i) + \mu = \gamma(x_j - x) & j = 1,...,n \\ \displaystyle\sum_{i=1}^{n} \lambda_i = 1 \end{cases} \tag{2}$$

where μ is the Lagrange parameter. Ordinary kriging may be extended to external drift kriging by Ahmed and DeMarsily (1987). A co-variable $Y(x)$ is assumed to be linearly related to the target variable and in order to minimize estimation variance under this assumption, the linear equation system can be modified to

$$\begin{cases} \sum_{i=1}^{n} \lambda_i \gamma(x_j - x_i) + \mu_1 + \mu_2 Y(x_j) = \gamma(x_j - x) \qquad j = 1,...,n \\ \sum_{i=1}^{n} \lambda_i = 1 \\ \sum_{i=1}^{n} \lambda_i Y(x_i) = Y(x) \end{cases} \qquad (3)$$

with the Lagrange parameters μ_1 and μ_2. Ordinary and external drift kriging can for instance be performed by the KT3D-routine of the Geostatistical Software Library (Deutsch and Journel, 1998).

Cross validation procedures allow to quantify the improvement of using covariates in the estimation procedure. A cross validation is typically applied to small data sets, like in this study, for which a Jack-knife validation is not possible since splitting the data into an estimation and a validation set would cause a change in the estimation model. Models based on a relative small number of observations are more sensitive towards further removal of data than models developed from larger data sets. With cross validation, the prediction performance is simply checked by dropping actual data one at a time and estimating the properties of the location from the co-variables and the neighboring data. This allows for computation of the error between the measurements and estimation for every sample location. In the first step, the root mean square error $RMSE$ between estimates and measurements is computed according to

$$RMSE = \sqrt{\frac{1}{n} SSE} \; . \qquad (4)$$

In the second step, the relative improvement I_r is calculated according to Simbahan et al. (2006),

$$I_r = \frac{RMSE_{OK} - RMSE_{EDK}}{RMSE_{OK}} \qquad (5)$$

where the index denotes the $RMSE$ for the reference ordinary krging OK or external drift kriging EDK. In case I_r is positive, the precision of the evaluated method is superior to the reference.

2.2 Stochastic simulation by simulated annealing

In a stochastic simulation rather the reproduction of basic features of the measured data is approached than an optimum estimation at unsampled locations. There are several algorithms available like e.g. sequential gaussian simulation or the turning bands method. An algorithm that is able to efficiently perform multi-criteria stochastic siumlations is the simulated annealing (Deutsch and Journel, 1998). This is a global optimization technique, based on an anlogy with the physical process of annealing. Roughly, there are five steps involved:

1. An initial candidate realisation is created by assigning a random value at each grid node by drawing from a prescribed population.

2. An objective function is computed to measure the difference between desired spatial features and those of the candidate realisation. In this study, three criteria were used in the objective function. The cumulative distribution $F^*(z)$ of the stochastic simulation should match the prespecified cumulative distribution $F(z)$ for a number of z values

$$O_h = \sum_z [F^*(z) - F(z)]^2.$$ (6)

The prespecified variogram $\gamma(h)$ should also be reproduced by the variogram of the stochastically generated realisation $\gamma^*(h)$

$$O_s = \sum_h \frac{[\gamma^*(h) - y(h)]^2}{\gamma(h)^2}.$$ (7)

The division by the square of the model semivariogram can be introduced to give more weight to the semivariance reproduction for small distances (Larocque et al., 2006). The use of a conditional distribution allows the realisations to be constrained to a secondary variable,

$$O_c = \sum_{i=0}^{n_s} \sum_{j=0}^{n_p} [f_i^*(j) - f_i(j)]^2$$ (8)

where ns and np are the number of secondary and primary classes; fi(j) is the conditional distribution of the primary variable (j = 1,…,np) given that the collocated secondary variable is in class i. The overall objective function value O is computed as the weighted sum of the three criteria

$$O = \varpi_h O_h + \varpi_s O_s + \varpi_c O_c.$$ (9)

The weights were set to 1.0, 5.0 and 1.0 for ώh, ώs and ώc, respectively.

3. The realisation is perturbed by swapping pairs of values taken at random locations.

4. The perturbation is accepted in case the objective function value is decreased; it is accepted with a certain probability even if the objection function value increased, which is done to avoid local optima.

5. The perturbation procedure is looped, while the probability with which unfavourable swaps are accepted is reduced until a minimum objective criterion is achieved.

For further details on simulated annealing in a geostatistical context refer to Deutsch and Cockerham (1994) and Deutsch and Journel (1998).

According to Leuangthong et al. (2004) minimum criteria exist that should be met by geostatistical simulations. First of all, the data values must be reproduced at their locations. Secondly, the distribution of the stochastic simulation should match the distribution of original data. This was checked using the cumulative probability density function by comparing the fractions of values of the original data and the stochastically generated cumulative probability density function (ccdf) $\hat{F}(u,z\,|\,(n))$ in p-probability intervals (PI) (Deutsch 1997; Goovaerts, 2001). Knowing the ccdf allows to compute the symmetric p-PI bounded by the *(1-p)/2* and *(1+p)/2* quantiles for any cumulative probability *u*. Knowing the ccdf of the stochastically generated data $\hat{F}(u,z\,|\,(n))$, *j = 1,…, N* and the original data *z(uj), j = 1,…, N* allowed calculating the fractions of true values falling into a given symmetric p-PI by

$$\bar{\xi}(p) = \frac{1}{N}\sum_{j=1}^{N}\xi(u_j,p) \quad \forall p \in [0,1]$$ (10)

where $\xi(u_j, p)$ was given by

$$\xi(u_j, p) = \begin{cases} 1 & F^{-1}(u_j, (1-p)/2) < z(u_j) \leq F^{-1}(u_j, (1+p)/2) \\ 0 & otherwise \end{cases} \qquad (11)$$

The agreement between simulated fractions and the fractions of the original data was finally assessed by the G-statistics

$$G = 1 - \int_0^1 [3a(p) - 2][\overline{\xi}(p) - p] dp \qquad (12)$$

where the indicator function $a(p)$ was given by

$$a(p) = \begin{cases} 1 & \overline{\xi}(p) \geq p \\ 0 & otherwise \end{cases} \qquad (13)$$

which causes a weight two times higher for the inaccurate case with $\overline{\xi} < p$. A weight of one is assigned to the accurate case, for which the fraction of values falling into the p-probability interval was equal to or larger than expected. The closer the G-value is to 1, the better the reproduction of the ccdf is. The following equation was proposed by Goovaerts (2000) to determine the accuracy of the reproduction of the variogram in a stochastic simulation,

$$\varepsilon_\gamma = \sum_{s=1}^{S} \frac{[\gamma(h_s) - \hat{\gamma}(h_s)]^2}{[\gamma(h_s)]^2} \qquad (14)$$

where S is a specific number of the first distance lags, 30 in this study, and $\hat{\gamma}(h_s)$ is the semivariance at lag h_s, calculated from the stochastic realisation. Note, that this criterion is identical to the one used to generate the stochastic simulation (Eq. 11). A small value of $\acute{\varepsilon}_r$ indicates good agreement between the reference variogram model and the variogram calculated from a stochastic realisation.

Ahuja, L.R., Ma, L.W., Timlin, D.J., 2006. Trans-disciplinary soil physics research critical to synthesis and modelling of agricultural systems. Soil Science Society of America Journal 70, 311–326.

Ahmed, S.; DeMarsily, G., 1987. Comparison of geostatistical methods for estimating transmissivity using data on transmissivity and specific capacity. Water Resources Research 23, 1717–1737.

Aiken, R.M., Jawson, M.D., Grahammer, K., Polymenopoulos, A.D., 1991. Positional, Spatially Correlated and Random Components of Variability in Carbon–Dioxide Efflux. Journal of Environmental Quality 20, 301–308.

Amelung, W., Cheshire, M.V., Guggenberger, G., 1996. Determination of neutral and acidic sugars in soil by capillary gas-liquid chromatography after trifluoroacetic acid hydrolysis. Soil Biology & Biochemistry 28, 1631–1639.

Amelung, W., Flach, K.-W., Zech, W., 1997. Climatic effects on soil organic matter composition in the great plains. Soil Science Society of America Journal 61, 115–123.

Amelung, W., Zech, W., Zhang, X., Follett, R.F., Tiessen, H., Knox, E., Flach, K.-W., 1998. Carbon, nitrogen, and sulfur pools in particle-size fractions as influenced by climate. Soil Science Society of America Journal 62, 172–181.

Amelung, W., Flach, K.W., Zech, W., 1999. Lignin in particle-size fractions of native grassland soils as influenced by climate. Soil Science Society of America Journal 63, 1222–1228.

Amelung, W., Zech, W., 1999. Minimisation of organic matter disruption during particle-size fractionation of grassland epipedons. Geoderma 92, 73–85.

Amelung, W., Zhang, X., 2001. Determination of amino acid enantiomers in soils. Soil Biology & Biochemistry 33, 553–562.

Amelung, W., Martius, C., Bandeira, A.G., Garcia, M.V.B., Zech, W., 2002. Lignin characteristics and density fractions of termite nests in an Amazonian rain forest - indicators of termite feeding guilds? Soil Biology & Biochemistry 34, 367–372.

Amelung, W., Brodowski, S., Sandhage-Hofmann, A., Bol, R., 2008. "Combining Biomarker with Stable Isotope Analyses for Assessing the Transformation and Turnover of Soil Organic Matter", p. 155–250 Advances in Agronomy, Vol 100, Vol. 100. Elsevier Academic Press Inc, San Diego.

Anderson, M.C., Kustas, W.P., Norman, J.M., 2003. Upscaling and downscaling - A regional view of the soil-plant-atmosphere continuum. Agronomy Journal 95, 1408–1423.

Angers, D.A., Bolinder, M.A., Carter, M.R., Gregorich, E.G., Drury, C.F., Liang, B.C., Voroney, R.P., Simard, R.R., Donald, R.G., Beyaert, R.P., Martel, J., 1997. Impact of tillage practices on organic carbon and nitrogen storage in cool, humid soils of eastern Canada. Soil & Tillage Research 41, 191–201.

Atkinson, P.M., Lloyd, C.D., 2007. Non-stationary variogram models for geostatistical sampling optimisation: An empirical investigation using elevation data. Computers & Geosciences 33, 1285–1300.

Bachmann, J., Guggenberger, G., Baumgartl, T., Ellerbrock, R.H., Urbanek, E., Goebel, M.O., Kaiser, K., Horn, R., Fischer, W.R., 2008. Physical carbon-sequestration mechanisms under special consideration of soil wettability. Journal of Plant Nutrition and Soil Science-Zeitschrift Für Pflanzenernährung und Bodenkunde 171, 14–26.

Baldock, J.A., Oades, J.M., Vassallo, A.M., Wilson, M.A., 1990. Solid-State Cp/Mas C–13 Nmr Analysis of Particle-Size and Density Fractions of a Soil Incubated with Uniformly Labeled C–13-Glucose. Australian Journal of Soil Research 28, 193–212.

Baldock, J.A., Oades, J.M., Waters, A.G., Peng, X., Vasallo, A.M., Wilson, M.A., 1992. Aspects of the chemical structure of soil organic materials as revealed by solid-state 13C NMR spectroscopy. Biogeochemistry 16, 1–42.

Baldock, J.A., Oades, J.M., Nelson, P.N., Skene, T.M., Golchin, A., Clarke, P., 1997. Assessing the extent of decomposition of natural organic materials using solid-state C–13 NMR spectroscopy. Australian Journal of Soil Research 35, 1061–1083.

Baldock, J.A., Skjemstad, J.O., 2000. Role of the soil matrix and minerals in protecting natural organic materials against biological attack. Organic Geochemistry 31, 697–710.

Baldock, J.A., Smernik, R.J., 2002. Chemical composition and bioavailability of thermally altered *Pinus resinosa* (Red pine) wood. Organic Geochemistry 33, 1093–1109.

Balesdent, J., Mariotti, A., Guillet, B., 1987. Natural C–13 Abundance as a Tracer for Studies of Soil Organic-Matter Dynamics. Soil Biology & Biochemistry 19, 25–30.

Batjes, N.H., 1996. Total carbon and nitrogen in the soils of the world. European Journal of Soil Science 47, 151–163.

Bellamy, P.H., Loveland, P.J., Bradley, R.I., Lark, R.M., Kirk, G.J.D., 2005. Carbon losses from all soils across England and Wales 1978–2003. Nature 437, 245–248.

Bernards, M.A., 2002. Demystifying suberin. Canadian Journal of Botany-Revue Canadienne De Botanique 80, 227–240.

Bol, R., Amelung, W., Friedrich, C., 2004. Role of aggregate surface and core fraction in the sequestration of carbon from dung in a temperate grassland soil. European Journal of Soil Science 55, 71–77.

Bol, R., Poirier, N., Balesdent, J., Gleixner, G., 2009. Molecular turnover time of soil organic matter in particle-size fractions of an arable soil. Rapid Communications in Mass Spectrometry 23, 2551–2558.

Boonmung, S., Riley, M.R., 2003. Quantitative analysis of added ammonium and nitrate in silica sand and soil using diffuse reflectance infrared spectroscopy. Spectroscopy Letters 36, 251–274.

Bornemann, L., Welp, G., Amelung, W., 2010. Particulate Organic Matter at the Field Scale: Rapid Acquisition Using Mid-infrared Spectroscopy. Soil Science Society of America Journal 74, 1147–1156, doi:10.2136/sssaj2009.0195.

Bornemann, L., Welp, G., Brodowski, S., Rodionov, A., Amelung, W., 2008. Rapid assessment of black carbon in soil organic matter using mid-infrared spectroscopy. Organic Geochemistry 39, 1537–1544.

Bornemann, L.C., Kookana, R.S., Welp, G., 2007. Differential sorption behaviour of aromatic hydrocarbons on charcoals prepared at different temperatures from grass and wood. Chemosphere 67, 1033–1042.

Bowman, R.A., Vigil, M.F., Nielsen, D.C., Anderson, R.L., 1999. Soil organic matter changes in intensively cropped dryland systems. Soil Science Society of America Journal 63, 186–191.

Braudeau, E., Mohtar, R.H., 2009. Modeling the soil system: Bridging the gap between pedology and soil-water physics. Global and Planetary Change 67, 51–61.

Brodowski, S., Amelung, W., Haumaier, L., Abetz, C., Zech, W., 2005a. Morphological and chemical properties of black carbon in physical soil fractions as revealed by scanning electron microscopy and energy-dispersive X-ray spectroscopy. Geoderma 128, 116–129.

Brodowski, S., Rodionov, A., Haumaier, L., Glaser, B., Amelung, W., 2005b. Revised black carbon assessment using benzene polycarboxylic acids. Organic Geochemistry 36, 1299–1310.

Brodowski, S., John, B., Flessa, H., Amelung, W., 2006. Aggregate-occluded black carbon in soil. European Journal of Soil Science 57, 539–546.

Brodowski, S., Amelung, W., Haumaier, L., Zech, W., 2007. Black carbon contribution to stable humus in German arable soils. Geoderma 139, 220–228.

Buurman, P., Peterse, F., Martin, G.A., 2007. Soil organic matter chemistry in allophanic soils: a pyrolysis-GC/MS study of a Costa Rican Andosol catena. European Journal of Soil Science 58, 1330–1347.

Cambardella, C.A., Elliott, E.T., 1992. Particulate soil organic-matter changes across a grassland cultivation sequence. Soil Science Society of America Journal 56, 777–783.

Cambardella, C.A., Elliott, E.T., 1993. Carbon and Nitrogen Distribution in Aggregates from Cultivated and Native Grassland Soils. Soil Science Society of America Journal 57,1071–1076.

Cambardella, C.A., 1998. "Experimental verification of simulated soil organic matter pools", p. 519–526, *In* R. Lal, et al., eds. Soil processes and the carbon cycle. Lewis Publishers, Boca Raton, Florida.

Carter, M.R., Gregorich, E.G., Angers, D.A., Donald, R.G., Bolinder, M.A., 1998. Organic C and N storage, and organic C fractions, in adjacent cultivated and forested soils of eastern Canada. Soil & Tillage Research 47, 253–261.

Carter, M.R., Angers, D.A., Gregorich, E.G., Bolinder, M.A., 2003. Characterizing organic matter retention for surface soils in eastern Canada using density and particle size fractions. Canadian Journal of Soil Science 83, 11–23.

Cerling, T.E., 1984. The Stable Isotopic Composition of Modern Soil Carbonate and Its Relationship to Climate. Earth and Planetary Science Letters 71, 229–240.

Chang, C.-W., Laird, D.A., Mausbach, M.J., Hurburgh, C.R.J., 2001. Near infrared reflectance spectroscopy – Principal components regression analysis of soil samples. Soil Science Society of America Journal 65, 480–490.

Chang, C.W., Laird, D.A., 2002. Near-infrared reflectance spectroscopic analysis of soil C and N. Soil Science 167, 110–116.

Chantigny, M.H., 2003. Dissolved and water-extractable organic matter in soils: a review on the influence of land use and management practices. Geoderma 113, 357–380.

Chen, C.R., Condron, L.M., Xu, Z.H., Davis, M.R., Sherlock, R.R., 2006. Root, rhizosphere and root-free respiration in soils under grassland and forest plants. European Journal of Soil Science 57, 58–66.

Chenu, C., Plante, A.F., 2006. Clay-sized organo-mineral complexes in a cultivation chronosequence: revisiting the concept of the 'primary organo-mineral complex'. European Journal of Soil Science 57, 596–607.

Christensen, B.T., 1992. Physical fractionation of soil and organic matter in primary particle size and density separates. Advances in soil science 20, 1–90.

Christensen, B.T., 1996. "Carbon in primary and secondary organomineral complexes", p. 97–165, *In* M. R. Carter and B. A. Stewart, eds. Structure and organic matter storage in agricultural soils, Vol. Adnaces in Soil Science. CRC Press, Boca Raton, Florida.

Christensen, B.T., 2001. Physical fractionation of soil and structural and functional complexity in organic matter turnover. European Journal of Soil Science 52, 345–353.

Clark, R.N., King, T.V.V., Klejwa, M., Swayze, G., Vergo, N., 1990. High spectral resolution reflectance spectroscopy of minerals. Journal of Geophysical Research, 12653–12680.

Clark, M.D., Gilmour, J.T. 1983. The effect of temperature on decomposition at optimum and saturated soil water contents. Soil Science Society of America Journal 47, 927–929.

Cockx, L., Van Meirvenne, M., Vitharana, U.W.A., Verbeke, L.P.C., Simpson, D., Saey, T., Van Coillie, F.A.B., 2009. Extracting Topsoil Information from EM38DD Sensor Data using a Neural Network Approach. Soil Science Society of America Journal 73, 2051–2058.

Colthup, N.B., Daly, L.H., Wiberley, S.E., 1990. Introduction to Infrared and Raman Spectroscopy, Academic Press Inc., San Diego.

Cornell, R.M., Schwertmann, U. 1996. The iron oxides, VCH Publishers, New York.

Cosby, B.J., Hornberger, G.M., Clapp, R.B., Ginn, T.R., 1984. A Statistical Exploration of the Relationships of Soil-Moisture Characteristics to the Physical-Properties of Soils. Water Resources Research 20, 682–690.

Coulson, C.B., Davies, R.I., Khan, E.J.A., 1959. Humic-Acid Investigations .2. Studies in the Fractionation of Humic Acids. Journal of Soil Science 10, 271–283.

Cressie, N. 1993. Statistics for spatial data, Wiley Interscience.

Czimczik, C.I., Masiello, C.A., 2007. Controls on black carbon storage in soils. Global Biogeochemical Cycles 21, GB3005/1–GB3005/8.

Daniel, K.W., Tripathi, N.K., Honda, K., 2003. Artificial neural network analysis of laboratory and in situ spectra for the estimation of macronutrients in soils of Lop Buri (Thailand). Australian Journal of Soil Research 41, 47–59.

Davidson, E.A., Janssens, I.A., 2006. Temperature sensitivity of soil carbon decomposition and feedbacks to climate change. Nature 440, 165–173.

De la Rosa, J.M., Knicker, H., Lopez-Capel, E., Manning, D.A.C., Gonzalez-Perez, J.A., Gonzalez-Vila, F.J., 2008. Direct detection of black carbon in soils by Py-GC/MS, carbon–13 NMR spectroscopy and thermogravimetric techniques. Soil Science Society of America Journal 72, 258–267.

Deutsch, C.V.; Cockerham, P.W., 1994. Practical considerations in the application of simulated annealing to stochastic simulation. Mathematical Geology 26, 67–82.

Deutsch, C.V.; Journel, A.G., 1998. GSLIB: Geostatistical Software library and user's guide, 2nd ed. Oxford University Press, New York, 369 p

Doner, H.E., Lynn, W.C., 1989. "Carbonate, Halide, Sulfate, and Sulfide Minerals", p. 297–324, In J. B. Dixon and S. B. Weed, eds. Minerals in Soil Environments, 2nd ed. Soil Science Society of America, Madison, Wisconsin, USA.

Dorodnikov, M., Fangmeier, A., Kuzyakov, Y., 2007. Thermal stability of soil organic matter pools and their delta C–13 values after C–3–C–4 vegetation change. Soil Biology & Biochemistry 39, 1173–1180.

Düwel, O., Utermann, J., 2008. "Humusversorgung der (Ober-) Böden in Deutschland– Status Quo", p. 115–120, In R. F. Hüttl, et al., eds. Zum Stand der Humusversorgung der Böden in Deutschland, Vol. 7. Cottbuser Schriften zur Ökosystemgenese und Landschaftsentwicklung, Cottbus.

Dugas, W.A., 1993. Micrometeorological and chamber measurements of CO2 flux from bare soil. Agric For Meteorol 67: 115–128.

Efron, B., 2004. The estimation of prediction error: Covariance penalties and cross-validation. Journal of the American Statistical Association 99, 619–632.

Emerson, W.W., 1959. The structure of soil crumbs Journal of Soil Science 5, 235–244.

Eswaran, H., Vandenberg, E., Reich, P., 1993. Organic-Carbon in Soils of the World. Soil Science Society of America Journal 57, 192–194.

Evershed, R.P., Bethell, P.H., Reynolds, P.J., Walsh, N.J., 1997. 5 beta-Stigmastanol and related 5 beta-stanols as biomarkers of manuring: Analysis of modern experimental material and assessment of the archaeological potential. Journal of Archaeological Science 24, 485–495.

Falge, E., Baldocchi, D., Olson, R., Anthoni, P., Aubinet, M., Bernhofer, C., Burba, G., Ceulemans, R., Clement, R., Dolman, H., Granier, A., Gross, P., Grunwald, T., Hollinger, D., Jensen, N.O., Katul, G., Keronen, P., Kowalski, A., Lai, C.T., Law, B.E., Meyers, T., Moncrieff, H., Moors, E., Munger, J.W., Pilegaard, K., Rannik, U., Rebmann, C., Suyker, A., Tenhunen, J., Tu, K., Verma, S., Vesala, T., Wilson, K., Wofsy, S., 2001. Gap filling strategies for defensible annual sums of net ecosystem exchange. Agricultural and Forest Meteorology 107, 43–69.

Falloon, P., Smith, P., Coleman, K., Marshall, S., 1998. Estimating the size of the inert organic matter pool from total organic carbon content for use in the Rothamsted carbon model. Soil Biology & Biochemistry 30, 1207–1211.

Falloon, P.D., Smith, P., 2000. Modelling refractory soil organic matter. Biology and Fertility of Soils 30, 388–398.

Feller, C., Beare, M.H., 1997. Physical control of soil organic matter dynamics in the tropics. Geoderma 79:69–116.

Fidencio, P.H., Ruisanchez, I., Poppi, R.J., 2001. Application of artificial neural networks to the classification of soils from Sao Paulo state using near infrared spectroscopy. The Analyst 126, 2194–2200.

Fierer, N., Craine, J.M., McLauchlan, K., Schimel, J.P., 2005. Litter quality and the temperature sensitivity of decomposition. Ecology 86, 320–326.

Flessa, H., Amelung, W., Helfrich, M., Wiesenberg, G.L.B., Gleixner, S., Brodowski, S., Rethemeyer, J., Kramer, C., Grootes, P.M., 2008. Storage and stability of organic matter in a Luvisol and Phaeozem with continuous maize cropping: A synthesis from the priority program SPP 1090. Journal of Plant Nutrition and Soil Science 171, 36–51.

Foti S. Z.; Balogh, J.; Nagy, Z.; Ürmös, Z.S.; Bartha, S.; Tuba, Z., 2008. Temporal and spatial variability and pattern of soil respiration in loess grassland. Community Ecology 9, 57–64.

Geladi, P., Kowalski, B.R., 1986. Partial Least-Squares Regression – a Tutorial. Analytica Chimica Acta 185, 1–17.

Geyer, W., Brueggemann, L., Hanschmann, G., 1997. Prediction of properties of soil humic substances from their ftir spectra using partial least squares regression. International Journal of Environmental and Analytical Chemistry 71, 181–193.

Glaser, B., Haumaier, L., Guggenberger, G., Zech, W., 1998. Black carbon in soils: the use of benzenecarboxylic acids as specific markers. Organic Geochemistry 29, 811–819.

Glaser, B., Amelung, W., 2003. Pyrogenic carbon in native grassland soils along a climasequence in North America. Global Biogeochemical Cycles 17, 33/1–33/8.

Glaser, B., Turrion, M.B., Alef, K., 2004. Amino sugars and muramic acid – biomarkers for soil microbial community structure analysis. Soil Biology & Biochemistry 36, 399–407.

Golchin, A., Clarke, P., Oades, J.M., Skjemstad, J.O., 1995. The Effects of Cultivation on the Composition of Organic-Matter and Structural Stability of Soils. Australian Journal of Soil Research 33, 975–993.

Golchin, A., Baldock, J.A., Clarke, P., Higashi, T., Oades, J.M., 1997. The effects of vegetation and burning on the chemical composition of soil organic matter of a volcanic ash soil as shown by C–13 NMR spectroscopy .2. Density fractions. Geoderma 76, 175–192.

Goldberg, E.D. 1985. Black Carbon in the Environment John Wiley & Sons, New York.

Gonzalez-Perez, J.A., Gonzalez-Vila, F.J., Almendros, G., Knicker, H., 2004. The effect of fire on soil organic matter – a review. Environmental International 30, 855–870.

Goovaerts, P. (2000) Estimation or simulation of soil properties? An optimization problem with conflicting criteria. Geoderma, 97: 165–186.

Graf, A.; Prolingheuer, N.; Schickling, A.; Schmidt, M.; Schneider, K.; Schüttemeyer, D.; Herbst, M.; Huisman, J.A.; Weihermüller, L.; Scharnagl, B.; Steenpass, C.; Harms, R.; Vereecken, H., 2010. Temporal downscaling of soil CO2 efflux measurements based on time-stable patterns. Vadose Zone J, in press.

Grayson, R., Blöschl, G. 2001. Spatial Patterns in Catchment Hydrology University Press, Cambridge.

Gregorich, E.G., Monreal, C.M., Schnitzer, M., Schulten, H.R., 1996. Transformation of plant residues into soil organic matter: Chemical characterization of plant tissue, isolated soil fractions, and whole soils. Soil Science 161, 680–693.

Gregorich, E.G., Beare, M.H., McKim, U.F., Skjemstad, J.O., 2006. Chemical and biological characteristics of physically uncomplexed organic matter. Soil Science Society of America Journal 70, 975–985.

Groeningen, J.W., Mutters, C.S., Horwath, W.R., Kessel, C.v., 2003. NIR and DRIFT-MIR spectrometry of soils for predicting soil and crop parameters in a flooded field. Plant and Soil 250, 155–165.

Guenzler, H., Gremlich, H.U., 2002. IR Spectroscopy – An Introduction Wiley-VCH, Weinheim.

Gulde, S., Chung, H., Amelung, W., Chang, C., Six, J., 2008. Soil carbon saturation controls labile and stable carbon pool dynamics. Soil Science Society of America Journal 72, 605–612.

Haaland, D.M., Thomas, E.V., 1988a. Partial least-squares methods for spectral analysis. 2. Application to simulated and glass spectral data. Analytical Chemistry 60, 1202–1208.

Haaland, D.M., Thomas, E.V., 1988b. Partial least-squares methods for spectral analyses. 1. Relation to other quantitative calibration methods and the extraction of qualitative information. Analytical Chemistry 60, 1193–1202.

Haberhauer, G., Rafferty, B., Strebl, F., Gerzabeck, M.H., 1998. Comparison of the composition of forest soil litter derived from three different sites at various decompositional stages using FTIR spectroscopy. Geoderma 83, 331–342.

Hammes, K., Schmidt, M.W.I., Smernic, R.J., Currie, L.A., Ball, W.P., Nguyen, T.H., Louchouarn, P., Houel, S., Gustafsson, O., Elmquist, M., Cornelissen, G., Skjemstad, J.O., Masiello, C.A., Song, J., Peng, P.a., Mitra, S., Dunn, J.C., Hatcher, P.G., Hockaday, W.C., Smith, D.M., Hartkopf-Fröder, C., Böhmer, A., Lüer, B., Huebert, B.J., Amelung, W., Brodowski, S., Huang, L., Zhang, W., Gschwend, P.M., Flores-Cervantes, D.X., Largeau, C., Rouzaud, J.N., Rumpel, C., Guggenberger, G., Kaiser, K., Rodionov, A., Gonzalez-Vila, F.J., Gonzalez-Perez, J.A., de la Rosa, J.M., Mannig, D.A.C., Lopez-Capel, E., Ding, L., 2007. Comparison of quantification methods to measure fire-derived (black / elemental) carbon in soils and sediments using reference materials from soil, water, sediment and the atmosphere. Global Biogeochemical Cycles 21.

Hasie, T., Tibshirani, R., Friedmann, J., 2001. The elements of statistical learning: data mining, interference and prediction. Springer, New York.

Hassink, J., Whitmore, A.P., Kubat, J., 1997. Size and density fractionation of soil organic matter and the physical capacity of soils to protect organic matter. European Journal of Agronomy 7, 189–199.

Hedges, J.I., Ertel, J.R., 1982. Characterization of Lignin by Gas Capillary Chromatography of Cupric Oxide Oxidation-Products. Analytical Chemistry 54, 174–178.

Hedley, C.B., Yule, I.Y., Eastwood, C.R., Shepherd, T.G., Arnold, G., 2004. Rapid identification of soil textural and management zones using electromagnetic induction sensing of soils. Australian Journal of Soil Research 42, 389–400.

Heitkamp, F., Raupp, J., Ludwig, B., 2009. Impact of fertilizer type and rate on carbon and nitrogen pools in a sandy Cambisol. Plant and Soil 319,259–275.

Herbst, M.; Prolingheuer, N.; Graf, A.; Huisman, J.A.; Weihermüller, L.; Vanderborght, J., 2009. Characterization and understanding of bare soil respiration spatial variability at plot scale. Vadose Zone J 8, 762–771.

Herbst, M., Hellebrand, H.J., Bauer, J., Huisman, J.A., Simunek, J., Weihermuller, L., Graf, A., Vanderborght, J., Vereecken, H., 2008. Multiyear heterotrophic soil respiration: Evaluation of a coupled CO_2 transport and carbon turnover model. Ecological Modelling 214, 271–283.

Hiller, D.A., Brümmer, G.W., 1997. Mikrosondenuntersuchungen an unterschiedlich stark mit Schwermetallen belasteten Böden. 2. Gehalte an Schwermetallen und anderen Elementen in Huminstoffaggregationen, Streustoffen und Holzkohlepartikeln. Journal of Plant Nutrition and Soil Science 160, 47–55.

Hockaday, W.C., Grannas, A.M., Kim, S., Hatcher, P.G., 2005. Direct molecular evidence for the degradation and mobility of black carbon in soils from ultrahigh-resolution mass spectral analysis of dissolved organic matter from a fire-impacted forest soil. Organic Geochemistry 37, 501–510.

Islam, K., Singh, B., McBratney, A., 2003. Simultaneous estimation of several soil properties by ultra-violet, visible, and near-infrared reflectance spectroscopy. Australian Journal of Soil Research 41, 1101–1114.

ISO10694, 1995. Soil quality – determination of organic and total carbon after dry combustion (elemental analysis).

ISO11277, 2002. Soil quality – Determination of particle size distribution in mineral soil material – Method by sieving and sedimentation

ISO13878, 1998. Soil quality – determination of total nitrogen content by dry combustion (elemental analysis).

Izaurralde, R.C., Haugen-Kozyra, K.H., Jans, D.C., McGill, W.B., Grant, R.F., Hiley, J.C., 1998. "Soil C Dynamics: Measurement, Simulation and Site-to-Region Scale up", *In* R. Lal, et al., eds. Assesment Methods for Soil Carbon. Lewis, Boca Raton, Florida.

Jahn, B.R., Linker, R., Upadhyaya, S.K., Shaviv, A., Slaughter, D.C., Shmulevich, I., 2006. Mid-infrared spectroscopic determination of soil nitrate content. Biosystems Engineering 94, 505–515.

Janik, L.J., Skjemstad, J.O., 1995. Characterization and Analysis of Soils Using Midinfrared Partial Least-Squares .2. Correlations with Some Laboratory Data. Australian Journal of Soil Research 33, 637–650.

Janik, L.J., Merry, R.H., Skjemstad, J.O., 1998. Can mid infrared diffuse reflectance analysis replace soil extractions. Australian Journal of Experimental Agriculture, 681–696.

Janik, L.J., Merry, R.H., Forrester, S.T., Lanyon, D.M., Rawson, A., 2007. Rapid prediction of soil water retention using mid infrared spectroscopy. Soil Science Society of America Journal 71, 507–514.

Jenkinson, D.S., Rayner, J.H., 1977. Turnover of Soil Organic-Matter in Some of Rothamsted Classical Experiments. Soil Science 123, 298–305.

Jenkinson, D.S., Adams, D.E., Wild, A., 1991. Model Estimates of CO2 Emissions from Soil in Response to Global Warming. Nature 351, 304–306.

Jenny, H. 1941. Factors of soil formation, a system of quantitative pedology Mc Graw-Hill, New York.

Jones, C., McConnell, C., Coleman, K., Cox, P., Falloon, P., Jenkinson, D., Powlson, D., 2005. Global climate change and soil carbon stocks; predictions from two contrasting models for the turnover of organic carbon in soil. Global Change Biology 11, 154–166.

Jones, M.J., 1973. The organic matter content of savanna soils of West Afrika. Journal of Soil Science 24, 42–53.

Jones, R.N., 1985. "Analytical Applications of Vibrational Spectroscopy – A Historical Review", p. 1, *In* J. R. Durig, ed. Chemical, Biological and Industrial Applications of Infrared Spectroscopy. John Wiley and Sons, Chichester.

Kaal, J., Rumpel, C., 2009. Can pyrolysis-GC/MS be used to estimate the degree of thermal alteration of black carbon? Organic Geochemistry 40, 1179–1187.

Kalbitz, K., Solinger, S., Park, J.H., Michalzik, B., Matzner, E., 2000. Controls on the dynamics of dissolved organic matter in soils: A review. Soil Science 165, 277–304.

Karapanagioti, H.K., James, G., Sabatini, D.A., Kalaitzidis, S., Christanis, K., Gustafsson, O., 2004. Evaluating charcoal presence in sediments and its effect on phenanthrene sorption. Water, Air, and Soil Pollution 4, 359–373.

Kerek, M., Drijber, R.A., Powers, M.J., Shearman, R.C., Gaussoin, R.E., Streich, A.M., 2002. Accumulation of microbial biomass within particulate organic matter of aging golf greens. Agronomy Journal 94, 455–461.

Kern, J.S., 1994. Spatial Patterns of Soil Organic-Carbon in the Contiguous United-States. Soil Science Society of America Journal 58, 439–455.

Khomik, M.; Altaf Arain, M.; McCaughey, J.H., 2006. Temporal and spatial variability of soil respiration in a boreal mixwood forest. Agricultural and Forest Meteorology 140, 244–256.

Knorr, W., Heimann, M., 2001. Uncertainties in global terrestrial biosphere modeling 1. A comprehensive sensitivity analysis with a new photosynthesis and energy balance scheme. Global Biogeochemical Cycles 15, 207–225.

Kögel-Knabner, I., 2002. The macromolecular organic composition of plant and microbial residues as inputs to soil organic matter. Soil Biology & Biochemistry 34, 139–162.

Kögel-Knabner, I., Guggenberger, G., Kleber, M., Kandeler, E., Kalbitz, K., Scheu, S., Eusterhues, K., Leinweber, P., 2008. Organo-mineral associations in temperate soils: Integrating biology, mineralogy, and organic matter chemistry. Journal of Plant Nutrition and Soil Science 171, 61–82.

Kögel, I., 1986. Estimation and Decomposition Pattern of the Lignin Component in Forest Humus Layers. Soil Biology & Biochemistry 18, 589–594.

Kölbl, A., Kögel-Knabner, I., 2004. Content and composition of free and occluded particulate organic matter in a differently textured arable Cambisol as revealed by solid-state 13–C NMR spectroscopy. Journal of Plant Nutrition and Soil Science 167, 45–53.

Kölbl, A., Leifeld, J., Kögel-Knabner, I., 2005. A comparison of two methods for the isolation of free and occluded particulate organic matter. Journal of Plant Nutrition and Soil Science 168, 660–667.

Koster, H.M. Ehrlicher, U., Gilg, H.A., Jordan, R., Murad, E., K. Onnich. 1999. Mineralogical and chemical characteristics of five nontronites and Fe-rich smectites. Clay Minerals 34, 579–599.

Konda, R.; Ohta, S.; Ishizuka, S.; Arai, S.; Ansori, S.; Tanaka, N.; Hardjono, A., 2008. Spatial structures of N2O, CO2, and CH4 fluxes from Acacia mangium plantation soils during a relatively dry season in Indonesia. Soil Biology & Biochemistry 40, 3021–3030. doi:10.1016/j.soilbio.2008.08.022

Kosugi, Y.; Mitani, T.; Itoh, M.; Noguchi, S.; Tani, M.; Matsuo, N.; Takanashi, S.; Ohkubo, S.; Nik, A.R., 2007. Spatial and temporal variation in soil respiration in a Southeast Asian tropical rainforest. Agricultural and Forest Meteorology 147, 35–47.

Kramer, C., Gleixner, G., 2006. Variable use of plant- and soil-derived carbon by microorganisms in agricultural soils. Soil Biology & Biochemistry 38, 3267–3278.

Kravchenko, A.N. ; Hao, X., 2008. Management practice effects on spatial variability characteristics of surface mineralizable C. Geoderma 144, 387–394.

Krull, E., Bray, S., Harms, B., Baxter, N., Bol, R., Farquhar, G., 2007. Development of a stable isotope index to assess decadal-scale vegetation change and application to woodlands of the Burdekin catchment, Australia. Global Change Biology 13, 1455–1468.

Kruskal, J.B., 1964. Nonmetric multidimensional scaling: a numerical method 29, 115–129.

Kuzyakova, I., Richter, C., 2003. Variability of soil parameters in a uniformity trial on a Luvisol evaluated by means of spatial statistics. Journal of Plant Nutrition and Soil Science 166, 348–356.

Larocque, G.; Dutilleul, P.; Pelletier, B.; Fyles, J.W., 2006. Conditional Gaussian co-simulation of regionalized components of soil variation. Geoderma 134, 1–16.

La Scala, N.; Marques Jr., J.; Pereira, G.T.; Cora, J.E., 2000. Short-term temporal changes in the spatial variability model of CO2 emissions from a Brazilian bare soil. Soil Biology & Biochemistry 32, 1459–1462.

Laird, D.A., Martens, D.A., Kingery, W.L., 2001. Nature of clay-humic complexes in an agricultural soil: I. Chemical, biochemical, and spectroscopic analyses. Soil Science Society of America Journal 65, 1413–1418.

Lal, R., 2008. Soil carbon stocks under present and future climate with specific reference to European ecoregions. Nutrient Cycling in Agroecosystems 81, 113–127.

Laskov, C., Amelung, W., Peiffer, S., 2002. Organic matter preservation in the sediment of an acidic mining lake. Environmental Science & Technology 36, 4218–4223.

Leifeld, J., 2006. Application of diffuse reflectance FT-IR spectroscopy and partial least squares regression to predict NMR properties of soil organic matter. European Journal of Soil Science 57, 846–857.

Leuangthong, O.; McLennan, J.A.; Deutsch, C.V., 2004. Minimum acceptance criteria for geostatistical realizations. Natural Resources Research 13, 131–141.

Li, X.D., Fu, H., Guo, D., Li, X.D., Wan, C.G., 2010. Partitioning soil respiration and assessing the carbon balance in a Setaria italica (L.) Beauv. Cropland on the Loess Plateau, Northern China. Soil Biology & Biochemistry 42, 337–346.

Liang, C., Zhang, X.D., Balser, T.C., 2007a. Net microbial amino sugar accumulation process in soil as influenced by different plant material inputs. Biology and Fertility of Soils 44, 1–7.

Liang, C., Zhang, X.D., Rubert, K.F., Balser, T.C., 2007b. Effect of plant materials on microbial transformation of amino sugars in three soil microcosms. Biology and Fertility of Soils 43, 631–639.

Liang, C., Fujinuma, R., Balser, T.C., 2008. Comparing PLFA and amino sugars for microbial analysis in an Upper Michigan old growth forest. Soil Biology & Biochemistry 40, 2063–2065.

Lichtfouse, E., Chenu, C., Baudin, F., Leblond, C., Da Silva, M., Behar, F., Derenne, S., Largeau, C., Wehrung, P., Albrecht, P., 1998. A novel pathway of soil organic matter formation by selective preservation of resistant straight-chain biopolymers: chemical and isotope evidence. Organic Geochemistry 28, 411–415.

Linker, R., Weiner, M., Shmulevich, I., Shaviv, A., 2006. Nitrate determination in soil pastes using attenuated total reflectance mid-infrared spectroscopy: Improved accuracy via soil identification. Biosystems Engineering 94, 111–118.

Loague, K., Green, R.E., 1991. Statistical and graphical methods for evaluating solute transport models: Overview and application. Journal of Contaminant Hydrology 7, 51–73.

Lohmann, R., McFarlane, J.K., Gschwend, P.M., 2005. Importance of black carbon to sorption of native PAHs, PCBs, and PCDDs in Boston and New York harbour sediments. Environmental Science and Technology 39, 141–148.

Lopez-Capel, E., Bol, R., Manning, D.A.C., 2005. Application of simultaneous thermal analysis mass spectrometry and stable carbon isotope analysis in a carbon sequestration study. Rapid Communications in Mass Spectrometry 19, 3192–3198.

Lowe, L.E., 1978. "Carbohydrates in soil", p. 65–93, *In* M. Schnitzer and S. U. Khan, eds. Soil Organic Matter. Elsevier, Amsterdam.

Ludwig, B., Khanna, P.K., 1998. "Use of near Infrared Spectroscopy to Determine Inorganic and Organic Carbon Fractions", *In* J. Kimble, et al., eds. Assessment methods for soil carbon. Lewis, Boca Raton, Florida.

Ludwig, B., Nitschke, R., Terhoeven-Urselmans, T., Michel, K., Flessa, H., 2008. Use of mid-infrared spectroscopy in the diffuse-reflectance mode for the prediction of the composition of organic matter in soil and litter. Journal of Plant Nutrition and Soil Science 171, 384–391.

Madejova, J., Keckes, J., Paalkova, H., Komadel, P., 2002. Identification of components in smectite/kaolinite mixtures. Clay Minerals 37, 377–388.

Mahieu, N., Powlson, D.S., Randall, E.W., 1999. Statistical analysis of published carbon–13 CPMAS NMR spectra of soil organic matter. Soil Science Society of America Journal 63, 307–319.

Manzoni, S., Porporato, A., 2009. Soil carbon and nitrogen mineralization: Theory and models across scales. Soil Biology & Biochemistry 41, 1355–1379.

Marschner, B., Brodowski, S., Dreves, A., Gleixner, G., Gude, A., Grootes, P.M., Hamer, U., Heim, A., Jandl, G., Ji, R., Kaiser, K., Kalbitz, K., Kramer, C., Leinweber, P., Rethemeyer, J., Schaeffer, A., Schmidt, M.W.I., Schwark, L., Wiesenberg, G.L.B., 2008. How relevant is recalcitrance for the stabilization of organic matter in soils? Journal of Plant Nutrition and Soil Science 171, 91–110.

Martens, H., Naes, T. 1989. Multivariate Calibration Wliley, Chichester.

Martin, J.G.; Bolstad, P.V., 2009. Variation of soil respiration at three spatial scales: Components within measurements, intra-site variation and patterns on the landscape. Soil Biology & Biochemistry 41, 530–543.

Mayer, L.M., Schick, L.L., Hardy, K.R., Wagal, R., McCarthy, J., 2004. Organic matter in small mesopores in sediments and soils. Geochimica et Cosmochimica Acta 68, 3863–3872.

McBratney, A.B., Webster, R., 1986. Choosing Functions for Semi-Variograms of Soil Properties and Fitting Them to Sampling Estimates. Journal of Soil Science 37, 617–639.

McBratney, A.B., Santos, M.L.M., Minasny, B., 2003. On digital soil mapping. Geoderma 117, 3–52.

McCarty, G.W., Reeves, J.B., Reeves, V.B., Follett, R.F., Kimble, J.M., 2002. Mid Infrared and Near Infrared Diffuse Reflectance Spectroscopy for Soil Carbon Measurement. Soil Science Society of America Journal 66, 640–646.

McCown, R.L., Hammer, G.L., Hargreaves, J.N.G., Holzworth, D.P., Freebairn, D.M., 1996. APSIM: A novel software system for model development, model testing and simulation in agricultural systems research. Agricultural Systems 50, 255–271.

McNairn, H., Brisco, B., 2004. The application of C-band polarimetric SAR for agriculture: a review. Canadian Journal of Remote Sensing 30, 525–542.

Meersmans, J., De Ridder, F., Canters, F., De Baets, S., Van Molle, M., 2008. A multiple regression approach to assess the spatial distribution of Soil Organic Carbon (SOC) at the regional scale (Flanders, Belgium). Geoderma 143, 1–13.

Mehra, O.P., Jackson, M.L., 1960. Iron oxide removal from soils and clays by a dithionite citrate system buffered with sodium bi-carbonate. Clays Clay Miner 7, 313–317.

Mendez-Millan, M., Dignac, M.F., Rumpel, C., Rasse, D.P., Derenne, S., 2010. Molecular dynamics of shoot vs. root biomarkers in an agricultural soil estimated by natural abundance C–13 labelling. Soil Biology & Biochemistry 42, 169–177.

Mertens, F.M., Paetzold, S., Welp, G., 2008. Spatial heterogeneity of soil properties and its mapping with apparent electrical conductivity. Journal of Plant Nutrition and Soil Science 171, 146–154.

Metay, A., Mary, B., Arrouays, D., Labreuche, J., Martin, M., Nicolardot, B., Germon, J.C., 2009. Effects of reduced or no tillage practices on C sequestration in soils in temperate regions. Canadian Journal of Soil Science 89, 623–634.

Miller, F.T., Guthrie, R.L., 1984. "Classification and distribution of soils containing rock fragments in the United States", *In* J. D. Nichols, et al., eds. Erosion and Productivity of Soils containing Rock Fragments, Vol. 13. Soil Science Society of America.

Mimmo, T., Reeves, J.B., McCarty, G.W., Galletti, G., 2002. Determination of biological measures by mid-infrared diffuse reflectance spectroscopy in soils within a landscape. Soil Science 167, 281–287.

Molz, F.J., Rajaram, H., Lu, S.L., 2004. Stochastic fractal-based models of heterogeneity in subsurface hydrology: Origins, applications, limitations, and future research questions. Reviews of Geophysics 42, 42.

Monreal, C.M., Schulten, H.R., Kodama, H., 1997. Age, turnover and molecular diversity of soil organic matter in aggregates of a Gleysol. Canadian Journal of Soil Science 77, 379–388.

Moron, A., Cozzolino, D., 2004. Determination of potentially mineralizable nitrogen and nitrogen in particulate organic matter fractions in soil by visible and near-infrared reflectance spectroscopy. Journal of Agricultural Science 142, 335–343.

Mueller, T.G., Pusuluri, N.B., Mathias, K.K., Cornelius, P.L., Barnhisel, R.I., Shearer, S.A., 2004. Map quality for ordinary kriging and inverse distance weighted interpolation. Soil Science Society of America Journal 68, 2042–2047.

Nguyen, T.H., Brown, R.A., Ball, W.P., 2004. An evaluation of thermal resistance as a measure of black carbon content in diesel soot, wood char, and sediment. Organic Geochemistry 35, 217–234.

Nierop, K.G.J., Verstraten, J.M., 2004. Rapid molecular assessment of the bioturbation extent in sandy soil horizons under, pine using ester-bound lipids by on-line thermally assisted hydrolysis and methylation-gas chromatography/mass spectrometry. Rapid Communications in Mass Spectrometry 18, 1081–1088.

Ninel, H., Schnitzer, M., Mehus, G.R., 1990. "Soil lipids: Origin, nature, contents, decomposition and effect on soil physical properties", p. 397–427, *In* J. M. Bollag and G. Stotzky, eds. Soil Biochemistry, Vol. 6. Marcel Dekker, New York.

Nuopponen, M.H., Birch, G.M., Sykes, R.J., Lee, S.J., Stewart, D., 2006. Estimation of wood density and chemical composition by means of diffuse reflectance mid-infrared fourier transform (DRIFT-MIR) spectroscopy. Journal of Agricultural and Food Chemistry 54, 34–40.

Oades, J.M., 1984. Soil Organic-Matter and Structural Stability – Mechanisms and Implications for Management. Plant and Soil 76, 319–337.

Ocio, J.A., Brookes, P.C., 1990. An Evaluation of Methods for Measuring the Microbial Biomass in Soils Following Recent Additions of Wheat Straw and the Characterization of the Biomass That Develops. Soil Biology & Biochemistry 22, 685–694.

Olk, D.C., Gregorich, E.G., 2006. Overview of the symposium proceedings, "Meaningful Pools in Determining Soil Carbon and Nitrogen Dynamics". Soil Science Society of America Journal 70, 967–974.

Otto, A., Simoneit, B.R.T., 2001. Chemosystematics and diagenesis of terpenoids in fossil conifer species and sediment from the Eocene Zeitz formation, Saxony, Germany. Geochimica Et Cosmochimica Acta 65, 3505–3527.

Otto, A., Shunthirasingham, C., Simpson, M.J., 2005. A comparison of plant and microbial biomarkers in grassland soils from the Prairie Ecozone of Canada. Organic Geochemistry 36, 425–448.

Otto, A., Simpson, M.J., 2006a. Sources and composition of hydrolysable aliphatic lipids and phenols in soils from western Canada. Organic Geochemistry 37, 385–407.

Otto, A., Simpson, M.J., 2006b. Evaluation of CuO oxidation parameters for determining the source and stage of lignin degradation in soil. Biogeochemistry 80, 121–142.

Parton, W.J., Schimel, D.S., Cole, C.V., Ojima, D.S., 1987. Analysis of Factors Controlling Soil Organic-Matter Levels in Great-Plains Grasslands. Soil Science Society of America Journal 51, 1173–1179.

Patterson, W.A., Edwards, K.J., Maguire, D.J., 1987. Microscopic charcoal as a fossil indicator of fire. Quartenary Science Review 6, 3–23.

Patzold, S., Mertens, F.M., Bornemann, L., Koleczek, B., Franke, J., Feilhauer, H., Welp, G., 2008. Soil heterogeneity at the field scale: a challenge for precision crop protection. Precision Agriculture 9, 367–390.

Panosso, A.R.; Marques Jr., J.; Pereira, G.T.; La Scala Jr., N., 2009. Spatial and temporal variability of soil CO2 emission in a sugarcane area under green and slash-and-burn managements. Soil & Tillage Research 105, 275–282. doi:10.1016/j.still.2009.09.008

Paul, E.A., Follett, R.F., Leavitt, S.W., Halvorson, A., Peterson, G.A., Lyon, D.J., 1997. Radiocarbon dating for determination of soil organic matter pool sizes and dynamics. Soil Science Society of America Journal 61, 1058–1067.

Paul, E.A., Morris, S.J., Conant, R.T., Plante, A.F., 2006. Does the acid hydrolysis-incubation method measure meaningful soil organic carbon pools? Soil Science Society of America Journal 70, 1023–1035.

Paul, J.W., Beauchamp, E.G., 1995. Availability of Manure Slurry Ammonium for Corn Using N–15-Labeled (Nh4)(2)So4. Canadian Journal of Soil Science 75, 35–42.

Paustian, K., Levine, E., Post, W.M., Ryzhova, I.M., 1997. The use of models to integrate information and understanding of soil C at the regional scale. Geoderma 79, 227–260.

Picollo, A., Pietrallemara, G., Mbagwu, J.S.C., 1997. Use of humic substances as soil conditioners to increase aggregate stability. Geoderma 75, 267–277.

Poesen, J., Lavee, H., 1994. Rock Fragments in Top Soils – Significance and Processes. Catena 23, 1–28.

Ponomarenko, E.V., Anderson, D.W., 2001. Importance of charred organic matter in Black Chernozem soils of Saskatchewan. Canadian Journal of Soil Science 81, 285–297.

Prechtel, A., von Lutzow, M., Schneider, B.U., Bens, O., Bannick, C.G., Kogel-Knabner, I., Huttl, R.F., 2009. Organic carbon in soils of Germany: Status quo and the need for new data to evaluate potentials and trends of soil carbon sequestration. Journal of Plant Nutrition and Soil Science 172, 601–614.

Pumpanen, J.; Kolari, P.; Ilvesniemi, H.; Minkkinen, K.; Vesala, T.; Niinistö, S.; Lohila, A.; Larmola, T.; Morero, M.; Pihlatie, M.; Janssens, I.; Yuste, J.C.; Grünzweig, J.M.; Reth, S.; Subke, J.-A.; Savage, K.; Kutsch, W.; Østreng, G.; Ziegler, W.; Anthoni, P.; Lindroth, A.; Hari, P. (2004) Comparison of different chamber techniques for measuring soil Co2 efflux. Agricultural and Forest Meteorology 123: 159–176.

Quenea, K., Largeau, C., Derenne, S., Spaccini, R., Bardoux, G., Mariotti, A., 2006. Molecular and isotopic study of lipids in particle size fractions of a sandy cultivated soil (Cestas cultivation sequence, southwest France): Sources, degradation, and comparison with Cestas forest soil. Organic Geochemistry 37, 20–44.

Reeves, J.B., McCarty, G.W., Reeves, V.B., 2001. Mid-infrared Diffuse Reflectance Spectroscopy for the Quantitative Analysis of Agricultural soils. Journal of Agricultural and Food Chemistry 49, 766–772.

Reeves, J.B., Van Kessel, J.A.S., 2002. Spectroscopic analysis of dried manures. Near-versus mid-infrared diffuse reflectance spectroscopy for the analysis of dried dairy manures. Journal of Near Infrared Spectroscopy 10, 93–101.

Reeves, J.B., Follett, R.F., McCarty, G.W., Kimble, J.M., 2006. Can near or mid-infrared diffuse reflectance spectroscopy be used to determine soil carbon pools? Communications in Soil Science and Plant Analysis 37, 2307–2325.

Reichstein, M., Rey, A., Freibauer, A., Tenhunen, J., Valentini, R., Banza, J., Casals, P., Cheng, Y.F., Grunzweig, J.M., Irvine, J., Joffre, R., Law, B.E., Loustau, D., Miglietta, F., Oechel, W., Ourcival, J.M., Pereira, J.S., Peressotti, A., Ponti, F., Qi, Y., Rambal, S., Rayment, M., Romanya, J., Rossi, F., Tedeschi, V., Tirone, G., Xu, M., Yakir, D., 2003. Modeling temporal and large-scale spatial variability of soil respiration from soil water availability, temperature and vegetation productivity indices. Global Biogeochemical Cycles 17,15.

Rethemeyer, J., Grootes, P.M., Brodowski, S., Ludwig, B. 2007. Evaluation of soil C-14 data for estimating inert organic matter in the RothC model. Radiocarbon 49, 1079–1091.

Ritchie, J.C., Spraberr, J., McHenry, J.R. 1974. Estimating Soil Erosion from Redistribution of Fallout Cs-137. Soil Science Society of America Journal 38, 137–139.

Rochette, P., Desjardins, R.L., Pattey, E., 1991. Spatial and temporal variability of soil respiration in agricultural fields. Canadian Journal of Soil Science 71, 189–196.

Rochette, P., Flanagan, L., B., 1997. Quantifying rhizosphere respiration in a corn crop under field conditions. Soil Science Society of America Journal 61, 466–474.

Rodionov, A., Amelung, W., Urusevskaja, I., Zech, W., 1999. Climatic effect on lignin and polysaccharides in particle-size fractions of zonal steppe soils, Russia. Journal of Plant Nutrition and Soil Science 162, 231–238.

Rodionov, A., Amelung, W., Haumeyer, L., Urusevskaja, I., Zech, W., 2006. Black carbon in the zonal steppe soils of Russia. Journal of Plant Nutrition and Soil Science 169, 363–369.

Rumpel, C., Janik, L.J., Skjemstad, J.O., Kogel-Knabner, I., 2001. Quantification of carbon derived from lignite in soils using mid-infrared spectroscopy and partial least squares. Organic Geochemistry 32, 831–839.

Rumpel, C., Chaplot, V., Planchon, O., Bernadou, J., Valentin, C., Mariotti, A., 2006. Preferential erosion of black carbon on steep slopes with slash and burn agriculture. Catena 65, 30–40.

Rumpel, C., Ba, A., Darboux, F., Chaplot, V., Planchon, O., 2009. Erosion budget and process selectivity of black carbon at meter scale. Geoderma 154, 131–137.

Ruzicka, S., Edgerton, D., Norman, M., Hill, T., 2000. The utility of ergosterol as a bioindicator of fungi in temperate soils. Soil Biology & Biochemistry 32, 989–1005.

Ryan, M.G., Law, B.E., 2005. Interpreting, measuring, and modeling soil respiration. Biogeochemistry 73, 3–27.

Sanderman, J., Amundson, R.G., Baldocchi, D.D., 2003. Application of eddy covariance measurements to the temperature dependence of soil organic matter mean residence time. Global Biogeochemical Cycles 17,15.

Schmidt, M.W.I., Skjemstad, J.O., Gehrt, E., Kögel-Knabner, I., 1999. Charred organic carbon in German chernozemic soils. European Journal of Soil Science 50, 351–365.

Schmidt, M.W.I., Noack, A.G., 2000. Black carbon in soils and sediments: Analysis, distribution, implications and current challenges. Global Biogeochemical Cycles 14, 777–793.

Schmidt, M.W.I., Skjemstad, J.O., Jäger, C., 2002. Carbon isotope geochemistry and nanomorphology of soil black carbon: Black chernozemic soils in central Europe originate from ancient biomass burning. Global Biogeochemical Cycles 16, doi:10.1029/2002GB001939.

Schoorl, J.M., Boix Fayos, C., de Meijer, R.J., van der Graaf, E.R., Veldkamp, A. 2004. The Cs-137 technique applied to steep Mediterranean slopes (Part I): the effects of lithology, slope morphology and land use. Catena 57, 15–34.

Schulten, H.R., Leinweber, P., Reuter, G., 1992. Initial Formation of Soil Organic-Matter from Grass Residues in a Long-Term Experiment. Biology and Fertility of Soils 14, 237–245.

Schulten, H.R., Leinweber, P., 1993. Pyrolysis-Field Ionization Mass-Spectrometry of Agricultural Soils and Humic Substances - Effect of Cropping Systems and Influence of the Mineral Matrix. Plant and Soil 151, 77–90.

Schutter, M.E., Fuhrmann, J.J., 1999. Microbial responses to coal fly ash under field conditions. Journal of Environmental Quality 28, 648–652.

Schwartz, D., deForesta, H., Mariotti, A., Balesdent, J., Massimba, J.P., Girardin, C., 1996. Present dynamics of the savanna-forest boundary in the Congolese Mayombe: A pedological, botanical and isotopic (C–13 and C–14) study. Oecologia 106, 516–524.

Sequaris, J.M., Guisado, G., Magarinos, M., Moreno, C., Burauel, P., Narres, H.D., Vereecken, H., 2010. Organic-carbon fractions in an agricultural topsoil assessed by the determination of the soil mineral surface area. Journal of Plant Nutrition Soil Science 173, 699–705.

Shepherd, K.D., Walsh, M.G., 2002. Development of reflectance spectral libraries for characterization of soil properties. Soil Science Society of America Journal 66, 988–998.

Simbahan, G.; Dobermann, A.; Goovaerts, P.; Ping, J.; Haddix, M.L., 2006. Fine-resolution mapping of soil organic carbon based on multivariate secondary data. Geoderma 132, 471–489.

Simonett, D.S. 1960. Soil genesis on Basalt in North Queensland International Congress of Soil Science, Madison, Wisconsin.

Simpson, M.J., Otto, A., Feng, X.J., 2008. Comparison of solid-state carbon–13 nuclear magnetic resonance and organic matter biomarkers for assessing soil organic matter degradation. Soil Science Society of America Journal 72, 268–276.

Six, J., Elliott, E.T., Paustian, K., Doran, J.W., 1998. Aggregation and soil organic matter accumulation in cultivated and native grassland soils. Soil Science Society of America Journal 62, 1367–1377.

Six, J., Paustian, K., Elliott, E.T., Combrink, C., 2000. Soil structure and organic matter: I. Distribution of aggregate-size classes and aggregate-associated carbon. Soil Science Society of America Journal 64, 681–689.

Six, J., Guggenberger, G., Paustian, K., Haumaier, L., Elliott, E.T., Zech, W., 2001. Sources and composition of soil organic matter fractions between and within soil aggregates. European Journal of Soil Science 52, 607–618.

Six, J., Conant, R.T., Paul, E.A., Paustian, K., 2002. Stabilization mechanisms of soil organic matter: Implications for C-saturation of soils. Plant and Soil 241, 155–176.

Six, J., Bossuyt, H., Degryze, S., Denef, K., 2004. A history of research on the link between (micro)aggregates, soil biota, and soil organic matter dynamics. Soil & Tillage Research 79, 7–31.

Skjemstad, J.O., Janik, L.J., Head, M.I., McLure, J.M., 1993. High energy ultraviolet photo oxidation: a novel technique for studying physically protected organic matter in clay- and silt-sized aggregates. Journal of Soil Science 44, 485–499.

Skjemstad, J.O., Spouncer, L.R., Cowie, B., Swift, R.S., 2004. Calibration of the Rothamsted organic carbon turnover model (RothC ver.26.3), using measurable soil organic carbon pools. Australian Journal of Soil Research 42, 79–88.

Smidt, E., Meissl, K., 2007. The applicability of Fourier transform infrared (FT-IR) spectroscopy in waste management. Waste Management 27, 268–276.

Smith, B.N., Epstein, S., 1971. 2 Categories of C–13/C–12 Ratios for Higher Plants. Plant Physiology 47, 380–386.

Smith, J.U., Smith, P., Monaghan, R., MacDonald, J., 2002. When is a measured soil organic matter fraction equivalent to a model pool? European Journal of Soil Science 53, 405–416.

Smith, K.A., Ball, T., Conen, F., Dobbie, K.E., Massheder, J., Rey, A., 2003. Exchange of greenhouse gases between soil and atmosphere: interactions of soil physical factors and biological processes. European Journal of Soil Science 54, 779–791.

Smith, P., Smith, J.U., Powlson, D.S., McGill, W.B., Arah, J.R.M., Chertov, O.G., Coleman, K., Franko, U., Frolking, S., Jenkinson, D.S., Jensen, L.S., Kelly, R.H., Klein-Gunnewiek, H., Komarov, A.S., Li, C., Molina, J.A.E., Mueller, T., Parton, W.J., Thornley, J.H.M., Whitmore, A.P., 1997. A comparison of the performance of nine soil organic matter models using datasets from seven long-term experiments. Geoderma 81, 153–225.

Smith, P., 2008. Land use change and soil organic carbon dynamics. Nutrient Cycling in Agroecosystems 81, 169–178.

Sohi, S.P., Mahieu, N., Arah, J.R.M., Powlson, D.S., Madari, B., Gaunt, J.L., 2001. A procedure for isolating soil organic matter fractions suitable for modeling. Soil Science Society of America Journal 65, 1121–1128.

Solomon, D., Lehmann, J., Kinyangi, J., Liang, B.Q., Schafer, T., 2005. Carbon K-edge NEXAFS and FTIR-ATR spectroscopic investigation of organic carbon speciation in soils. Soil Science Society of America Journal 69, 107–119.

Solomon, D., Lehmann, J., Kinyangi, J., Amelung, W., Lobe, I., Pell, A., Riha, S., Ngoze, S., Verchot, L., Mbugua, D., Skjemstad, J., Schafer, T., 2007. Long-term impacts of anthropogenic perturbations on dynamics and speciation of organic carbon in tropical forest and subtropical grassland ecosystems. Global Change Biology 13, 511–530.

Song, J., Peng, P.a., Huang, W., 2002. Black carbon and kerogen in soils and sediments: 1. Quantification and characterization. Environmental Science and Technology 36, 3960–3967.

Soussana, J.F., Loiseau, P., Vuichard, N., Ceschia, E., Balesdent, J., Chevallier, T., Arrouays, D., 2004. (Carbon cycling and sequestration opportunities in temperate grasslands. Soil Use and Management 20, 219–230.

Stendahl, J., Lundin, L., Nilsson, T., 2009. The stone and boulder content of Swedish forest soils. Catena 77, 285–291.

Stevenson, F.J., 1966. Lipids in Soil. Journal of the American Oil Chemists Society 43,203–212.

Stewart, C.E., Plante, A.F., Paustian, K., Conant, R.T., Six, J., 2008. Soil carbon saturation: Linking concept and measurable carbon pools. Soil Science Society of America Journal 72, 379–392.

Stewart, C.E., Paustian, K., Conant, R.T., Plante, A.F., Six, J. 2007. Soil carbon saturation: concept, evidence and evaluation. Biogeochemistry 86, 19–31.

Tatzber, M., Stemmer, M., Spiegel, H., Katzlberger, C., Haberhauer, G., Mentler, A., Gerzabek, M.H., 2007. FTIR-spectroscopic characterization of humic acids and humin fractions obtained by advanced NaOH, $Na_4P_2O_7$, and Na_2CO_3 extraction procedures. Journal of Plant Nutrition and Soil Science, 6, 522–529.

Terhoeven-Urselmans, T., Michel, K., Helfrich, M., Flessa, H., Ludwig, B., 2006. Near-infrared spectroscopy cam predict the composition of organic matter in soil and litter. Journal of Plant Nutrition and Soil Science 169, 168–174.

Topp, G.C., Davis, J.L., 1985. Measurement of Soil-Water Content Using Time-Domain Reflectrometry (TDR) - a Field-Evaluation. Soil Science Society of America Journal 49, 19–24.

Trumbore, S.E., Zheng, S.H., 1996. Comparison of fractionation methods for soil organic matter C–14 analysis. Radiocarbon 38, 219–229.

Van Genuchten, P.P.L., Simunek, J., 2004. "Integrated modeling of vadose-zone flow and solute transport", p. 37–69, In R. A. Feddes, et al., eds. Frontis Workshop on Unsaturated-Zone Modeling: Progress, Challenges, and Applications, Wageningen.

Viscarra-Rossel, R.A., McGlynn, R.N., McBratney, A.B., 2006a. Determining the composition of mineral-organic mixes using UV–vis–NIR diffuse reflectance spectroscopy. Geoderma 137, 70–82.

Viscarra-Rossel, R.A., Walvoort, D.J.J., McBratney, A.B., Janik, L.J., Skjemstad, J.O., 2006b. Visible, near infrared, mid infrared or combined diffuse reflectance spectroscopy for simultaneous assessment of various soil properties. Geoderma 131, 59–75.

Viscarra-Rossel, R.A., 2007a. ParLeS: Software for chemometric analysis of spectroscopic data. Chemometrics and Intelligent Laboratory Systems.

Viscarra-Rossel, R.A., 2007b. Robust modelling of soil diffuse reflectance spectra by "bagging-partial least squares regression". Journal of Near Infrared Spectroscopy 15, 39–47.

Visser, H., de Nijs, T., 2006. The Map Comparison Kit. Environmental Modelling & Software 21, 346–358.

Voet, D., Voet, J.G. 1995. Biochemistry John Wiley New York.

Vogel, H.J., Roth, K., 2003. Moving through scales of flow and transport in soil. Journal of Hydrology 272, 95–106.

von Lützow, M., Leifeld, J., Kainz, M., Kögel-Knabner, I., Munch, J.C., 2002. Indications for soil organic matter quality in soils under different management. Geoderma 105, 243–258.

von Lützow, M., Kögel-Knabner, I., Ekschmitt, K., Matzner, E., Guggenberger, G., Marschner, B., Flessa, H., 2006. Stabilization of organic matter in temperate soils: mechanisms and their relevance under different soil conditions – a review. European Journal of Soil Science 57, 426–445.

von Lützow, M., Kögel-Knabner, I., Ekschmittb, K., Flessa, H., Guggenberger, G., Matzner, E., Marschner, B., 2007. SOM fractionation methods: Relevance to functional pools and to stabilization mechanisms. Soil Biology & Biochemistry 39, 2183–2207.

Wagai, R., Mayer, L.M., Kitayarna, K., Knicker, H., 2008. Climate and parent material controls on organic matter storage in surface soils: A three-pool, density-separation approach. Geoderma 147, 23–33.

Wander, M., 2004. "Soil organic matter fractions and their relevance to soil function", *In* M. Magdoff and R. R. Weil, eds. Soil organic matter in sustainable agriculture. CRC Press, Boca Raton, Florida.

Wang, Y.Q., Zhang, X.C., Zhang, J.L., Li, S.J., 2009. Spatial Variability of Soil Organic Carbon in a Watershed on the Loess Plateau. Pedosphere 19, 486–495.

Wattel-Koekkoek, E.J.W., van Genuchten, P.P.L., Buurman, P., van Lagen, B., 2001. Amount and composition of clay-associated soil organic matter in a range of kaolinitic and smectitic soils. Geoderma 99, 27–49.

Watts, C.W., Dexter, A.R., 1997. The influence of organic matter in reducing the destabilization of soil by simulated tillage. Soil & Tillage Research 42, 253–275.

Webster, E.A., Chudek, J.A., Hopkins, D.W., 1997. Fates of C–13 from enriched glucose and glycine in an organic soil determined by solid-state NMR. Biology and Fertility of Soils 25, 389–395.

Wengel, M., Kothe, E., Schmidt, C.M., Heide, K., Gleixner, G., 2006. Degradation of organic matter from black shales and charcoal by the wood-rotting fungus Schizophyllum commune and release of DOC and heavy metals in the aqueous phase. Science of the Total Environment 367, 383–393.

Werth, M., Kuzyakov, Y., 2009. Three-source partitioning of CO2 efflux from maize field soil by C–13 natural abundance. Journal of Plant Nutrition and Soil Science 172, 487–499.

Williams, P.C., Sobering, D.C., 1993. Comparison of commercial near infrared transmittance and reflectance instruments for analysis of whole grains and seeds. Journal of Near Infrared Spectroscopy, 12, 25–32.

Wilson, K.B., Meyers, T.P., 2001. The spatial variability of energy and carbon dioxide fluxes at the floor of a deciduous forest. Boundary-Layer Meteorology 98, 443–473.

Wilson, M.A. 1987. NMR Techniques and Applications in Geochemistry and Soil Chemistry Pergamon Press, Oxford.

Wiseman, C.L.S., Puttmann, W., 2005. Soil organic carbon and its sorptive preservation in central Germany. European Journal of Soil Science 56, 65–76.

Wiseman, C.L.S., Puttmann, W., 2006. Interactions between mineral phases in the preservation of soil organic matter. Geoderma 134, 109–118.

WRB, I.W.G. 2007. World Reference Base for Soil Resources 2006, first update 2007 FAO, Rome.

Yanai, J.; Mishima, A.; Funakawa, S.; Akshalov, K.; Kosaki, T., 2005. Spatial variability of organic matter dynamics in the semi-arid croplands of northern Kazakhstan. Soil Sci Plant Nutr 51, 261–269.

Yang, H., Yu, J.Z., 2002. Uncertainties in charring correction in the analysis of elemental and organic carbon in atmospheric particles by thermal/optical methods. Environmental Science and Technology 36, 5199–5204.

Yavitt, J.B., Harms, K.E., Garcia, M.N., Wright, S.J., He, F., Mirabello, M.J., 2009. Spatial heterogeneity of soil chemical properties in a lowland tropical moist forest, Panama. Australian Journal of Soil Research 47, 674–687.

Ye, L., Tang, H., Zhu, J., Verdoodt, A., Van Ranst, E., 2008. Spatial patterns and effects of soil organic carbon on grain productivity assessment in China. Soil Use and Management 24, 80–91.

Zadeh, L., 1965. Fuzzy sets. Information and Control, 338–353.

Zelles, L., 1999. Fatty acid patterns of phospholipids and lipopolysaccharides in the characterisation of microbial communities in soil: a review. Biology and Fertility of Soils 29, 111–129.

Zhang, J.H., Nie, X.J., Su, Z.A., 2008. Soil Profile Properties in Relation to Soil Redistribution by Intense Tillage on a Steep Hillslope. Soil Science Society of America Journal 72, 1767–1773.

Zimmermann, M., Leifeld, J., Fuhrer, J., 2007a. Quantifying soil organic carbon fractions by infrared-spectroscopy. Soil Biology and Biochemistry 39, 224–231.

Zimmermann, M., Leifeld, J., Schmidt, M.W.I., Smith, P., Fuhrer, J., 2007b. Measured soil organic matter fractions can be related to pools in the RothC model. European Journal of Soil Science 58, 658–667.

Zsolnay, A., 2003. Dissolved organic matter: artefacts, definitions, and functions. Geoderma 113, 187–209.